A STUDY OF THE RELATIONSHIP BETWEEN PERMEABILITY DISTRIBUTIONS AND SMALL SCALE SEDIMENTARY FEATURES IN A FLUVIAL FORMATION

by

Madeline Gotkowitz

Submitted in Partial Fulfillment
of the Requirements for the Degree of
Master of Science in Hydrology

New Mexico Institute of Mining and Technology
Socorro, New Mexico

October, 1993

Abstract

This study focuses on styles of small-scale heterogeneity found in fluvial sand and soil bodies. Over 1,700 in situ measurements of air permeability were taken in an outcrop-based study which joins observations of sedimentary features with their associated permeability distributions. The relationship between sedimentology and hydrologic parameters provides a geologic framework to assess geostatistical hypotheses.

The soils in the study area are found to have a significantly lower permeability than the channel sand deposits. The soil deposits showed a significant lack of observable small scale sedimentary structures, which is reflected in the experimental variograms. The permeability distribution in these study sites appears to be adequately represented by a continuous gaussian random field model. The presence of calcium carbonate nodules in the soils is related to the permeability distribution. Correlation lengths in the channel sands perpendicular to stratigraphy are significantly shorter than those observed parallel to stratigraphy.

A sedimentological, bounding surfaces model is evaluated with regard to permeability distributions. In deposits of little sedimentary structure, the mean and variance may adequately characterize the permeability distribution. Where significant sedimentary structure exists, the bounding surfaces model can be used to determine the scales of variability present in the permeability distribution and may also be used to infer an appropriate choice of random field model.

Acknowledgements

Many people have helped me throughout my graduate school career. Drs. Fred Phillips, John Wilson, Allen Gutjahr, and Dave Love provided excellent teaching, guidance, and critical reviews. This research was funded by the Subsurface Science Program, Office of Energy Research, U.S. Department of Energy under contract no. DE-FG04-89ER60843.

I owe much to Matt and Ruth Davis. Many of the ideas presented here belong to them, and the field work was accomplished with their help and ingenuity. Even geostatistics is fun when Matt and Ruth are around.

TABLE OF CONTENTS

LIST OF TABLES

LIST OF FIGURES

CHAPTER 1: INTRODUCTION

The growing problem of contaminated groundwater resources has led to increased interest in the effects of geologic heterogeneity on flow and transport processes in the subsurface. Spatial variability in aquifer material must be adequately characterized in order to predict dispersion of a contaminant plume, because spatial variation in hydraulic conductivity is a dominant control on velocity variations within groundwater systems (Schwartz, 1977). The actual nature of aquifer heterogeneity is deterministic. However, because of the difficulties inherent in determining subsurface characteristics, a stochastic framework is often employed as a practical means of describing subsurface parameters, such as hydraulic conductivity distributions. Stochastic transport models of the hydraulic conductivity field have been developed for groundwater hydrology and petroleum engineering (e.g. Dagan, 1982; Gelhar and Axness, 1983). The mean, variance and correlation length of the random variable (in this case, hydraulic conductivity) must be estimated. An assumption is often made in these models that the variance of the random variable will reach an asymptotic value as the volume of the sampled region increases (Journel and Huijbregts, 1978). Alternatively, it has been suggested that the variance of hydraulic conductivity is scale-dependent (Neuman, 1990; Wheatcraft and Tyler, 1988). Investigators have applied both fractal and nested models to the problem of characterizing subsurface heterogeneity (Kemblowski and Wen, 1993; Burrough,

1983).

Further evaluation of these hypotheses requires empirical data. Researchers have obtained very large numbers of permeability measurements from cores or in-situ flow tests, however the expense involved makes this an impractical approach for routine use (Smith, 1981; Woodbury and Sudicky, 1991). Incorporation of qualitative geologic information may help to constrain the number of hydraulic conductivity measurements necessary for estimation of these statistical moments by relating geologic variation to variation in hydraulic conductivity (Davis et al, 1993; Phillips and Wilson, 1989; Anderson, 1989; Poeter and Gaylord, 1990). Specifically, we would like to come to a detailed understanding of the relationship between depositional environment, sedimentological features, and permeability distributions. Empirical, outcrop-based studies of permeability patterns will improve our understanding of hydrogeological heterogeneity preserved in the subsurface. These studies should also allow us to ascertain which random field models accurately represent styles of heterogeneity found in particular depositional environments.

Several workers have completed outcrop based studies of geologic heterogeneity. Goggin et al. (1988), found that distinct permeability modes could be related to the stratification types identified within an eolian sandstone deposit. Dreyer et al. (1990), suggest a relationship between permeability patterns and depositional facies distribution in

delta plain/coastal plain channel sand bodies. Davis et al. (1993) looked at architectural element-scale heterogeneity in a fluvial/interfluvial environment and concluded that the external geometry and spatial assemblage of the elements are dominant controls on the spatial correlation structure at that scale of observation.

This study is an extension of work by Davis et al.(1993, 1991) and Lohmann (1992), with an emphasis on the styles of heterogeneity within two architectural elements found at the Sierra Ladrones field site. Here, we would like to arrive at a method of incorporating "soft" geologic information and "hard" permeability data into a characterization of the permeability distribution of an aquifer at a relatively small scale (on the order of meters). As large numbers of contaminated aquifers are located in alluvial/fluvial sedimentary environments, this study focuses on styles of small-scale heterogeneity found in fluvial sand and soil bodies. We used an in-situ mini air permeameter (Davis et al. 1994, in press) to conduct an extensive outcrop-based study which joins observations of small scale sedimentary features with their associated permeability distributions.

The relationship between sedimentology and hydrologic parameters provides a geologic framework to assess geostatistical hypotheses. If areas within an architectural element exhibit similar permeability patterns then, once those patterns have been identified, the task of characterizing aquifer heterogeneity might be aided by finding a representation of the spatial

distribution of the elements. The small-scale studies presented here have been carried out to investigate three topics related to this: what is the nature of geologic and hydrogeologic variation within fluvial sand and soil deposits?; is there a connection between observable geologic features and the correlation structure of the associated permeability distribution?; and finally, to compare and contrast the styles of heterogeneity found within and between the sands and soils of the study area.

CHAPTER 2: STUDY SITES

Over 1700 measurements of permeability were obtained at seven outcrop locations within the Albuquerque Basin of central New Mexico. Six of the study sites, referred to as SS1, SS2, SS3, SS4, SS5 and SS6, are located at the Bosque site. One study, ES1, is located at the Escondida site.

2.1 Bosque Site

The Bosque site is located in the Pliocene-Pleistocene Sierra Ladrones Formation in a location which is interpreted to be of fluvial/interfluvial origin. This is the site of previous studies by Davis et al.(1993 and 1991), Davis (1993), and Lohmann (1992). The deposits are interpreted as marginal ancestral Rio Grande floodplain and tributary deposits (Davis et al., 1993).

Six architectural elements have been identified at the Bosque site (Davis et al., 1993). Two of these were considered appropriate for this small-scale study based on the range of permeabilities found within them and their overall importance within the fluvial depositional regime. Studies SS1, SS2, SS3 and SS5 are located in a channel sand element, CH-2. Studies SS4 and SS6 are in a sandy paleosol element, Ps.

2.1.1 CH-2 Element

The CH-2 element consists of low-energy channel sands with grain size ranging from very fine to medium. Sedimentary structures commonly include continuous and discontinuous

horizontal lamination, foresets of inclined planar crossbedding, ripple cross laminated sands and climbing ripple stratification. Clay drapes from 0.5 to 1.5 cm thick are locally abundant, and are often interbedded with very fine sands, and laminated clay and silt. Lohmann (1992) describes these deposits as proximal flood plain sands and axial channel fill.

2.1.2 Ps Element

The Ps element consists of an orange-red sandy paleosol composed of moderately to well-sorted, very fine to fine sand with scattered zones of white calcium carbonate accumulation. Some of these deposits display weak sedimentary structures, although in general, the processes involved in pedogenesis have destroyed the sedimentary structure of the parent material. Lohmann (1992) attributed this element to a combination of fluvial and eolian floodplain sands.

2.2 Escondida Site

One small scale study presented here, ES1, was conducted at an area within the Sierra Ladrones Formation located approximately 60 km to the south of the Bosque field site, near Escondida, New Mexico. The deposits at this site (ES1) are interpreted as high-energy fluvial deposits of the Rio Grande axial drainage system. While this study does not benefit from the extensive work previously conducted at the Bosque site, it was felt that extending the small scale studies to a site judged

to be more strictly fluvial than inter-fluvial in nature would further generalize the results of this project.

CHAPTER 3: FIELD METHODS

3.1 Site Selection

Five of the Bosque study sites were chosen based on their being representative of the CH-2 or Ps elements. SS3 is in the CH-2 element but is not typical of deposits found at the site. Both SS3 and the Escondida site study, ES1, were selected because they display fluvial sedimentary features different than those common to the Bosque site. Other site selection criteria included good vertical exposure with few surface irregularities such as animal burrows or fractures, the presence of dry, weakly lithified material within the range of measurement of the air permeameter, and ease of accessibility.

3.2 Sampling Scheme

Sampling locations were located on a grid in order to optimize the process of variogram estimation. For computational purposes, the grid spacing should be less than the correlation length of the property being sampled for. As the correlation length of each study area was unknown at the outset of each study, a random approach was developed to assure sampling throughout a range of spacings. This method was adapted from that developed by Davis (1991). Analysis of the initial data sets showed an insufficient number of measurements taken at small separation distances. As described in section 4.2.1, each Bosque field site was sampled a second time at very short lags to cover

the range of scales needed for variogram estimation.

The air-permeameter measures approximately one cubic centimeter of material (Davis et al., 1994). With this in mind, sampling locations were held to a minimum of two centimeters spacing. This then determined the smallest scale of heterogeneity which could be detected in this study. Repeated measurements were made at several locations at each study site in order to estimate the measurement error associated with the air-permeameter. This value was used to determine the nugget value of the experimental variograms.

A rough form of photogrammetry was used in the Bosque studies SS1 through SS5 to plan and implement the sampling strategy. Photographs of the outcrop areas were taken at a scale which allowed the identification of significant features on the outcrop. These photographs were taken with sufficient overlap so that photo-mosaics of each study area could be made. Control points were drawn on the photomosaic in an orthogonal grid at dimensions which provided for the desired number of control points to be distributed throughout the study area. A pair of random numbers from a uniform distribution between zero and one was generated for each control point. One of these random values was multiplied by the grid spacing in the x direction, the other was multiplied by the grid spacing in the y direction. These numbers served as the sampling dimensions for that particular control point. A third random number between zero and one was generated for each control point. If the random number was less

than 0.50, that control point was designated as a "four". The control point was the location of the first measurement, and three other measurements were obtained at distances away from the control point equal to the sampling dimensions generated for that control point, as illustrated in Figure 1. If the random number was equal to or greater than 0.50, that control point was designated as a "nine". In this case, the control point served as the location for the first measurement, and a grid of three rows of three sampling locations was laid out from there (Figure 1). The sampling locations of each study site are shown in Appendix D.

It was expected that this sampling scheme would provide an adequate distribution of pairs of data points for variogram estimation without biasing the sampling to a particular scale of heterogeneity. However, it was later determined that this process did not yield a sufficient number of measurements at very short distances. The study sites were sampled again as described in Section 4.2.1.

The photomosaic was used in the field to identify the locations of control points on the outcrop. The sampling locations were measured from each control point, and each location was recorded as an x,y distance from the first control point.

Measurements at study site ES1 were taken along a vertical transect. The measurements were spaced at a variety of intervals and were planned so as to yield sufficient data for variogram

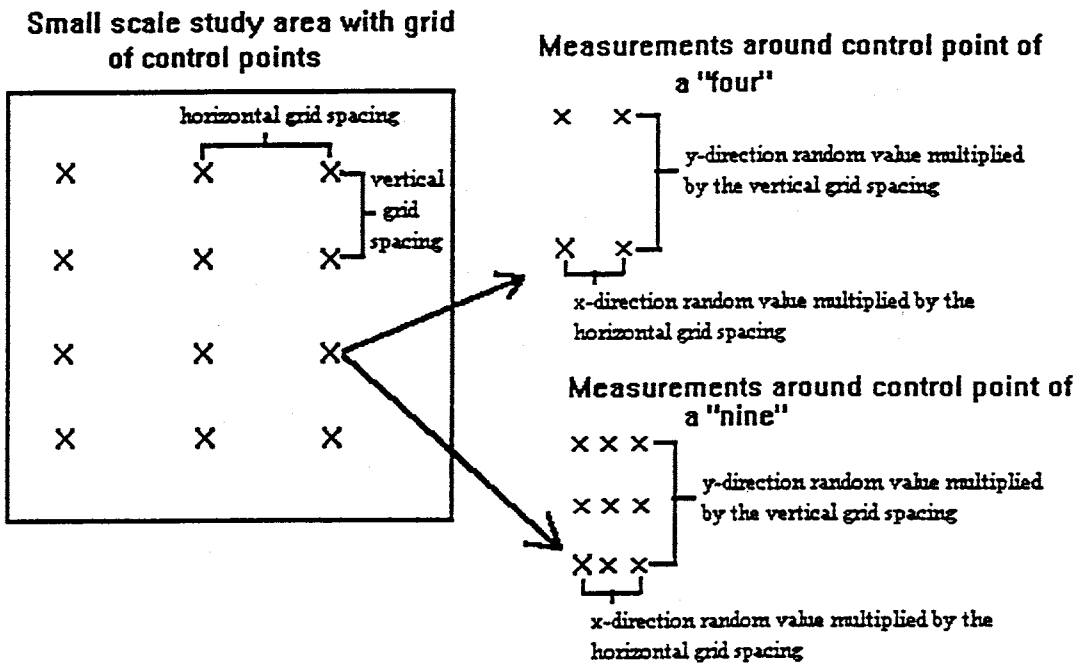

Figure 1. Illustration of orthogonal grid of control points and sampling locations around control points.

estimation within particular subsets of the transect. This sampling design was implemented in order to better characterize the variability associated with particular components of the bounding surfaces sedimentary model (discussed below). Study SS6, part of the Ps element at the Bosque site, was sampled at various spacings along several horizontal transects.

3.3 Permeability Mapping

3.3.1 The air mini-permeameter

Measurements of permeability were obtained with a lightweight syringe air mini-permeameter developed by Davis et al. (1994). Due to its portability and the use of small air pressures, the permeameter is well-suited to obtaining in-situ measurements of dry material along a geologic outcrop. This allows the measurement of weakly lithified, permeable materials, such as fine grained sands and soils.

The permeameter operates by injecting air into an outcrop through a rubber tip seal held against the outcrop surface. A ground glass syringe is used as a mechanical pressure source; as the piston falls through the syringe casing, a constant pressure is applied to the outcrop. The flow rate is calculated by timing the rate at which the piston falls. The permeability is calculated from Darcy's law and the applied pressure, measured flow rate, and geometry of the tip seal. The bulk sampling volume of the air-permeameter is approximately 1 cubic centimeter. Interested readers are referred to Davis et al.

(1994) for a detailed description of the methodology of the air-permeameter calibration.

3.3.2 Measuring procedure

Free-fall time, or the time recorded when the syringe is allowed to fall with the tip seal open to the air, was measured regularly throughout the studies to ensure against air-permeameter malfunction. The range of the permeameter is suited for the measurement of weakly lithified sands and soils. There are features within each study area which have associated permeabilities beyond the range of the permeameter, such as clay balls and clay drapes, calcite nodules, lenses of loose material, fractures, and holes. Sampling points which fell on these areas were recorded as a "non-measurement".

Each study site was prepared by digging away the colluvial cover to reach a vertical face of undisturbed deposit. The outcrop was then allowed to dry for a few days before sampling took place to ensure that soil moisture would not affect measured permeabilities.

3.4 Mapping of sedimentary features

Heterogeneity observed within each study site was mapped according to the hierarchical system of bounding surfaces in fluvial deposits developed by Allen (1983) and furthered by Miall (1990). We used this model to identify regions within each small-scale study area. Each region is relatively homogeneous in

small scale sedimentary features. The quantitative permeability data sets were then evaluated within and between these regions. The bounding surfaces model is preferred over other ad hoc definitions of hydrofacies because it is both well established in the literature and can be generalized to other depositional environments. If we find that assemblages of these regions exhibit a certain permeability pattern, then the spatial variability of permeability can be related to the spatial characteristics of the bounding surfaces model.

The bounding surfaces model identifies internal divisions in sandstone bodies which separate packets of genetically related strata. At the scale of interest in the studies presented here, zeroth, first and second order contacts are of interest.

Zeroth order boundaries are non-erosional, concordant bedding contacts which might arise from deposition of a stratum parallel to the unit beneath it. First order contacts are usually erosional and bound individual cross-bedding sets. First order boundaries separate similar lithofacies, and are interpreted as the result of bedform migration under steady flow conditions. Second order contacts separate cosets of differing lithofacies and are usually erosional. These second order boundaries signify a change in flow conditions.

CHAPTER 4: STATISTICAL ANALYSIS

The purpose of the statistical analyses used here is to characterize the spatial distribution of permeability with a random field model. We would like to identify the component of the measured permeability distribution due to random noise and the component due to spatial correlation.

Data sets which are spatially correlated pose certain statistical difficulties. Particularly, assumptions regarding independence of measurements may be violated. Other workers suggest methods to assure independence of measurements where spatial correlation is expected, including randomly selecting a subset of data (Woodbury and Sudicky, 1991) and selecting a subset of data based on a minimum separation distance greater than the correlation length (Sudicky, 1986; Hess, et al.,1992). Use of these methods would severely restrict sample sizes of the small scale studies presented here, which tend to exhibit a correlation length up to half the distance included in each study area. Several alternative methods of analysis have been employed in order to overcome these difficulties, including the use of graphical techniques and non-parametric tests.

4.1 Distribution Characterization and Comparisons

4.1.1 Lognormality of hydraulic conductivity

In groundwater studies, hydraulic conductivity values are commonly assumed to follow a lognormal distribution (Freeze and Cherry, 1979). In this study, the natural log transform is used:

$$Y=\ln(k)$$

where k is permeability in darcies.

The non-parametric Kolomogorov-Smirnov test is used to compare the transformed empirical data to the theoretical normal distribution (Till, 1974). This test relies on comparisons of the expected and the observed relative frequencies to detect differences in location, skewness or dispersion of a distribution. "D_{max}", which is the maximum difference between the expected (normal) and the observed frequency distribution, is compared to "D_{crit}". For a two-tailed test at the 5 per cent significance level (i.e. α = .05), an asymptotic value of D_{crit} for large sample sizes is given by:

$$D_{crit} = 1.36\,[\frac{n_1+n_2}{n_1 n_2}]^{1/2}$$

where n_1 and n_2 are the number of locations on the distributions which are compared (n_1=n_2 where n_1 is the sample size of the empirical distribution). If D_{max} is less than D_{crit}, the null hypothesis that the empirical distribution is normal cannot be rejected. Although this test assumes independent observations and this data is presumably correlated and not independent, the results of the Kolomogorov-Smirnov test give a reasonable guideline for judging equality of distributions.

4.1.2 Identification of populations

We would like to determine if regions within each study site

have similar permeability distributions, and if study sites located within the same architectural element have similar permeability distributions. Probability plots and box plots are used to visually evaluate and compare empirical distributions. Box plots show the 25th and 75th percentiles as end lines on a box. The mid line of the box represents the 50th percentile, and capped bars indicate the 10th and 90th percentile points. The 5th and 95th percentiles are marked with circles. The Kolomogorov-Smirnov test is used to formalize the comparison of distributions, testing the hypothesis that two empirical data sets have similar distributions in terms of their location, skewness and dispersion. In this case, D_{max} is equal to the greatest difference between the two empirical distributions and D_{crit} is calculated as given above, where n_1 and n_2 are the sample sizes of the two empirical distributions.

4.2 Correlation Structure

4.2.1 Variogram calculation

Experimental variograms were calculated in the horizontal and vertical directions for each of the small scale study sites. We expect these directions to be the principal directions of anisotropy, as they are generally perpendicular and parallel to stratigraphy in the study areas. Where structure was observed to run counter to this, other likely directions were explored in the variogram calculation.

Variogram calculation is affected by the presence of

geographically distinct populations (Armstrong, 1984). In our case, the appearance in the variogram of heterogeneous populations is of particular interest. Intuitively, our goal of identifying regions of differing mean permeabilities within each study area suggests that the assumption of stationarity in the random field model will not be met over each study area. We can justify the use of this model if we assume that each region is an area of local stationarity. These regions are stratigraphically determined, and are laterally extensive. Thus, horizontal variograms calculated with a small search window will reflect the variance found *within* these regions of equal mean permeability, as pairs of points with large vertical separations are not included in the calculations if the search window is small.

Vertical variograms *will* reflect the pairing of points from differing sub-populations, as the vertical search window samples from the stacked assemblages of these locally stationary, laterally continuous regions. A repetition of facies or discrete lenses of differing permeabilities will often result in a "hole" effect in the variogram (Isaaks and Sristava, 1989). This hole, which is a drop in variogram value as lag size increases, may occur at roughly the spacing between adjacent layers. Variograms presented here were calculated with as small a search window as possible while maintaining a sufficient number of pairs. Each lag class contains a minimum of forty pairs, although most have significantly more pairs than this. The results of each variogram calculation, including the number of pairs and average

distance associated with each lag class, is presented in Appendix B.

Mathematical models were fit to experimental variograms; however it was found that the sampling design did not provide sufficient information to estimate the variogram at very short separation distances. To correct this, a second round of sampling was carried out about a year after the initial field work took place. The outcrop surfaces had undergone a winter's weathering between these sampling episodes, and there was not identical moisture content at the time of each sampling. Due to the significant time lapse and resulting alteration of the outcrops, the two data sets from each site were not combined. The measurements of permeability obtained in the second round of sampling were used only to calculate values of the variogram at lags of 0, 2 and 4 centimeters. These points are represented with hollow triangles on the variograms; the original variogram estimates are marked by filled triangles.

4.2.2 Trend analysis

In addition to the case of geographically distinct sub-populations, the assumption of stationarity may be violated by a gradual change in permeability values over a large region. One goal of this study is to identify trends in permeability attributable to deterministic causes, such as small scale sedimentary features. Examples of this include an overall fining-upwards sequence in a sand deposit, or an irregular

precipitation of calcium carbonate throughout a soil unit.

If a significant linear trend is present in the data set, the variogram will have a quadratic shape (Gutjahr, 1991). A nonlinear trend can be much harder to detect or identify from the variogram estimation (Starks and Fang, 1982; Rehfeldt et al., 1992). All sample sets which displayed evidence of drift in the data values were analyzed for a trend by fitting a planar drift model of the form:

$$k = ax+by+c$$

where k is permeability in darcies, x and y are location coordinates on the sampling grid in centimeters, and a, b and c are coefficients found by multiple linear regression.

In the case of the ES1 study, where data was collected along a transect, a linear model was fit to assess drift:

$$k = ax+b$$

The fitted model was subtracted from the data and residuals used to calculate the variogram. In all of the cases where a trend was suspected, no significant differences were seen between the variograms with and without the trend surface removed from the data. Therefore, no variograms with trends removed from the data have been presented here.

4.2.3 Extreme values

Another issue in the calculation of experimental variograms is the treatment of extreme values. Some sampling locations

which fell on materials with extreme values of permeability, such as clay or gravel, could not be measured with the permeameter. These unsuccessful attempted measurements were not included in the variogram data sets. Removing outliers is a standard technique for attaining reasonable estimates of the variogram (Armstrong, 1984), and this was the approach taken here. The lack of spatial continuity of the features with extreme permeability values serves as a physical justification for the elimination of these extreme values. For example, a scattering of clay balls with an average diameter of five centimeters might not significantly alter the effective permeability of a sand layer two meters wide, but their inclusion in the estimation of the variogram will completely mask the correlation structure of the sand layer.

4.2.4 Nugget effect

The value of the variogram at a lag distance of zero is zero, however experimental measurement error and/or short scale variability may lead to differing sample values at extremely short lags (Isaaks and Srivastava, 1989). This results in a discontinuity near the origin of the variogram which is called the nugget effect. The second round of sampling at the Bosque sites was designed to evaluate the nugget effect by testing the repeatability of measurements in the field. Causes of variation in repeated measurements made with the mini-permeameter are due to inaccuracies in placing the permeameter tip seal at exactly

the same location, alteration of the outcrop surface by air flow through the tip seal, and operator errors in holding the instrument level and maintaining a constant pressure in applying the tip seal to the outcrop surface. Small random variation in the rate of piston fall and timing circuits may also contribute to measurement error.

Variogram nugget values were calculated from at least 315 pairs of measurements at each Bosque site. All of these values were less than 0.04 and were within the range (0.01 to 0.05) of the variance of repeated measurements made on fabricated samples under laboratory conditions by Davis et al.(1994).

CHAPTER 5: RESULTS AND DISCUSSION

5.1 Channel Sands and Floodplain Soils at the Bosque Site

5.1.1 CH=2 Element

SS1, SS2 and SS5 are located within a single channel scour in the CH-2 element (Figure 2). SS1 and SS2 are oriented parallel to the inferred paleoflow direction, while SS5 is perpendicular to the inferred paleoflow direction.

SS1 is approximately 2.1 meters wide and 1.6 meters high (Figure 3). Three second order bounding surfaces separate the outcrop into four regions. The lowest 0.7 meters in the area is designated as Region 1. It consists of even and wavy parallel, thickly laminated upper-fine and lower-medium sands. There is soft-sediment deformation near a large (0.1 meter in diameter) clay ball in the lower right-hand corner of the unit. Region 2 is a 0.2 meter layer of coarse sand which contains scattered pebbles, discontinuous clay drapes, and small (from 2 to 5 centimeters in diameter) clay balls. This is overlain by Region 3, which is 0.7 meters thick, with even, parallel, horizontal laminae. Within this region, grain size fines upward from a coarse sand, which is cleaner than that found in the unit below, to a fine sand at the top. There are climbing ripples present at the top of Region 3. Region 4 is approximately 0.15 meters high and consists of even, parallel laminae dipping east.

SS2 is about 10 meters above and to the east of SS1, and is approximately 1.5 meters high and 1.5 meters wide. It is similar to SS1 in the predominance of medium and fine sands. SS2

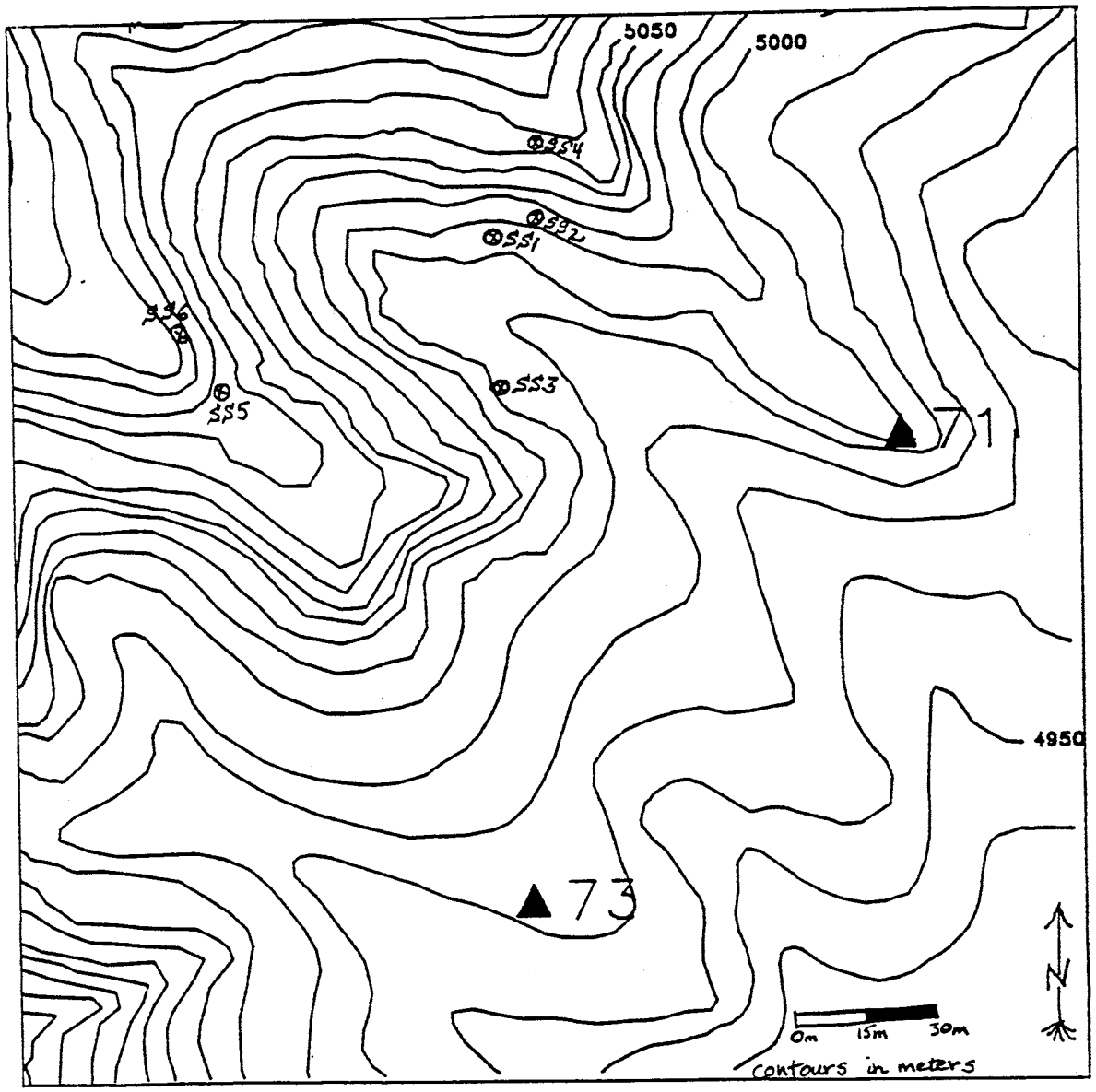

Figure 2. Relative locations of six Bosque study sites. Locations marked as 71 and 73 identify survey points from earlier work at the site (Davis, 1993).

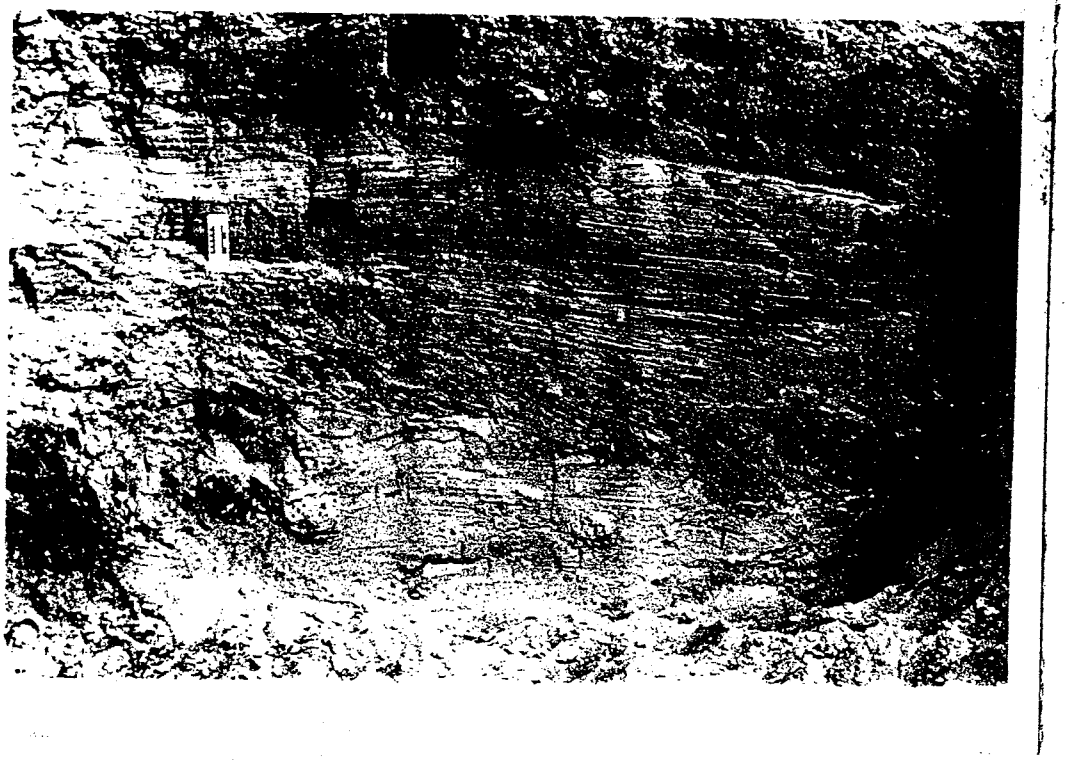

ɟure 3. Photograph of SS1. Bounding surfaces identified by
ɜhed line, regions identified by number. Scale card is 15
ıtimeters long.

is generally more homogeneous than SS1 in both lithology and small scale structures, with low-angle to planar cross-bedding throughout the outcrop (Figure 4).

Three second order bounding surfaces were identified within SS2, dividing the outcrop into four regions. The lowest 0.5 meter makes up Region 1, which consists of low angle, cross-laminated sand. The laminae are 2 to 4 millimeters thick, alternating between bands of lower-coarse and lower-fine sands. Region 2 is about 0.4 meters high and is similar to Region 1 but volumetrically contains more fine sand. This is overlain by Region 3, a 0.3-meter-thick area of coarse sand interbedded with thinly laminated fine sand. The uppermost unit, Region 4, is a coarse sand scour fill about 0.2 meters thick topped by about 0.15 meters of bedded coarse and medium sand.

SS5 is located approximately 65 meters to the south of SS1 and is about 20 meters higher up on the escarpment. The prepared outcrop is 1.2 meters high and 3.4 meters wide, slightly wider than SS1 and SS2 study areas. The outcrop is relatively homogeneous and consists predominantly of medium and fine grained sands with low-angle to planar cross-bedding (Figure 5). SS5 differs from SS1 and SS2 in that there are many lateral truncations in bedding and discontinuous clay drapes. There are no distinct changes in grain size or lithology across the truncations. Many discontinuous zeroth and first order bounding surfaces are present in the outcrop, however no second order surfaces were identified.

igure 4. Photograph of SS2. Bounding surfaces identified by ashed line, regions identified by number. Scale card is 15 entimeters long.

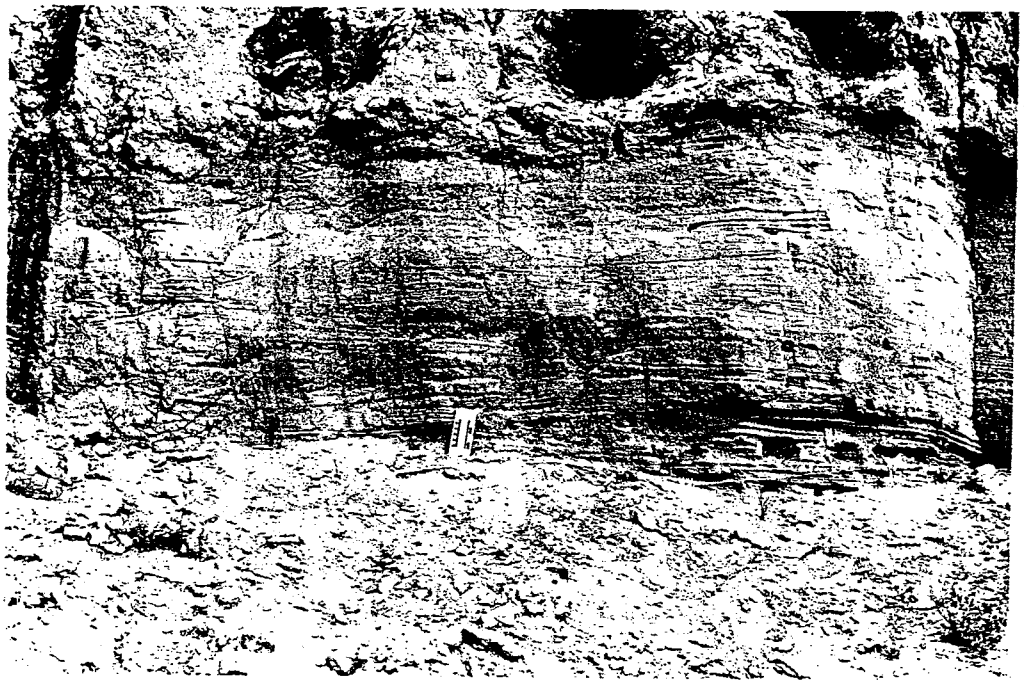

igure 5. Photograph of SS5. Bounding surfaces identified by ashed line, regions identified by number. Scale card is 15 entimeters long.

The primary depositional processes influencing the spatial distribution of permeability in these channel sand deposits are variations in flow velocity, volume and direction. These variations are responsible for the discrete boundaries seen in the outcrops as changes in flow conditions alter both bedforms and the mean grain size of material deposited. While one scale of variability may characterize a certain region, stacking of these regions superimposes a larger scale of variability. Journel and Huijbregts (1978) suggest that nested structures can be represented as the sum of several variograms, where each variogram characterizes the variability at a particular scale:

$$\gamma(h) = \gamma_0(h) + \gamma_1(h) + \ldots \gamma_i(h)$$

We hypothesize here that the correlation structure within the CH-2 element can be represented as a nested model.

Air-permeability was measured at 142 of the 151 sample locations generated on SS1 (see Appendix D). All non-measurements were due to the presence of clay balls. One hundred twenty-eight measurements were made on SS2 from 130 sample locations. One non-measurement was due to a calcite nodule, the other to a hole in the outcrop. SS5 yielded 192 air-permeameter measurements from 198 sample locations. Non-measurements were due to the presence of insect holes in the outcrop.

Statistics of the natural logarithm transforms of the three data sets are presented in Table 1. Probability plots and box plots of the data sets are shown in Figure 6. The Kolomogorov-Smirnov test of distributions does not clearly indicate that the

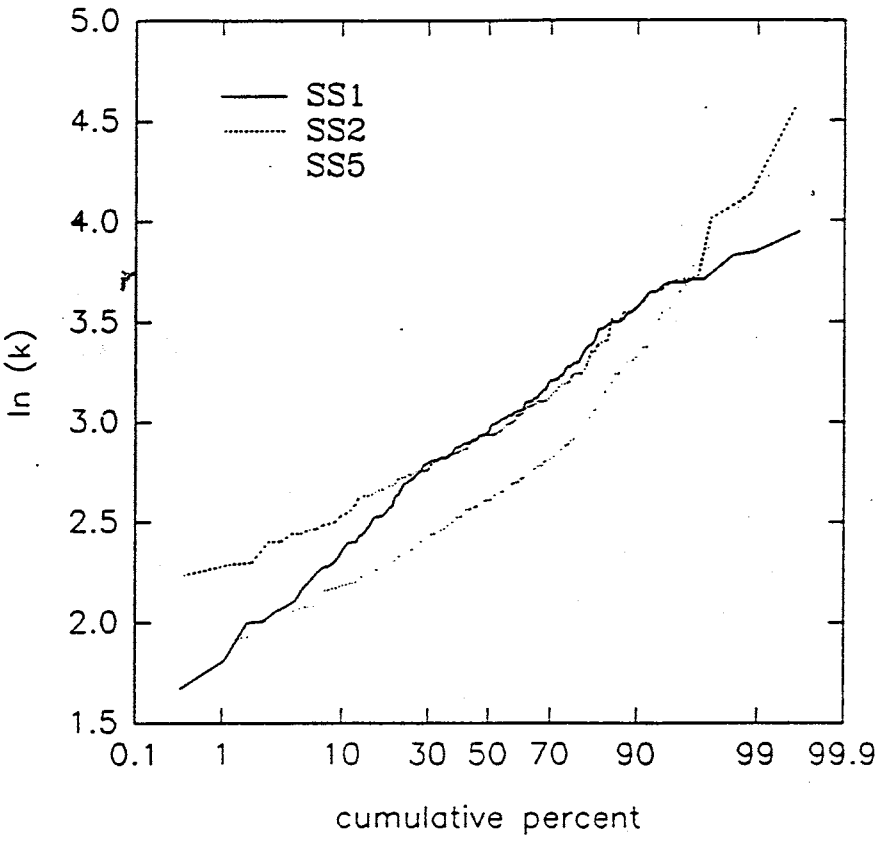

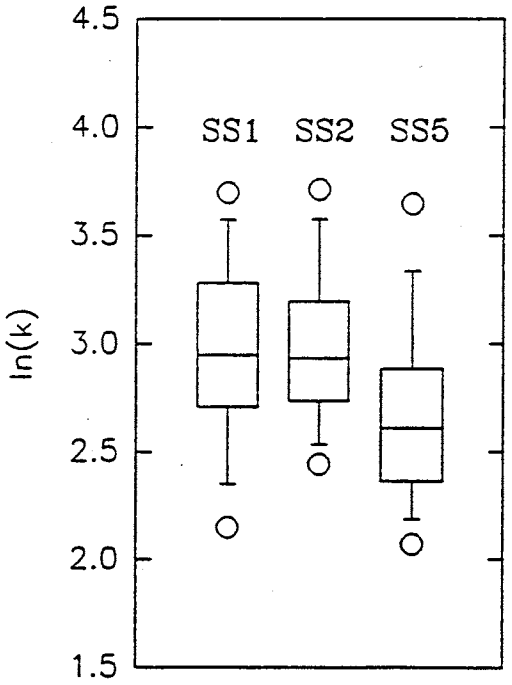

Figure 6. Probability plots and box plots of CH-2 element studies.

natural logarithm transform of the SS1 data set is normally distributed (α = .05, D_{max} = 0.07, D_{crit}= 0.07). The null hypothesis that the distributions are normal is rejected in the case of SS2 (α = .05, D_{max} = .19, D_{crit}= .08) and SS5 (α = :05, D_{max} = 0.10, D_{crit}= 0.06). The test of distributions also shows that SS1 and SS2 have the same distribution (α = .05, D_{max} = 0.05, D_{crit}= 0.17), but SS1 and SS5 (α = .05, D_{max} = 0.36, D_{crit}= 0.15), and SS2 and SS5 (α = .05, D_{max} = 0.38, D_{crit}= 0.16) do not have equal distributions.

Table 1. Statistics of CH-2 element studies.

	SS1	SS2	SS5
N	142	128	192
mean	2.96	3.00	2.69
variance	0.21	0.16	0.23

Experimental variograms are shown in Figure 7. The first three estimates on each variogram, indicated by hollow triangles, were obtained from the second set of measurements made at each site. This included 132 additional measurements from SS1 and SS2 and 126 at SS5. The treatment of these additional measurements in the variogram calculation is discussed in Section 4.2.1. Exponential models were fitted to those from SS1 and SS2:

$$\gamma_{h,SS1}(\xi) = .024 + .165[1-exp(-\frac{|\xi|}{16})]$$

$$\gamma_{v,SS1}(\xi) = .024 + .180[1-exp(-\frac{|\xi|}{8})]$$

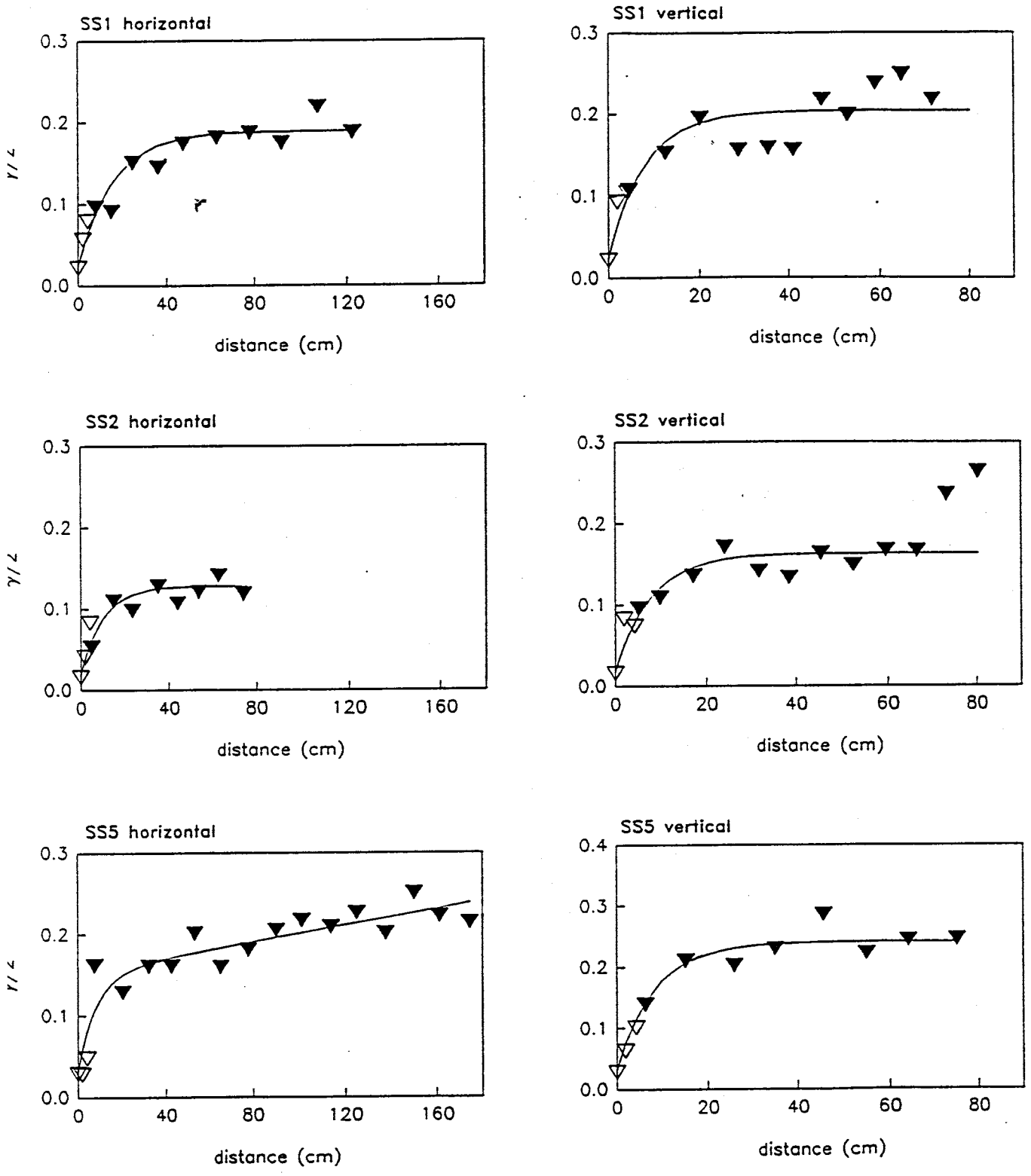

Figure 7. Directional variograms of CH-2 element studies. Hollow triangles indicate variogram estimates made from second sampling of area.

$$\gamma_{h,SS2}(\xi) = .018 + .110\left[1 - \exp\left(-\frac{|\xi|}{10}\right)\right]$$

$$\gamma_{v,SS2}(\xi) = .018 + .145\left[1 - \exp\left(-\frac{|\xi|}{8}\right)\right]$$

The exponential model yielded a good fit to the experimental variograms. Burroughs (1983) showed that if processes affecting a given area act over closely related scales, the resulting variogram will consist of a set of straight lines which approximate a curve. Changes in the flow regime are evidenced in the outcrop by bounding surfaces, as discussed in Section 5.2. These bounding surfaces have a hierarchical structure, but the hierarchy does not have consistent spatial dimensions associated with it; the processes which result in the various types of bounding surfaces act at closely related scales. The good fit of the exponential model to these experimental variograms supports this claim, as the variation in permeability within the study sites is the result of a changes in flow conditions within the confines of the channel depositional regime. Both horizontal variograms exhibit a significantly greater range than those in the vertical direction. We expect to see this directional anisotropy as the stratigraphy is relatively continuous in the horizontal direction while variations in bedforms and grain size are apparent in the vertical direction.

The SS5 vertical variogram was also fit with an exponential model with a relatively short range:

$$\gamma_{v,SS5}(\xi) = .031 + .210\left[1 - \exp\left(-\frac{|\xi|}{8.33}\right)\right]$$

A nested exponential and linear model was fit to the SS5 horizontal variogram:

$$\gamma_{h,SS5}(\xi) = .031 + .120\left[1 - \exp\left(-\frac{|\xi|}{8.33}\right)\right] + \frac{.1}{200}(|\xi|)$$

A simple exponential model was fit to the SS5 horizontal variogram, but the nested exponential and linear model was judged to provide a significantly better fit to the variogram. This might be explained by directional anisotropy, as SS5 is oriented perpendicular to the paleoflow direction and SS1 and SS2 are oriented parallel to the paleoflow direction. SS5 also displays significantly more lateral discontinuity in small scale geologic features than do the SS1 and SS2 study areas. However, as SS5 has a greater horizontal sampling domain than SS1 and SS2, the applicability of the nested model might also be due to larger scale heterogeneity captured by a larger sampling area.

5.1.2 Ps Element

SS4 and SS6 are located approximately 80 meters apart, across the same arroyo which separates SS5 from SS1 and SS2 (Figure 2). The SS4 and SS6 study areas are in a single sandy, orange-red paleosol element that lacks sedimentary structures in both locations. Grain size is very fine throughout both study

areas. SS4 is 1.5 meters high and 2.4 meters wide. Thirty-one calcite nodules averaging 4.4 cm in diameter are scattered in the central portion of the outcrop (Figure 8). SS6 is about 0.7 meters high and 1.1 meters wide. Calcite deposits are much more ubiquitous in SS6 than in SS4 (Figure 9). One hundred twenty-seven nodules were counted in the SS6 study area. These had an average diameter of 0.7 cm. The calcite nodules cover about 3% of the SS4 and 2% of the SS6 study areas. Data from the survey of calcite nodules is presented in Appendix C.

Whereas depositional processes control the heterogeneity in the CH-2 sands, here the geologic control on the heterogeneity is pedogenic. The primary pedogenic processes influencing the spatial distribution of permeability are the translocation of clay material and the precipitation of calcium carbonate. The heterogeneity in permeability resulting from the calcite deposits is distinctly different than that observed in the CH-2 sand deposits. While variation in grain size and bedding is apparent in the sands, the soils appear homogeneous and structureless except for the discrete change from soil to calcite nodule.

Two hundred sixteen sample locations were identified in SS4, of which 213 air-permeameter measurements were obtained. Two of the non-measurements were due to the presence of calcite nodules, the third fell on a fracture in the outcrop. The fracture is believed to be a result of surface exposure. One hundred three air-permeameter measurements were obtained in SS6 from 104 sampling locations. The non-measurement was due to calcite.

.gure 8. Photograph of SS4. Shovel is approximately one meter
›ng.

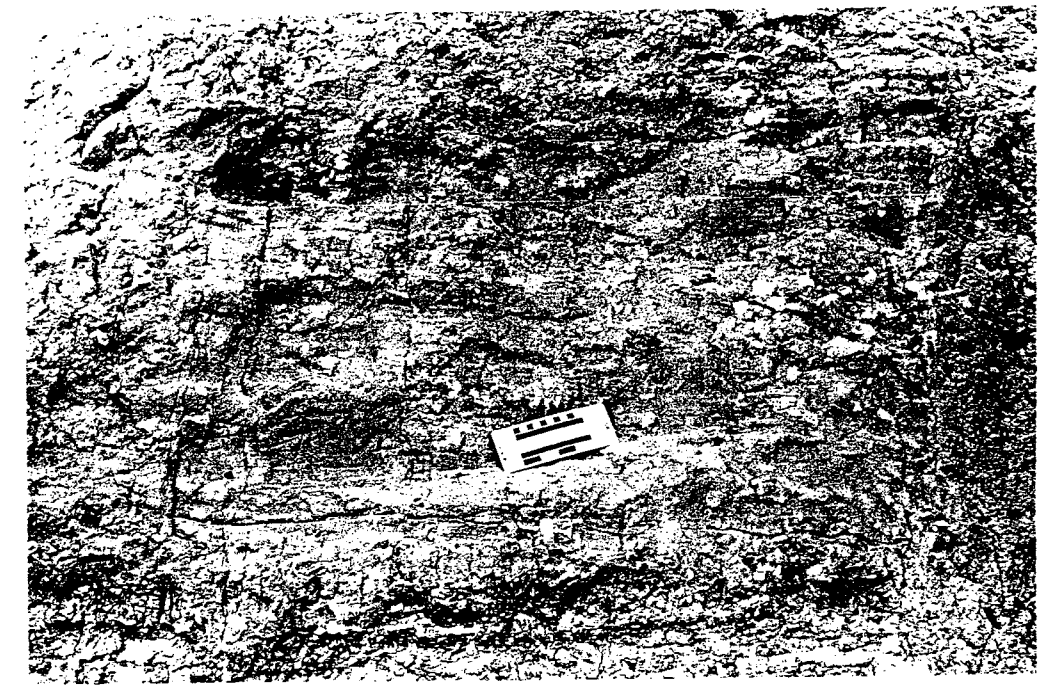

Figure 9. Photograph of SS6. Scale card is 15 centimeters long.

Statistics of the transformed data appear in Table 2. Probability plots and box plots of the data sets are shown in Figure 10. The Kolomogorov-Smirnov test indicates that SS6 is normally distributed (α = 0.05, D_{crit}=0.09, D_{max}=0.06), although the null hypothesis of a normal distribution is rejected in the case of SS4 (α = 0.05, D_{crit}=0.06, D_{max}=0.07). The test result is not definitive in comparing the distributions found at SS4 and SS6, as the D_{crit} value is equal to the D_{max} value (α = 0.05, D_{crit}=0.16, D_{max}=0.16).

Table 2. Statistics of Ps studies.

	SS4	SS6
N	216	134
mean	1.94	1.91
variance	0.12	0.25

Measurements made directly on the calcite nodules were not successful due to the very low permeability of the calcite. The lower end of the air permeameter range is about 0.5 darcy (Davis et al., 1994), so the permeability of the calcite is assumed to be lower than this value. There is a gradational transition from calcite to soil moving out from the center of each nodule. An additional 70 measurements were made at both SS4 and SS6 in order to assess the average dimensions of the region of reduced permeability around the center of the calcite nodules. These measurements were not included in the statistics of the Ps studies shown in Table 2 or in the variogram estimates, as they were not randomly sampled. The data from this survey is presented in Appendix C. Figure 11 shows box plots of measurements taken at distances of 2,4 and 6 cm from the center

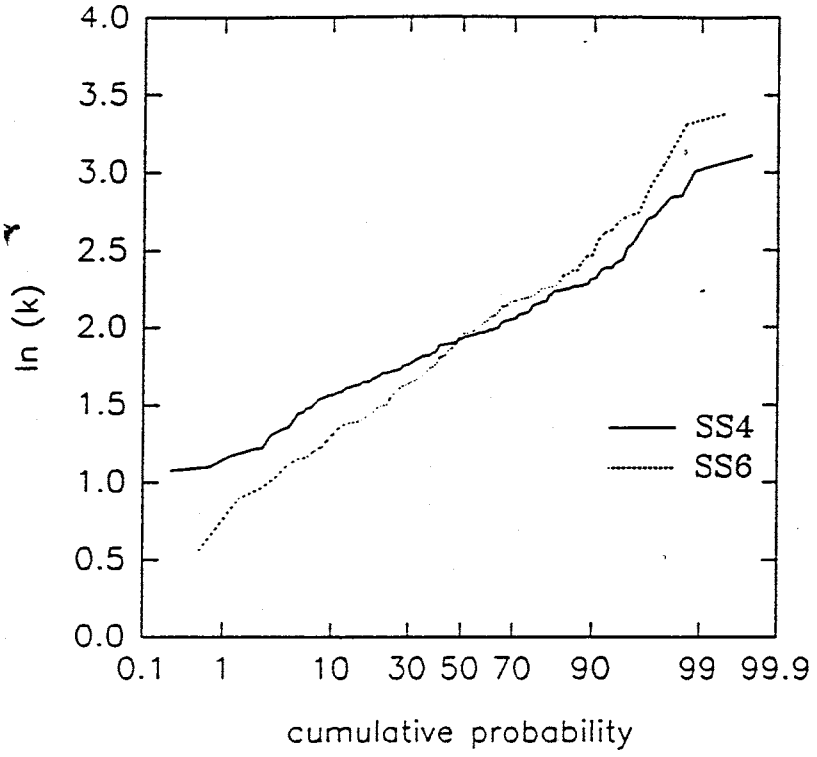

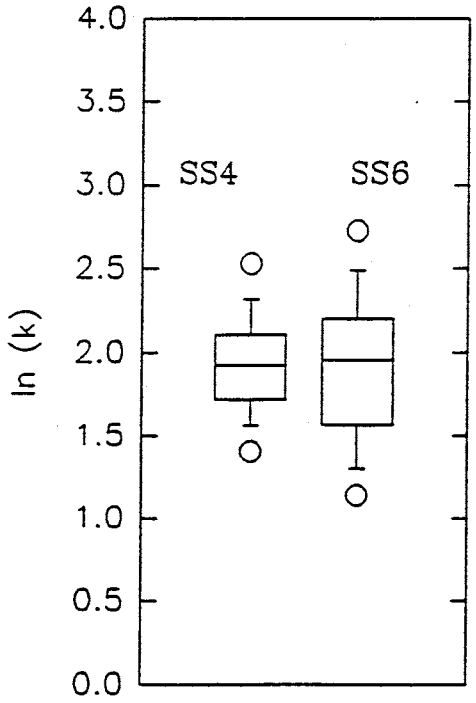

Figure 10. Probability plots and box plots of Ps element studies.

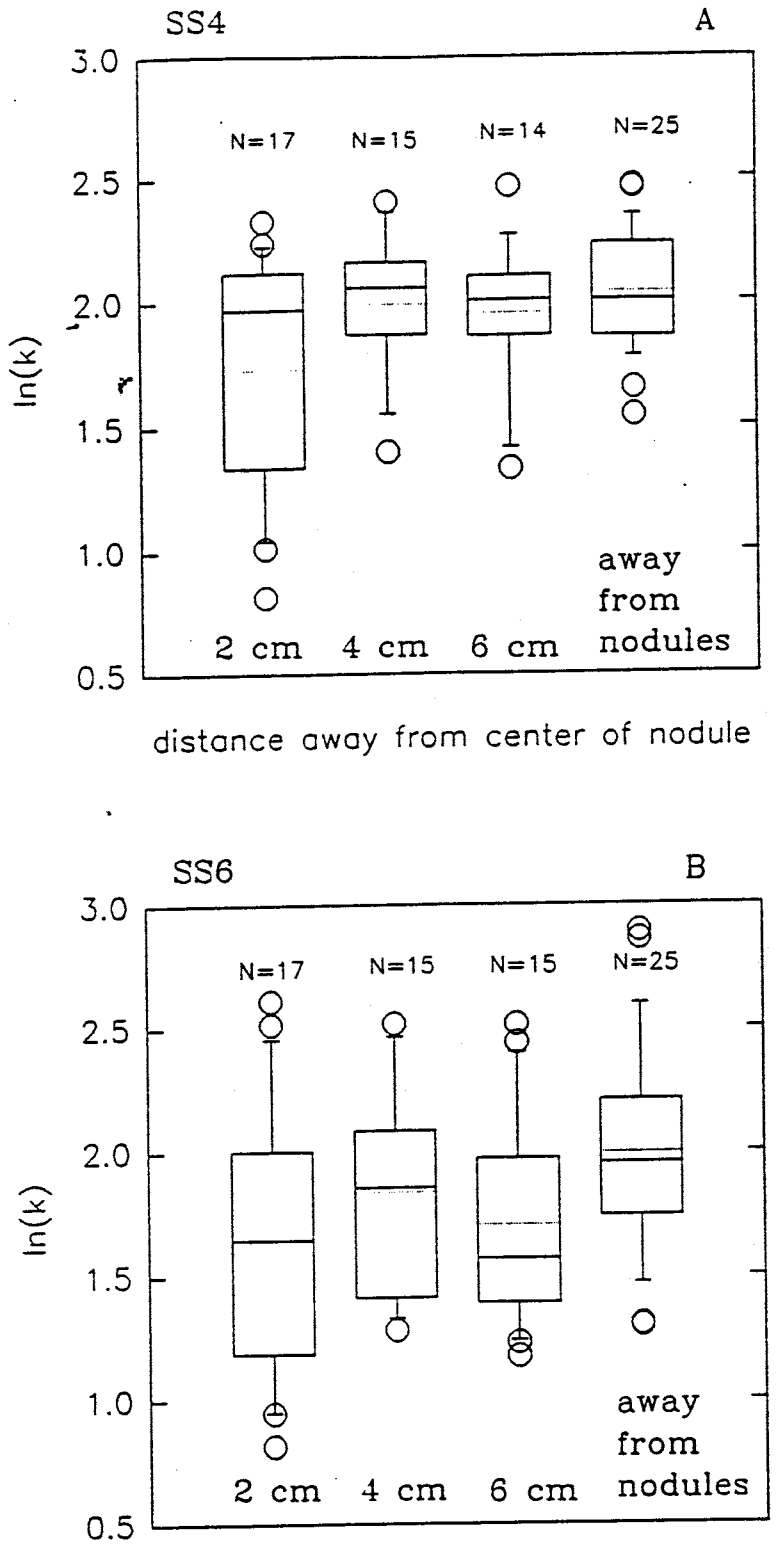

Figure 11. Box plots of SS4 and SS6 permeability measurements at 2cm, 4cm, 6cm and far away from calcite nodules. Dotted lines show the sample average, solid lines mark the 25th, 50th and 75th percentiles. Data outside the 10th and 90th percentiles are marked by circles.

of each of four nodules at SS4 and SS6. Some of these measurements fell on points which were very white with calcium, depending on the diameter of the particular nodule sampled. Permeability measurements were also taken at 25 locations judged to be as far away as possible from any calcite (labeled as "away from nodules" in Figure 11).

The SS4 box plot (Figure 11a), shows a smaller mean permeability at 2 cm distance, which reflects the presence of large nodules in that study area. The SS6 box plot (Figure 11b) shows a general increase in average permeability with distance, however there is a smaller region of lower permeability around each nodule than in SS4. This reflects the small size of the nodules in SS6.

Experimental variograms are shown in Figure 12. The estimates marked by hollow triangles were obtained from the second set of measurements, which included 126 additional measurements at each location. Both the horizontal and vertical SS4 variograms were fit with a gaussian model of the form:

$$\gamma_{SS4}(\xi) = .027 + .07(1-\exp(-|\xi|^2/10^2))$$

The SS6 horizontal variogram was fit with a gaussian model of the form:

$$\gamma_{SS6,h}(\xi) = .031+.20(1-\exp(-|\xi|^2/6^2))$$

The SS6 vertical variogram was fit with a slightly shorter range:

$$\gamma_{SS6,v}(\xi) = .031+.20(1-\exp(-|\xi|^2/2^2))$$

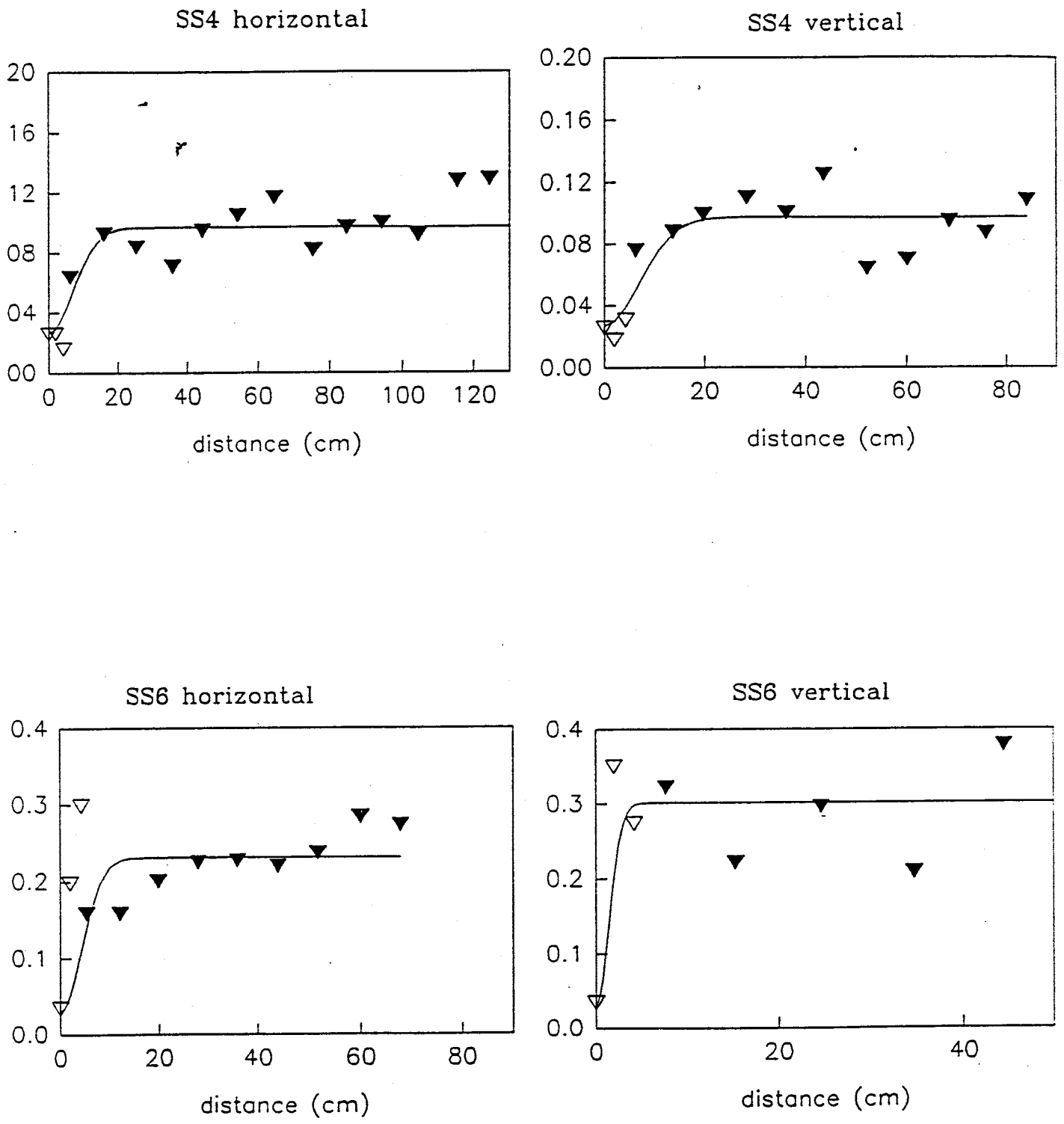

Figure 12. Directional variograms of Ps element studies.

The gaussian models fit the experimental variograms well by rising to the sill value over a very short range. The deposition of calcite nodules in these soil deposits is reflected in the variogram. The SS6 variograms display an extremely short range of 2 and 6 centimeters. One expects to see a high variance between measurements taken at short distances because there are so many calcite nodules scattered throughout the soil. There is a high probability that of two measurements taken at a short distance, one will fall on the soil and one will fall on or very near calcite. In SS4, where there are large areas with no nodules present, variogram estimates at short lags remain clustered around the nugget value.

Both SS4 and SS6 variograms have relatively short ranges. The SS4 horizontal and vertical variograms are fit with the same model parameters, indicating statistical isotropy. The SS6 directional variograms have very similar ranges (2 and 6 centimeters), which furthers the claim that the Ps deposits may be isotropic. The lack of spatial correlation in these deposits may be a reflection of the lack of apparent sedimentary structures.

5.2 The Bounding Surfaces Model

One goal of this study was to look beyond the site-specific characteristics of the Bosque study area in order to relate observable sedimentary features in any location to a permeability distribution. The bounding surfaces model provides an

established path through which we can evaluate and further generalize our findings, as the spatial distribution of these bounding surfaces has been studied in various depositional environments. Particularly, we would like to know if we can measure variation in permeability across these bounding surfaces, and if the presence of these surfaces is reflected in the correlation structure of the permeability field.

The model identifies zeroth order boundaries as non-erosional, concordant bedding contacts which might arise from deposition of a stratum parallel to the unit beneath it. First order contacts are usually erosional and bound individual cross-bedding sets. First order boundaries separate similar lithofacies, and are interpreted as the result of bedform migration under steady flow conditions. Second order contacts separate cosets of differing lithofacies and are usually erosional. These second order boundaries signify a change in flow conditions. Because the second order surfaces separate areas deposited under different flow regimes, we expect that usually they separate areas of different mean permeability, but this will not be the case if differing lithofacies have similar mean permeability.

Results of the SS1 and SS2 studies are compared to findings from another location, the Escondida site, in light of the bounding surfaces model. An additional small-scale study, SS3, is also presented.

5.2.1 Escondida Study (ES-1)

The ES1 study area, Figure 13, is part of a high energy, channel-fill sand deposit. The outcrop is oriented perpendicular to the inferred paleoflow direction. The study involved a vertical transect 180 centimeters in length which crossed four second order surfaces, nine first order surfaces and two zeroth order surfaces, as shown in Figure 14. Five regions are defined by the second order surfaces. The uppermost 50 centimeters, Region 1, encompasses seven first order surfaces. The sand is of fine to medium grain size, with coarse lag deposits at the base of some of the first order boundaries. Region 2 is 42 centimeters in length and contains one zeroth order and one first order boundaries. Grain size within this region varies from coarse to pebbly sands. This is followed by Region 3, which is 56 centimeters long and contains one first order surface. Grain size is similar to that found in Region 2. The next 27 centimeters of the transect, Region 4, contains a single zeroth order contact. Grain size here ranges from fine to medium. Region 6 consists of the bottom five centimeters of the study area, where grain size ranges from medium to coarse sand.

Seventy-five permeability measurements were taken at a variety of intervals ranging from 1.5 to 6 centimeters. Statistics of the natural log transform of the ES1 data are shown in Table 3. The null hypothesis that the transformed data are normally distributed is rejected (α = 0.05, D_{crit}=0.10, D_{max}=0.12).

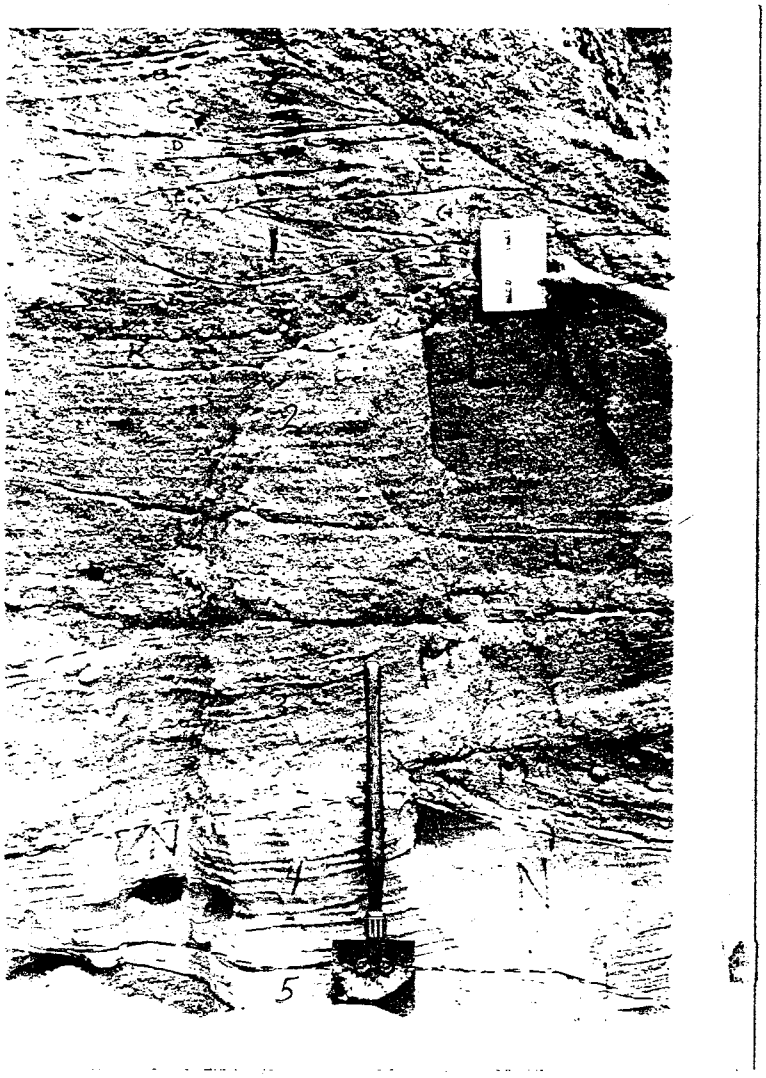

gure 13. Photograph of ES1 study area. Bounding surfaces entified by dashed line, regions identified by number. Notebook 19 centimeters long.

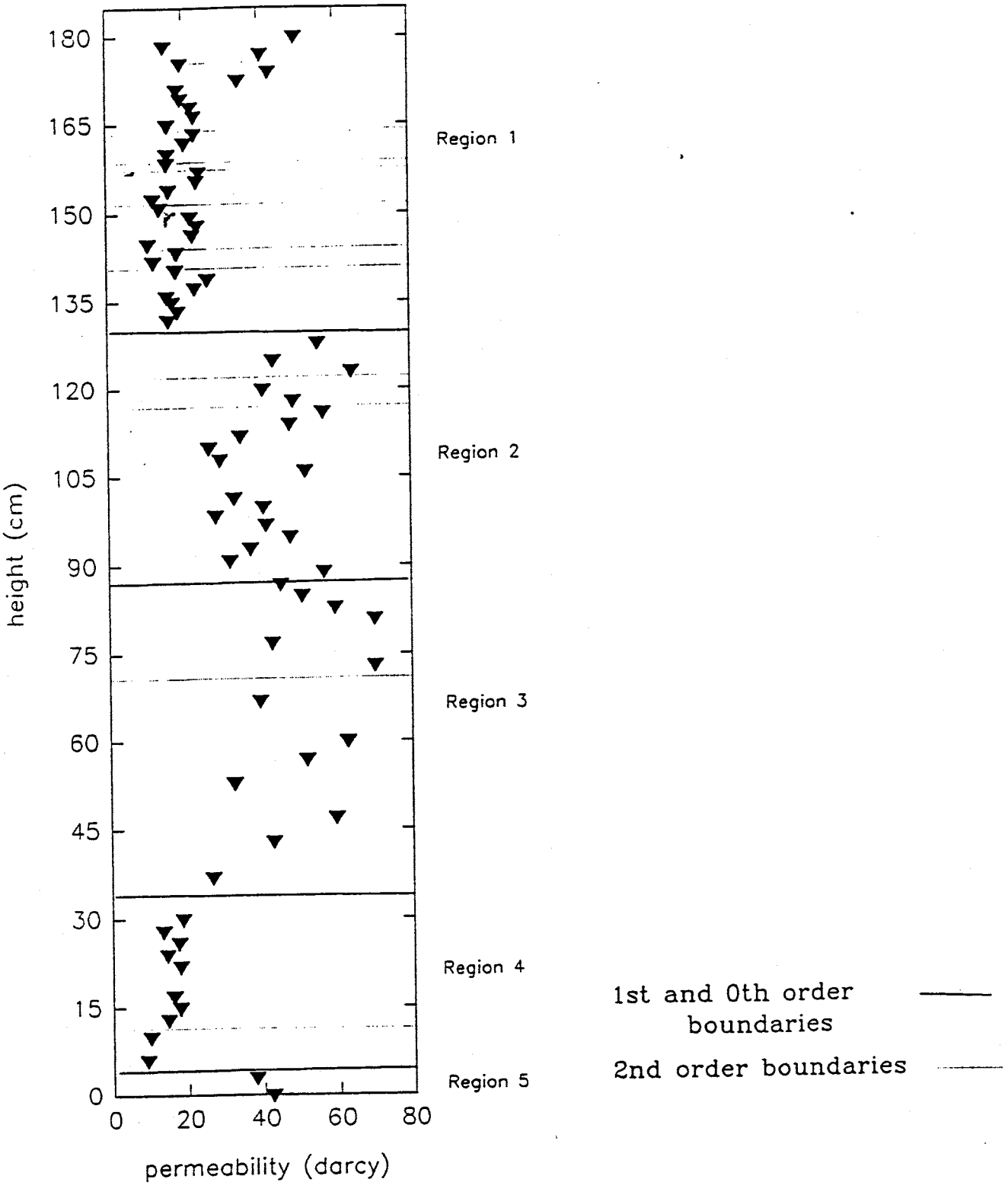

Figure 14. Diagram of ES1 transect. Permeability in darcies is graphed with the location along transect at which each measurement was obtained. Positions of 0th, 1st and 2nd order boundaries are also shown.

Table 3. Statistics of ES1 and ES1 Regions.

	ES1	Region 1	Region 2	Region 3	Region 4	Region 5
n	75	33	19	11	10	2
mean	3.28	3.01	3.73	3.82	2.67	3.69
variance	0.27	0.12	0.07	0.07	0.06	0.01

A box plot of the five ES1 regions is shown in Figure 15c. Results of the Kolomogorov-Smirnov test of distributions of these regions are given in Table 4. The null hypothesis of equal distributions cannot be rejected in the case of Regions 1 and 4 and Regions 2 and 3. Region 5 was too small to consider in this analysis.

Table 4. Comparisons of distributions within ES1.

regions	D_{crit}	D_{max}	result
1 and 2	0.39	0.84	not equal
1 and 3	0.44	0.85	not equal
1 and 4	0.49	0.45	equal
2 and 3	0.49	0.25	equal
2 and 4	0.53	1.00	not equal
3 and 4	0.57	1.00	not equal

Figure 14 is a diagram of bounding surface locations, and the magnitude and locations of permeability measurements along the ES1 transect. This reflects both the box plot of ES1 regions and the findings of the Kolomogorov-Smirnov test, showing the similar ranges of permeability in Regions 1 and 4 and Regions 2 and 3. The diagram also illustrates that second order boundaries generally separate areas of differing mean permeability, except in the case of the Regions 2 and 3. The first and zeroth order contacts show no obvious or conclusive relationship to the permeability distribution.

Variograms were calculated within individual regions of

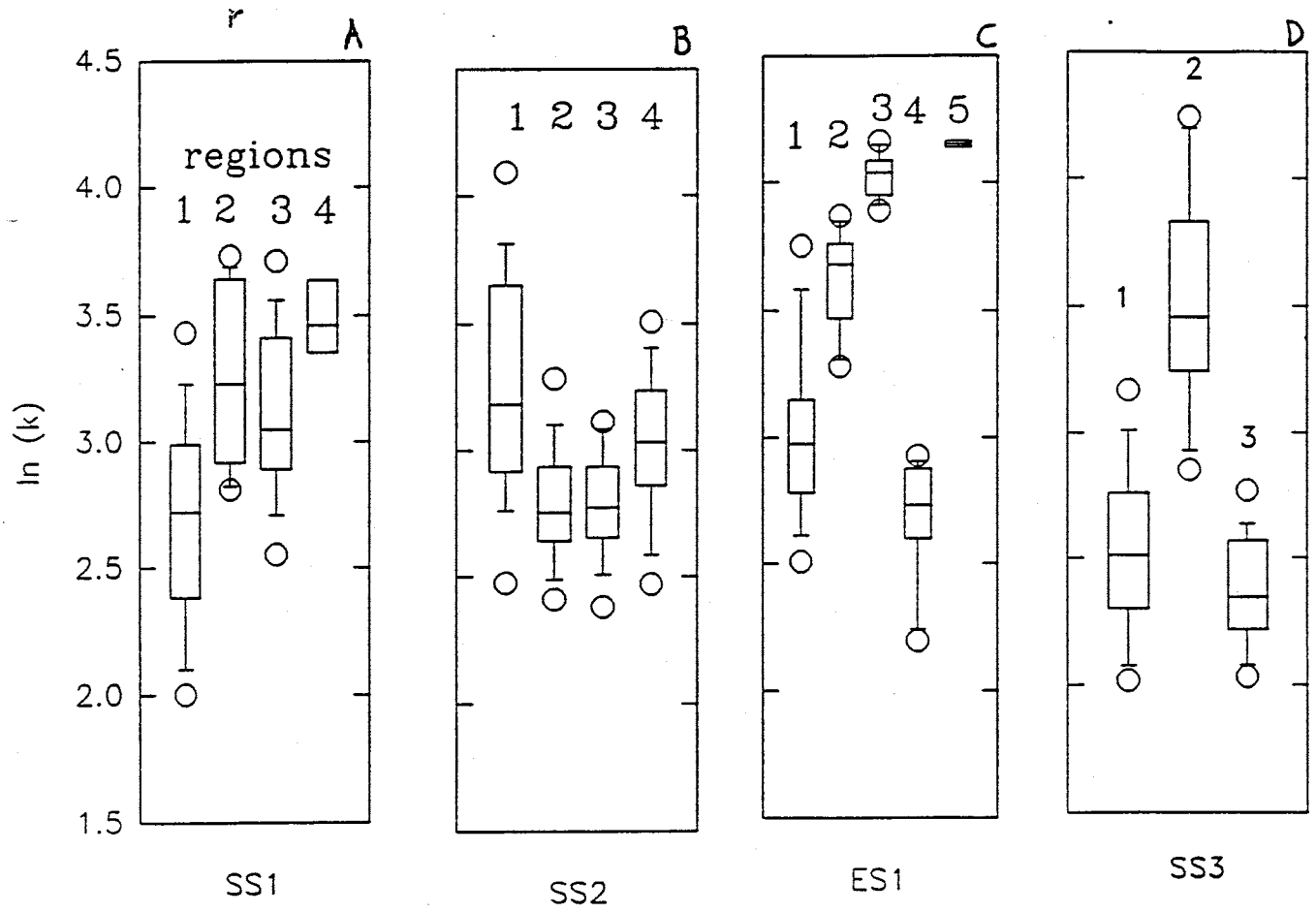

Figure 15. Box plots of distributions measured within regions of SS1, SS2, ES1, and SS3.

sufficient sample size. These showed weak correlation. The variogram of the entire ES1 data set is shown in Figure 16a. The dashed line indicates the distance at which the lag reaches half the dimension of the sample space, which is a standard "rule of thumb" for the distance included in variogram calculations (Isaaks and Srivastava, 1989). Points beyond this lag are presented in the variograms in Figure 16 in order to show holes in the variogram structures.

The ES1 variogram was fitted with a nested exponential and linear model of the form:

$$\gamma_{v,ES1}(\xi) = .04 + .30\left[1-\exp\left(-\frac{|\xi|}{33.3}\right)\right] + \frac{.36}{300}(|\xi|)$$

The model fits the ES1 data reasonably well until a hole is encountered at a lag of about 100 centimeters. This distance is close to the sum of Regions 2 and 3, 98 centimeters. The drop in the variogram value at this distance reflects the pairing of points in Regions 1 and 4. The greatest value the variogram reaches is about 0.45, which is much greater than the overall variance of the data set, 0.27.

5.2.2 Small Scale Study SS3

SS3 is located at the Bosque field site and is situated across a small arroyo from SS1 and SS2 (see Figure 2). This particular study was not presented in the context of the CH-2 studies because it is not typical of the deposits seen throughout

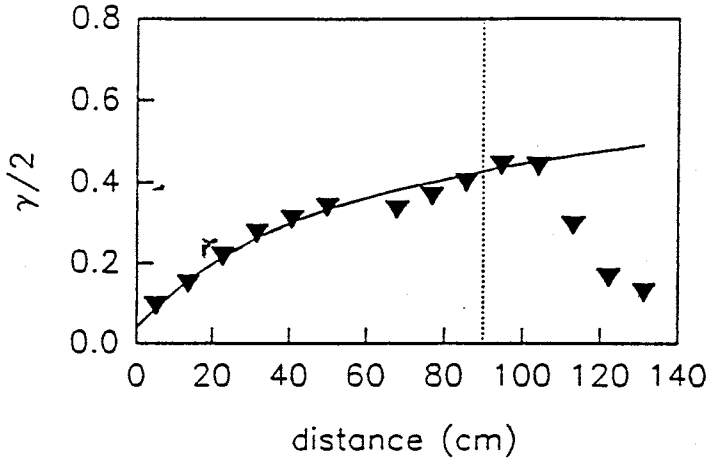

A

ES1 variogram

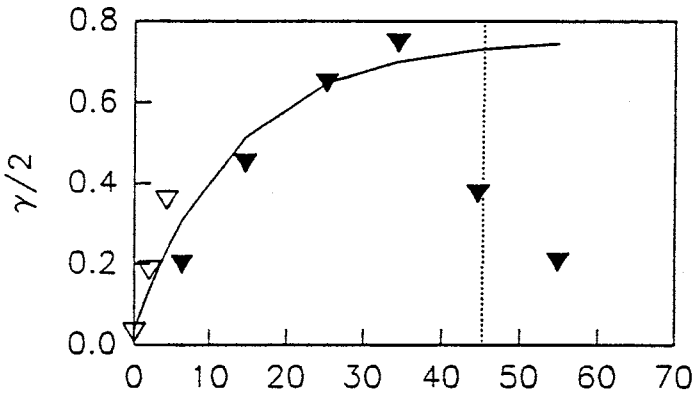

B

SS3 vertical variogram

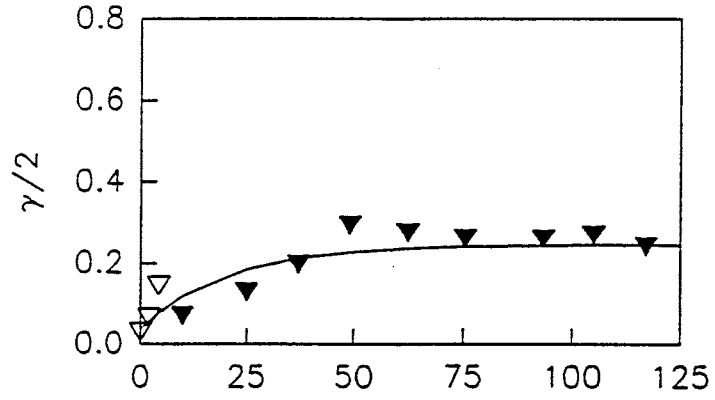

C

SS3 horizontal variogram

Figure 16. Variograms of ES1 and SS3. Dashed lines in ES1 and SS2 vertical variograms indicate the distance at which half the sampling distance is reached.

the area. The appearance of SS3 is very different from SS1, SS2 and SS5 in that it has three distinct layers (Figure 17). Grain size varies greatly between these regions, (from pebbly to fine sand), but both grain size and style of cross-bedding are relatively homogeneous within each region.

The area covered in the study is interpreted as deposits of two waning flow episodes. The lowest part of the exposure, Region 1, is the uppermost sequence in the flood transition, with bedding typical of a lower flow regime, ripple flow. Region 1 is approximately 0.2 meters high, consisting of thickly laminated, lower-medium sand with planar bedding. The central and upper regions together represent an entire upward grading, waning flow sequence. The central region, Region 2, is approximately 0.2 meters high, with thickly laminated planar bedding. It is dominated by very-coarse sand, but also includes some poorly sorted lower-medium and upper-fine sands. The pebbly lag of the upper flow regime sequence is at the base of Region 2. Pebbles up to 5 millimeters in diameter are present in this layer. Region 3 fines upward from an area of planar flow into a lower flow regime ripple flow, as seen in Region 1. It is approximately 0.5 meter thick and consists of thickly laminated fine sand, with some coarse sand.

One hundred nine air-permeameter measurements were obtained from 117 sample locations. All non-measurements were due to the presence of poorly consolidated, very coarse material. Statistics of the natural log transform of the SS3 data are shown

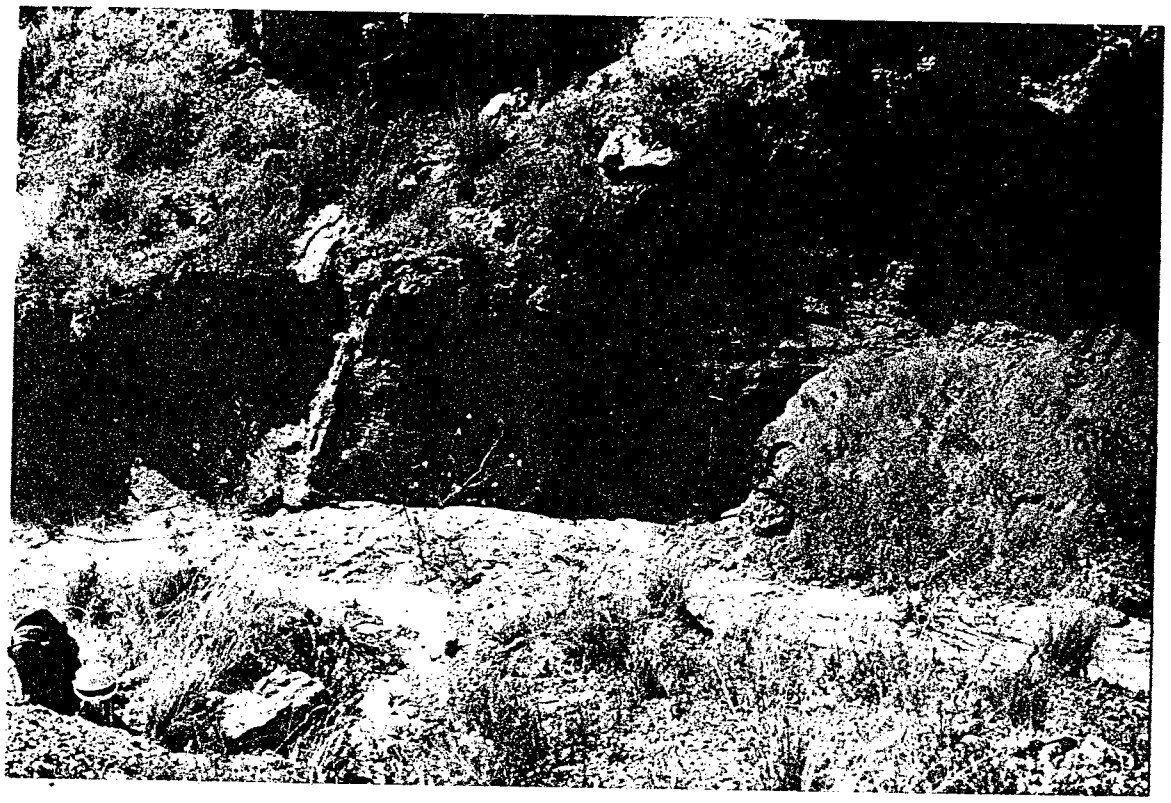

Figure 17. Photograph of SS3 study area. Bounding surfaces identified by dashed line, regions identified by number. Shovel is about 1 meter long.

in Table 5. The null hypothesis that the data follow the normal distribution is rejected (α=0.05, D_{crit} =0.084, D_{max}=.151).

Table 5. Statistics of SS3 and SS3 Regions.

	SS3	Region 1	Region 2	Region 3
N	109	27	32	50
mean	2.75	2.53	3.52	2.38
variance	0.35	0.13	0.19	0.05

A box plot of the SS3 regions, Figure 15d, reveals the similarity of Regions 1 and 3. The Kolomogorov-Smirnov test confirms that these regions have similar permeability distributions (Table 6).

Table 6. SS3 regions test of equal distributions.

Regions	D_{crit}	D_{max}	result
1 and 2	0.36	0.73	not equal
1 and 3	0.32	0.20	equal
2 and 3	0.31	0.87	not equal

The bounding surfaces model applied to this site does not identify these regional divisions, as the only second order surface present is that between Region 1 and Region 2. This boundary represents a hiatus in deposition, as this is the boundary between successive flood events. A zeroth order boundary, a non-erosional concordant bedding contact, separates Regions 2 and 3. In this case, the progressive fining upwards sequence which results in a change in hydrogeologic parameters between Regions 2 and 3 is not coincident with a second order boundary.

One hundred twenty-six additional measurements were made at SS3 and variogram estimates calculated from these data are indicated with hollow triangles. The horizontal experimental variogram is shown in Figure 16c, and was fitted with an

exponential model:

$$\gamma_{h,SS3}(\xi) = .036 + .21[1-\exp(-\frac{|\xi|}{20})]$$

The horizontal variogram reaches a sill at 0.24, which is significantly lower than the sample variance of 0.35. This is due to the greater lateral continuity observed in the outcrop, as few pairs of points from different regions are considered in this variogram.

The vertical experimental variogram of SS3 is shown in Figure 16b, and was fit with an exponential model of the form:

$$\gamma_{v,SS3}(\xi) = .036 + .72[1-\exp(-\frac{|\xi|}{13.33})]$$

The variogram reflects the vertical dimensions of the three regions. The variogram reaches a maximum value at a lag near 30 centimeters. This distance is the average thickness of the three regions, and is the distance where pairs of data from Regions 1 and 2 and from Regions 2 and 3 make up a majority of the pairs in the lag class. A hole effect appears at a lag distance of about 40 centimeters. This is the approximate thickness of Region 1 and 2 combined, and so reflects the decrease in variance found when data pairs from Regions 1 and 3 are compared while the number of pairs from Regions 1 and 2 and Regions 2 and 3 are neglected. The exponential variogram model fits only the rising limb of the variogram and does not capture the effect of the

stacking of similar regions separated by a higher permeability unit. The maximum value of the experimental variogram, about 0.65, is much greater than the variance of the SS3 data set, 0.35.

5.2.3 CH-2 Studies

As discussed earlier, four regions separated by second order surfaces were identified in both SS1 and SS2. Statistics and results of comparisons of the regions within SS1 are given in Tables 7 and 8. Region 4 is too small to consider. The null hypothesis that Regions 2 and 3 have similar permeability distributions is accepted.

Table 7. Statistics of SS1 and SS1 regions

	SS1	Region 1	Region 2	Region 3	Region 4
N	142	61	19	59	3
mean	2.96	2.69	3.25	3.12	3.49
variance	0.21	0.20	0.12	0.12	0.04

Table 8. SS1 regions test of equal distributions

Regions	D_{crit}	D_{max}	result
1 and 2	0.3573	0.52	not equal
1 and 3	0.2483	0.42	not equal
2 and 3	0.3587	0.17	equal

Results of the SS2 regions analysis are given in Tables 9 and 10. The null hypothesis that Regions 1 and 4 and Regions 2 and 3 have similar distributions is accepted.

Table 9. Statistics of SS2 and SS2 regions.

	SS2	Region 1	Region 2	Region 3	Region 4
N	128	42	34	21	31
mean	3.00	3.26	2.80	2.78	3.03
variance	0.16	0.22	0.07	0.04	0.09

Table 10. SS2 regions test of equal distributions.

Regions	D_{crit}	D_{max}	result
1 and 2	0.31	0.42	not equal
1 and 3	0.37	0.46	not equal
1 and 4	0.32	0.32	equal
2 and 3	0.38	0.06	equal
2 and 4	0.34	0.35	not equal
3 and 4	0.39	0.40	not equal

Box plots of the SS1 and SS2 regions are shown in Figure 15a and b. Relative to the regions within ES1 and SS3, SS1 and SS2 each contain regions which are relatively similar. Both the SS1 and SS2 vertical experimental variograms reach a sill at values very close to the sample variance (Figure 7). Neither of the ES1 and SS3 vertical variograms reach a sill, and each climbs to a maximum variogram value much greater than their respective sample variances. In ES1 and SS3, second order surfaces separate regions of distinctly different permeability distributions, and the experimental variogram reflects this by rising to a value much greater than the variance and falling in value as lags are reached which equal the distance between similar regions. In SS1 and SS2, second order surfaces separate areas of relatively similar permeability distributions, the variogram reaches an asymptotic value, and a simple exponential model adequately represents the permeability structure.

The holes seen in the variogram structures of ES1 and SS3 may be the result of the particular arrangement and thicknesses of the regions in each area, such as regions which are much thinner than the section measured with quasi-periodic strata. The finite "window" from which measurements are taken in SS3 is bound by upper and lower regions of similar mean permeability,

which leads to similar measurements in pairs at large lag distances. While the particular arrangement of regions sampled may reveal the hole in these cases, there is also a significant difference in the source of variability in ES1 and SS3 than in SS1 and SS2. Table 11 shows the variance of the means of the regions found within each study along with the variance of that study. Both SS1 and SS2 show much lower variances between regions than overall, while ES1 and SS3 have about the same amount of variance between regions and in the complete data set. It seems than that if second order bounding surfaces separate regions which have a low variance between the regions, an exponential variogram model which reaches a sill at the sample variance may be appropriate. The experimental results presented here indicate that if a higher degree of variability is found between regions, the vertical experimental variogram will likely rise to a value greater than the sample variance and may decrease in value as lags near the vertical dimension of the layers are reached.

Table 11. Comparison of overall and between regions variances.

	SS1	SS2	ES1	SS3
overall variance	0.21	0.16	0.27	0.35
variance between regions	0.11	0.05	0.26	0.38

CHAPTER 6: CONCLUSIONS

Figure 18 shows box plots of each small scale study. It is apparent that the soils of the Ps element have a significantly lower permeability than the channel sands of the CH-2 element and the Escondida site. The variance within each study site is much is much less than one.

Studies conducted in the Ps (paleosol) element (SS4 and SS6) showed a significant lack of observable small scale sedimentary structures. The experimental variograms show little spatial correlation, which we believe is a result of this lack of sedimentary structure. The permeability distribution in these study sites appears to be adequately represented by a continuous gaussian random field model. The SS4 experimental variograms indicate that the SS4 deposit is statistically isotropic, as the directional variograms are fit with the same model. Statistical isotropy within the Ps element is also indicated by the results of the SS6 study, where the ranges of the horizontal and vertical variograms are close in value (6 and 2 centimeters, respectively). The short range of the SS6 experimental variograms may be caused by the widespread calcium carbonate deposits. A longer range was observed in the SS4 variograms, which may be a result of fewer calcite nodules which are concentrated in one area of the outcrop.

The CH-2 study areas displayed nested scales of heterogeneity as regions within each study site act as areas of local second order stationarity. Where depositional processes

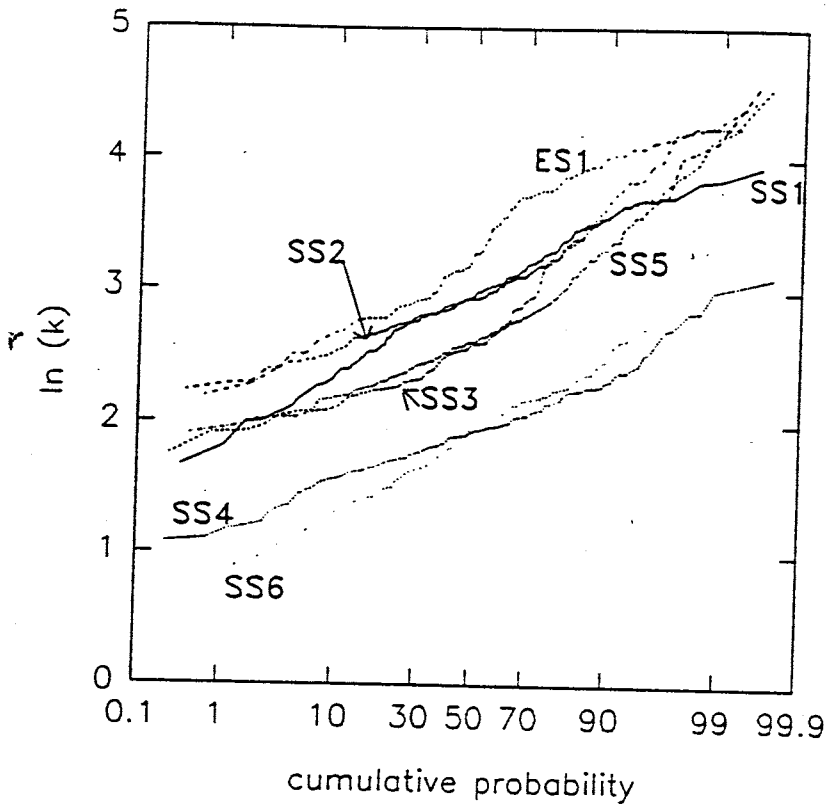

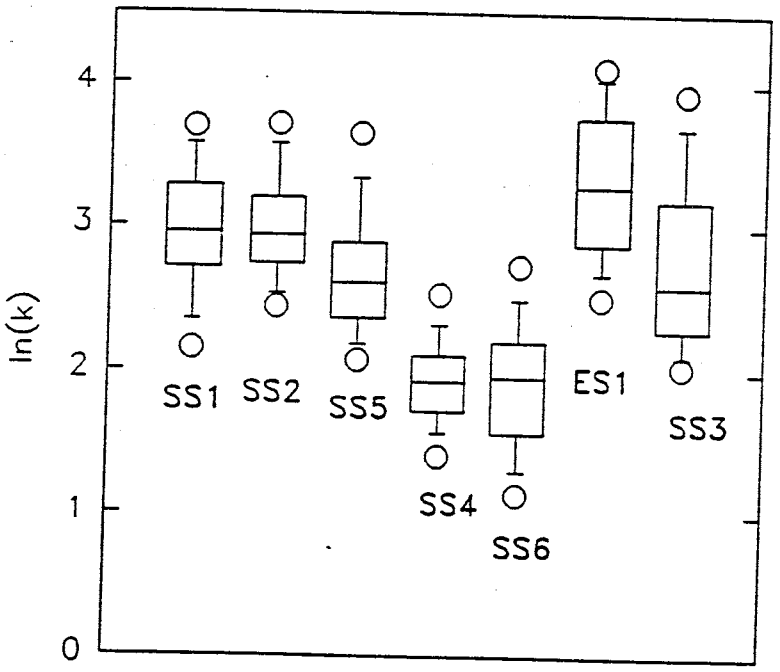

Figure 18. Probability plots and box plots of all small scale studies.

act at closely related scales the correlation structure might be adequately represented by an exponential variogram model, as in SS1 and SS2. The SS5 study site included a larger sample domain and was oriented perpendicular to the inferred direction of paleoflow. A more complex, nested model was required to fit the experimental SS5 variogram, possibly due to additional scales of heterogeneity encountered across the larger sample domain or due to directional anisotropy encountered by sampling perpendicular to paleoflow direction. Correlation lengths in the CH-2 element perpendicular to stratigraphy are significantly shorter than those observed parallel to stratigraphy. The extensive lateral continuity observed in the outcrops may cause the longer correlation lengths, while changes in grain size and bedform seen across stratigraphic layers lead to less spatial correlation in the vertical direction.

The bounding surfaces model may be used to identify permeability structure in geologic outcrops. The ES1 study indicates that zeroth and first order surfaces, which separate areas of similar lithofacies, do not appear to represent significant hydrogeologic variation. However, continuous fining-up deposits may contain regions of significantly different mean permeability on either side of these lower order boundaries, as in SS3.

Second order surfaces, which are lithologic boundaries, often separate regions of different mean permeability. If the variability of mean permeabilities found between these regions is

much less than the overall variability in permeability found in the area, an exponential variogram model which rises to a sill equal to the overall variance adequately characterizes the permeability distribution in the vertical direction. In deposits where the variability between regions bounded by second order surfaces is as great as the overall variability, the variogram will rise to a value much greater than the overall variance. Given a particular arrangement of strata and sampling "window", the experimental variogram may also display a significant drop in value at lag distances equal to the separation distance between similar regions.

These findings suggest types of geologic information which may be used to supplement or plan an efficient sampling scheme of permeability measurements. In deposits of little sedimentary structure, spatial correlation may occur over such a short range that the mean and variance may adequately characterize the permeability distribution. Where significant sedimentary structure exists, information concerning the distribution of second order bounding surfaces and the mean permeability of each lithofacies can be used to determine the scales of variability present in the permeability distribution and may also be used to infer an appropriate choice of random field model.

REFERENCES

Allen,J.R.L., 1983. Studies in fluviatile sedimentation: bars,bar-complexes and sandstone sheets (low sinuosity braided streams) in the Brownstones (L.Devonian), Welsh Borders. *Sed.Geol.* 33:237-293.

Anderson, M.P., 1989. Hydrogeologic facies models to delineate large-scale spatial trends in glacial and glaciofluvial sediments. *Geological Society of America Bulletin*, 101:501-511.

Armstrong,M., 1984. Common problems seen in variograms. *Mathematical Geology*, 16:305-313.

Brannan,J.R. and J.S.Haselow, 1993. Compound Random Field Models of Multiple Scale Hydraulic Conductivity. Water Resour. Res., 29:365-372.

Burrough,P.A., 1983. Multiscale sources of spatial variation in soil. II. A non-Brownian fractal model and its application in soil survey. *Journal of Soil Science*, 34:599-620.

Dagan,G., 1982. Stochastic modeling of groundwater flow by unconditional and conditional probabilities,2, The solute transport. *Water Resour. Res.*, 18:835-848.

Davis,J.M., S.J.Colarullo, R.C.Lohmann, F.M.Phillips, 1991. Alluvial aquifer heterogeneities in the Rio Grande Valley: Implications for ground water contamination. New Mexico Water Resources Research Institute Technical Completion Report Project # 1345681.

Davis,J.M., 1991. Technical Completion Report, Greater Confinement Disposal Heterogeneity Study, Nevada Test Site, Area 5, Radioactive Waste Management Site. Reynold's Electric & Engineering Co.

Davis,J.M., 1993. A conceptual geologic and sedimentological model of aquifer heterogeneity based on outcrop studies. New Mexico Institute of Mining and Technology PhD dissertation.

Davis,J.M., R.C.Lohmann, F.M. Phillips, J.L.Wilson, 1993. Architecture of the Sierra Ladrones Formation, central New Mexico: Depositional controls on the permeability correlation structure. *GSA Bulletin*, 105:998-1007.

Davis, J.M., J.L.Wilson, F.M.Phillips, 1994. A portable air-minipermeameter for rapid in-situ field measurements. *Ground Water, 32.*

Dreyer,T., A.Scheie, and O.Walderhaug, 1990. Minipermeameter-based study of permeability trends in channel sand bodies. *AAPG Bulletin*, 74:359-374.

Freeze, R.A. and J.A.Cherry, 1979. *Groundwater*. Englewood Cliffs, New Jersey: Prentice-Hall, Inc. pp 604.

Gelhar L.W., and C.L.Axness, 1983. Three-dimensional stochastic analysis of macrodispersion in aquifers. *Water Resour. Res.*, 19:161-180.

Goggin,D.J., M.A.Chandler, G.Kocurek, and L.W.Lake, 1988. Patterns of permeability in Eolian deposits: Page sandstone (Jurassic), Northeastern Arizona. *SPE Formation Evaluation*, June, 1988:297-306.

Gotway, C.A., and N.A.C.Cressie, 1990. A spatial analysis of variance applied to soil-water infiltration. *Water Resour. Res.*, 26: 2695-2703.

Gutjahr, A., 1991. Geostatistics for sampling design and analysis in *Groundwater Residue Sampling Design*, American Chemical Society, p.48-90.

Hess, K.M., S.H. Wolf, M.A. Celia, 1992. Large-scale natural gradient tracer test in sand and gravel, Cape Cod, Massachusetts, 3, hydraulic conductivity variability and calculated macrodispersivities. *Water Resour.Res.*, 28:2011-2027.

Isaaks, E.H. and R.M.Srivastava, 1989. *An Introduction to Applied Geostatistics*. New York:Oxford University Press. pp 561.

Journel, A.G., and Ch.J.Huijbregts, 1978. *Mining Geostatistics*. London:Academic Press. pp 600.

Kemblowski, M.W., and J. Wen, 1993. *Contaminant spreading in soils with fractal permeability distribution*. Water Resour. Res., 29:419-425.

Lohmann, R.C., 1992. A sedimantological approach to hydrologic characterization: a detailed three-dimensional study of an outcrop of the Sierra Ladrones Formation, Albuquerque Basin. Unpublished independent study, New Mexico Institute of Mining and Technology.

May, R.B., M.E. Masson and M.A.Hunter, 1990. *Applications of statistics in behavioral research*. Harper and Row: New York, 571pp.

Miall, A.D., 1990. *Principles of sedimentary basin analysis*. New York: Springer-Verlag. pp 540.

Miall, A.D., 1978. Lithofacies types and the vertical profile models of braided river deposits: a summary. In *Fluvial Sedimentology*, ed. A.D.Miall, 597-604, *Can.Soc.Petrol.Geol.Mem.5.*

Neuman, S.P., 1990. Universal scaling of hydraulic conductivities and dispersivities in geologic media. *Water Resour. Res.*, 26:1749-1758.

Phillips, F.M. and J.L.Wilson, 1989. An approach to estimating hydraulic conductivity spatial correlation scales using geological characteristics. *Water Resour. Res.*, 25:141-143.

Poeter,E., and D.R.Gaylord, 1990. Influence of aquifer heterogeneity on contaminant transport at the Hanford site. *Groundwater*, 28:900-909.

Rehfeldt, K.R., J.M.Boggs, and L.W.Gelhar, 1992. Field study of dispersion in a heterogeneous aquifer: 3. Geostatistical analysis of hydraulic conductivity. Water Resour. Res., 28:3309-3324.

Schwartz,F.W., 1977. Macroscopic dispersion in porous media: the controlling factors. *Water Resour. Res.*, 13:743-752.

Smith,L., 1981. Spatial Variability of flow parameters in a stratified sand. *Mathematical Geology*, 13:1-21.

Starks,T.H. and J.H.Fang, 1982. The effect of drift on the experimental semivariogram. *Mathematical Geology*, 14:309-319.

Sudicky, E.A., 1986. A natural gradient experiment on solute transport in a sand aquifer: Spatial variability of hydraulic conductivity and its role in the dispersion process. *Water Resour. Res.*, 22:2069-2082.

Till, R.T., 1974. *Statistical Methods for the earth scientist.* Wiley and Sons: New York. 154 pp.

Wheatcraft, S.W., and S.W. Tyler, 1988. An explanation of scale-dependent dispersivity in heterogeneous aquifers using concepts of fractal geometry. *Water Resour. Res.*, 24:566-578.

Woodbury,A.D., and E.A.Sudicky, 1991. The geostatistical characteristics of the Borden aquifer. *Water Resour. Res.*, 27:533-546.

Initial sampling data for each study site is given with x, y coordinates from arbitrary origin. Second sampling data are not given in relation to first set because of changes in the outcrop surface and moisture content between the two sampling dates. Second sampling data are given in terms of "R", which indicates repeated measurements at a single location, and "S", which indicate a series of nine measurements taken on a grid at 2 cm intervals. Each set of nine "S" measurements are given with x, y locations relative to an arbitrary origin.

ss1 data
July 29, 1992

region	facies	n	time(s)	x	y	q(cc/s)	k(darcy)
I	1	1	2.09	7	0	26.34	20.10
I	1	2	1.66	7	14	33.16	27.39
I	1	3	1.83	12	14	30.08	23.93
I	1	4	5.85	12	0	9.41	6.23
I	1	5	nm	7	34	mud ball	
I	1	6	nm	7	41	mud ball	
I	1	7	2.22	7	48	24.80	18.62
I	1	8	3.54	18.5	48	15.55	10.76
I	1	9	2.99	18.5	41	18.41	13.04
I	1	10	3.19	18.5	34	17.26	12.10
I	1	11	3.27	30	48	16.83	11.77
I	1	12	3.43	30	41	16.05	11.15
I	1	13	2.57	30	34	21.42	15.57
I	1	14	nm	7	70	mud clasts	
II	2	15	1.53	7	83	35.98	30.85
II	2	16	2.1	7	96	26.21	19.98
II	2	17	1.39	25	96	39.60	35.80
II	2	18	1.38	25	83	39.89	36.22
I	1	19	2.05	25	70	26.85	20.60
I	1	20	2.62	43	70	21.01	15.22
II	2	21	nm	43	83	mud ball	
II	2	22	1.88	43	96	29.28	23.08
II	2	23	1.47	7	94	37.45	32.78
II	2	24	1.83	7	96	30.08	23.93
II	2	25	1.99	18.5	96	27.66	21.41
II	2	26	1.73	18.5	94	31.82	25.84
III	4	27	2.09	0	137	26.34	20.10
III	4	28	2.24	4	137	24.57	18.42
III	4	29	1.68	8	137	32.76	26.93
I	1	30	2.27	45	0	24.25	18.11
I	1	31	3.87	45	15	14.22	9.74
I	1	32	2.15	55.5	15	25.60	19.39
I	1	33	2.29	55.5	0	24.04	17.92
I	1	34	1.9	47	25	28.97	22.75
I	1	35	4.27	47	33	12.89	8.75
I	1	36	4.08	65	25	13.49	9.19
I	1	37	5.1	65	33	10.79	7.22
I	1	38	4.29	47	53	12.83	8.70
I	1	39	3.66	52	53	15.04	10.37
I	1	40	3.98	57	53	13.83	9.45
III	3	41	1.97	55	94	27.94	21.69
III	3	42	1.35	55	98	40.77	37.55
III	3	43	1.77	75	98	31.10	25.04
III	3	44	1.28	75	94	43.00	41.08
III	4	45	1.89	57	133	29.12	22.91
III	4	46	2.33	57	137	23.62	17.54
III	5	47	1.77	57	141	31.10	25.04
III	5	48	2.56	66	141	21.50	15.65
III	4	49	2.66	66	137	20.69	14.95
III	4	50	1.75	66	133	31.45	25.43
III	4	51	2	75	133	27.52	21.27
III	4	52	1.91	75	137	28.82	22.60

SS1 additional sampling
July 30, 1993

	t	k [darcy]	q[cc/s]
R1	1.70	28.36	32.68
	1.61	30.74	34.50
	1.60	31.03	34.72
	1.63	30.17	34.08
	1.64	29.90	33.87
	1.63	30.17	34.08
	1.92	23.91	28.93
	1.74	27.43	31.93
	1.91	24.08	29.08
	2.66	15.80	20.88
	1.55	32.57	35.84
	1.99	22.79	27.91
	2.20	19.99	25.25
	2.62	16.09	21.20
	2.56	16.55	21.70
R2	1.70	28.36	32.68
	1.63	30.17	34.08
	1.68	28.85	33.07
	1.83	25.54	30.36
	1.88	24.61	29.55
	1.66	29.37	33.46
	1.66	29.37	33.46
	1.61	30.74	34.50
	1.63	30.17	34.08
	1.66	29.37	33.46
	1.99	22.79	27.91
	1.82	25.74	30.52
	1.58	31.62	35.16
	1.44	36.62	38.58
	1.79	26.34	31.03
R3	1.59	31.32	34.94
	1.62	30.45	34.29
	1.49	34.65	37.28
	1.53	33.23	36.31
	1.59	31.32	34.94
	1.66	29.37	33.46
	1.66	29.37	33.46
	1.52	33.58	36.55
	1.41	37.92	39.40
	1.59	31.32	34.94
	1.57	31.93	35.38
	1.55	32.57	35.84
	1.79	26.34	31.03
	1.67	29.11	33.26
	1.59	31.32	34.94
R4	2.16	20.47	25.72
	2.04	22.05	27.23
	2.16	20.47	25.72
	1.68	28.85	33.07
	1.83	25.54	30.36
	1.89	24.43	29.39
	2.22	19.76	25.02
	2.19	20.11	25.37

	2.02	22.34	27.50		
	2.07	21.63	26.84		
	2.02	22.34	27.50		
	2.02	22.34	27.50		
	2.06	21.77	26.97		
	2.10	21.23	26.45		
	2.20	19.99	25.25		
				x	y
S1	2.59	16.32	21.45	0	0
	2.42	17.73	22.95	2	0
	2.30	18.89	24.15	4	0
	2.52	16.87	22.04	0	2
	2.41	17.82	23.05	2	2
	2.29	19.00	24.26	4	2
	2.05	21.91	27.10	0	4
	2.78	14.99	19.98	2	4
	3.22	12.63	17.25	4	4
S2	1.05	68.30	52.90	0	0
	1.05	68.30	52.90	2	0
	1.21	50.03	45.91	4	0
	0.90	107.30	61.72	0	2
	1.81	25.94	30.69	2	2
	1.56	32.25	35.61	4	2
	1.19	51.72	46.68	0	4
	1.36	40.32	40.85	2	4
	1.48	35.03	37.53	4	4
S3	1.17	53.55	47.48	0	0
	1.04	69.95	53.41	2	0
	1.28	44.94	43.40	4	0
	1.04	69.95	53.41	0	2
	0.95	89.80	58.47	2	2
	1.24	47.70	44.80	4	2
	1.70	28.36	32.68	0	4
	1.74	27.43	31.93	2	4
	1.83	25.54	30.36	4	4
S4	1.45	36.21	38.31	0	0
	1.28	44.94	43.40	2	0
	1.34	41.38	41.46	4	0
	1.52	33.58	36.55	0	2
	1.50	34.29	37.03	2	2
	1.57	31.93	35.38	4	2
	1.63	30.17	34.08	0	4
	1.28	44.94	43.40	2	4
	1.38	39.32	40.25	4	4
S5	2.20	19.99	25.25	0	0
	2.91	14.20	19.09	2	0
	3.06	13.39	18.15	4	0
	3.31	12.23	16.78	0	2
	2.46	17.38	22.58	2	2
	2.47	17.29	22.49	4	2
	2.96	13.92	18.77	0	4
	2.85	14.56	19.49	2	4
	2.67	15.73	20.81	4	4
S6	0.98	81.95	56.68	0	0
	1.33	41.93	41.77	2	0
	1.34	41.38	41.46	4	0
	1.27	45.59	43.74	0	2
	1.09	62.49	50.96	2	2
	1.15	55.51	48.30	4	2
	1.54	32.90	36.07	0	4

	2.06	21.77	26.97	2	4
	1.73	27.65	32.11	4	4
S7	1.22	49.23	45.53	0	0
	1.13	57.64	49.16	2	0
	1.24	47.70	44.80	4	0
	1.63	30.17	34.08	0	2
	1.10	61.19	50.50	2	2
	1.63	30.17	34.08	4	2
	1.50	34.29	37.03	0	4
	1.43	37.04	38.85	2	4
	1.49	34.65	37.28	4	4
S8	1.51	33.93	36.79	0	0
	1.62	30.45	34.29	2	0
	1.52	33.58	36.55	4	0
	1.84	25.35	30.19	0	2
	1.66	29.37	33.46	2	2
	1.52	33.58	36.55	4	2
	1.68	28.85	33.07	0	4
	1.95	23.42	28.49	2	4
	2.00	22.63	27.78	4	4

SS2 data
August 11, 1992

facies	n	time(s)	x(cm)	y(cm)	q(cc/s)	k(darcy)
f1	1	1.91	4.0	7.0	28.82	22.60
f1	2	0.79	4.0	13.0	69.68	143.80
f1	3	0.95	14.0	13.0	57.94	76.93
f1	4	1.22	14.0	7.0	45.12	44.74
f1	5	2.98	9.0	38.0	18.47	13.09
f2	6	1.88	9.0	45.0	29.28	23.08
f2	7	1.68	11.5	45.0	32.76	26.93
f1	8	1.24	11.5	38.0	44.39	43.44
f3	9	1.76	0.0	71.0	31.28	25.24
f3	10	2.45	0.0	85.0	22.47	16.50
f3	11	3.30	16.0	85.0	16.68	11.65
f3	12	1.91	16.0	71.0	28.82	22.60
f4	13	1.87	8.0	101.0	29.44	23.24
f4	14	2.24	8.0	107.0	24.57	18.42
f4	15	1.91	8.0	113.0	28.82	22.60
f3	16	2.02	10.0	113.0	27.25	21.00
f4	17	2.83	10.0	107.0	19.45	13.90
f4	18	1.68	10.0	101.0	32.76	26.93
f4	19	1.72	12.0	107.0	32.00	26.05
f4	20	2.06	12.0	113.0	26.72	20.47
f4	21	2.33	12.0	101.0	23.62	17.54
f5	22	1.77	23.0	136.0	31.10	25.04
f5	23	1.81	23.0	139.5	30.41	24.29
f5	24	1.89	23.0	143.0	29.12	22.91
f5	25	1.84	25.0	143.0	29.92	23.75
f5	26	2.82	25.0	139.5	19.52	13.95
f5	27	2.03	25.0	136.0	27.12	20.86
f5	28	1.90	27.0	136.0	28.97	22.75
f5	29	3.46	27.0	139.5	15.91	11.04
f5	30	1.84	27.0	143.0	29.92	23.75
f1	31	1.57	34.0	7.0	35.06	29.69
f1	32	1.27	34.0	12.0	43.34	41.65
f1	33	1.14	34.0	17.0	48.29	50.87
f1	34	1.17	34.0	17.0	47.05	48.37
f1	35	1.13	34.0	12.0	48.71	51.77
f1	36	1.94	34.0	7.0	28.37	22.14
f1	37	2.04	34.0	7.0	26.98	20.73
f1	38	1.17	34.0	12.0	47.05	48.37
f1	39	1.12	34.0	17.0	49.15	52.70
f1	40	2.07	43.0	40.0	26.59	20.35
f2	41	1.27	43.0	55.0	43.34	41.65
f2	42	1.13	48.0	55.0	48.71	51.77
f1	43	1.57	48.0	40.0	35.06	29.69
f3	44	2.21	47.0	70.0	24.91	18.73
f3	45	1.24	47.0	77.5	44.39	43.44
f3	46	2.05	47.0	85.0	26.85	20.60
f3	47	2.88	50.0	85.0	19.11	13.62
f3	48	2.09	50.0	77.5	26.34	20.10
f3	49	nm	50.0	70.0	hole	
f3	50	1.82	53.0	70.0	30.24	24.11
f3	51	1.68	53.0	77.5	32.76	26.93
f3	52	2.02	53.0	85.0	27.25	21.00
f3	53	2.55	49.0	94.0	21.59	15.72

f4	54	2.14	49.0	98.0	25.72	19.50
f4	55	2.09	49.0	102.0	26.34	20.10
f4	56	1.91	53.0	102.0	28.82	22.60
f4	57	2.42	53.0	98.0	22.75	16.74
f3	58	2.77	53.0	94.0	19.87	14.25
f3	59	2.99	57.0	94.0	18.41	13.04
f4	60	3.27	57.0	98.0	16.83	11.77
f4	61	1.65	57.0	102.0	33.36	27.63
f5	62	2.13	49.0	137.0	25.84	19.62
f5	63	1.52	49.0	142.0	36.21	31.16
f5	64	2.09	49.0	147.0	26.34	20.10
f5	65	2.67	57.5	147.0	20.62	14.88
f5	66	1.62	57.5	142.0	33.98	28.36
f5	67	1.36	57.5	137.0	40.47	37.09
f5	68	1.27	66.0	137.0	43.34	41.65
f5	69	2.02	66.0	142.0	27.25	21.00
f5	70	2.46	66.0	147.0	22.38	16.41
f1	71	1.73	75.0	0.0	31.82	25.84
f1	72	0.97	75.0	11.0	56.75	72.88
f1	73	1.16	91.5	11.0	47.45	49.17
f1	74	1.52	91.5	0.0	36.21	31.16
f1	75	1.82	81.0	40.0	30.24	24.11
f1	76	1.63	81.0	44.0	33.77	28.11
f1	77	2.05	97.0	44.0	26.85	20.60
f1	78	1.71	97.0	40.0	32.19	26.27
f3	79	1.77	85.0	62.0	31.10	25.04
f3	80	1.91	85.0	69.0	28.82	22.60
f3	81	2.28	85.0	76.0	24.14	18.02
f3	82	2.27	89.0	76.0	24.25	18.11
f3	83	1.68	89.0	69.0	32.76	26.93
f3	84	1.46	89.0	62.0	37.70	33.13
f3	85	1.92	93.0	62.0	28.67	22.44
f3	86	1.52	93.0	69.0	36.21	31.16
f3	87	2.10	93.0	76.0	26.21	19.98
f4	88	2.20	85.0	101.0	25.02	18.84
f4	89	2.39	85.0	101.0	23.03	17.00
f4	90	2.27	88.0	101.0	24.25	18.11
f4	91	2.15	88.0	101.0	25.60	19.39
f5	92	1.70	83.0	125.0	32.38	26.48
f5	93	1.58	83.0	127.0	34.84	29.41
f5	94	1.91	85.0	127.0	28.82	22.60
f5	95	1.38	85.0	125.0	39.89	36.22
f1	96	1.41	111.0	4.0	39.04	34.99
f1	97	1.20	111.0	12.0	45.87	46.12
f1	98	0.92	121.0	12.0	59.83	84.01
f1	99	2.21	121.0	4.0	24.91	18.73
f1	100	1.41	114.0	34.0	39.04	34.99
f1	101	1.95	114.0	37.0	28.23	21.99
f1	102	2.88	114.0	40.0	19.11	13.62
f1	103	1.97	117.0	40.0	27.94	21.69
f1	104	1.94	117.0	37.0	28.37	22.14
f1	105	2.19	117.0	34.0	25.13	18.94
f1	106	1.60	120.0	34.0	34.40	28.88
f1	107	2.74	120.0	37.0	20.09	14.43
f1	108	1.92	120.0	40.0	28.67	22.44
f3	109	2.24	130.0	58.0	24.57	18.42
f3	110	nm	130.0	63.0	nodule	
f3	111	2.34	130.0	68.0	23.52	17.45
f3	112	2.37	132.0	68.0	23.23	17.18
f3	113	2.39	132.0	63.0	23.03	17.00

f3	114	2.20	132.0	58.0	25.02	18.84
f3	115	2.44	134.0	58.0	22.56	16.58
f3	116	2.64	134.0	63.0	20.85	15.08
f3	117	2.35	134.0	68.0	23.42	17.36
f3	118	2.76	135.0	90.0	19.94	14.31
f4	119	2.45	135.0	96.0	22.47	16.50
f3	120	2.24	143.0	96.0	24.57	18.42
f4	121	2.61	143.0	90.0	21.09	15.29
f5	122	1.67	130.0	127.0	32.96	27.16
f5	123	1.53	130.0	134.0	35.98	30.85
f6	124	2.09	130.0	141.0	26.34	20.10
f5	125	1.71	138.0	141.0	32.19	26.27
f5	126	1.37	138.0	134.0	40.18	36.65
f6	127	1.36	138.0	127.0	40.47	37.09
f5	128	1.23	146.0	127.0	44.75	44.08
f5	129	1.50	146.0	134.0	36.70	31.79
f6	130	1.58	146.0	141.0	34.84	29.41

ss2 additional sampling
July 30, 1993

	k [darcy]	q[cc/s]	t[seconds]
R1	18.79	24.05	2.31
	18.79	24.05	2.31
	20.47	25.72	2.16
	17.92	23.15	2.40
	18.49	23.74	2.34
	21.10	26.33	2.11
	17.82	23.05	2.41
	17.73	22.95	2.42
	18.69	23.94	2.32
	17.29	22.49	2.47
	17.38	22.58	2.46
	18.39	23.64	2.35
	18.29	23.54	2.36
	17.38	22.58	2.46
	17.64	22.86	2.43
R2	31.62	35.16	1.58
	30.17	34.08	1.63
	54.51	47.89	1.16
	25.94	30.69	1.81
	23.58	28.63	1.94
	22.19	27.36	2.03
	38.84	39.96	1.39
	32.25	35.61	1.56
	26.55	31.21	1.78
	22.79	27.91	1.99
	22.63	27.78	2.00
	27.65	32.11	1.73
	24.97	29.87	1.86
	27.88	32.30	1.72
	27.20	31.74	1.75
R3	15.38	20.42	2.72
	15.25	20.27	2.74
	15.59	20.65	2.69
	18.01	23.24	2.39
	17.73	22.95	2.42
	16.87	22.04	2.52
	17.04	22.22	2.50
	17.04	22.22	2.50
	18.10	23.34	2.38
	13.76	18.58	2.99
	15.59	20.65	2.69
	16.47	21.61	2.57
	15.12	20.13	2.76
	14.32	19.22	2.89
	14.62	19.56	2.84
R4	29.37	33.46	1.66
	26.55	31.21	1.78
	33.23	36.31	1.53
	27.43	31.93	1.74
	31.03	34.72	1.60
	31.62	35.16	1.58
	28.85	33.07	1.68
	36.21	38.31	1.45
	29.11	33.26	1.67

	27.88	32.30	1.72		
	30.17	34.08	1.63		
	30.17	34.08	1.63		
	30.17	34.08	1.63		
	29.37	33.46	1.66		
	28.61	32.87	1.69		
				x	y
S1	24.97	29.87	1.86	0	0
	35.03	37.53	1.48	2	0
	22.34	27.50	2.02	4	0
	37.92	39.40	1.41	0	2
	46.98	44.44	1.25	2	2
	30.45	34.29	1.62	4	2
	31.32	34.94	1.59	0	4
	30.17	34.08	1.63	2	4
	24.08	29.08	1.91	4	4
S2	25.74	30.52	1.82	0	0
	23.42	28.49	1.95	2	0
	27.43	31.93	1.74	4	0
	35.41	37.79	1.47	0	2
	54.51	47.89	1.16	2	2
	30.17	34.08	1.63	4	2
	39.32	40.25	1.38	0	4
	47.70	44.80	1.24	2	4
	37.92	39.40	1.41	4	4
S3	18.49	23.74	2.34	0	0
	15.87	20.96	2.65	2	0
	15.52	20.57	2.70	4	0
	20.22	25.48	2.18	0	2
	23.74	28.78	1.93	2	2
	21.36	26.58	2.09	4	2
	21.10	26.33	2.11	0	4
	18.29	23.54	2.36	2	4
	15.80	20.88	2.66	4	4
S4	26.14	30.86	1.80	0	0
	26.77	31.38	1.77	2	0
	26.77	31.38	1.77	4	0
	29.37	33.46	1.66	0	2
	26.98	31.56	1.76	2	2
	27.43	31.93	1.74	4	2
	18.49	23.74	2.34	0	4
	25.16	30.03	1.85	2	4
	22.19	27.36	2.03	4	4
S5	11.99	16.48	3.37	0	0
	17.29	22.49	2.47	2	0
	39.32	40.25	1.38	4	0
	32.57	35.84	1.55	0	2
	22.63	27.78	2.00	2	2
	21.91	27.10	2.05	4	2
	15.52	20.57	2.70	0	4
	13.19	17.92	3.10	2	4
	12.54	17.15	3.24	4	4
S6	23.42	28.49	1.95	0	0
	22.34	27.50	2.02	2	0
	24.79	29.71	1.87	4	0
	36.21	38.31	1.45	0	2
	26.55	31.21	1.78	2	2
	20.59	25.84	2.15	4	2
	50.03	45.91	1.21	0	4
	28.36	32.68	1.70	2	4

	21.49	26.71	2.08	4	4
S7	34.65	37.28	1.49	0	0
	27.43	31.93	1.74	2	0
	22.63	27.78	2.00	4	0
	46.27	44.09	1.26	0	2
	47.70	44.80	1.24	2	2
	45.59	43.74	1.27	4	2
	19.87	25.14	2.21	0	4
	25.16	30.03	1.85	2	4
	27.43	31.93	1.74	4	4
S8	32.90	36.07	1.54	0	0
	30.74	34.50	1.61	2	0
	48.45	45.16	1.23	4	0
	37.92	39.40	1.41	0	2
	25.94	30.69	1.81	2	2
	39.32	40.25	1.38	4	2
	37.92	39.40	1.41	0	4
	39.82	40.55	1.37	2	4
	20.97	26.20	2.12	4	4

SS3 data
September 4, 1992

region	facies	n	time(s)	x(cm)	y(cm)	q(cc/s)	k(darcy)
1	1	1	2.62	0	0	21.01	15.22
1	1	2	2.94	20	0	18.72	13.29
1	1	3	2.01	0	19	27.39	21.13
1	1	4	2.2	20	19	25.02	18.84
2	2	5	2.52	-2	27	21.84	15.94
2	2	6	2.01	6	27	27.39	21.13
2	2	7	1.82	14	27	30.24	24.11
2	2	8	1.53	-2	30	35.98	30.85
2	2	9	0.9	-2	33	61.16	89.57
2	2	10	1	6	30	55.05	67.59
2	2	11	1.22	6	33	45.12	44.74
2	2	12	1.38	14	30	39.89	36.22
2	2	13	1.1	14	33	50.04	54.67
1	3	14	2.02	-4	53	27.25	21.00
1	3	15	2.53	11	53	21.76	15.87
1	3	16	nm	-4	70	loose gravel	
1	3	17	nm	11	70	loose gravel	
1	1	18	3.6	34	0	15.29	10.56
1	1	19	3.93	47	0	14.01	9.58
1	1	20	1.91	60	0	28.82	22.60
1	1	21	2.23	34	12	24.68	18.52
2	2	22	1.56	34	24	35.29	29.97
1	1	23	4.68	47	12	11.76	7.92
2	2	24	1.42	47	24	38.76	34.60
1	1	25	4.08	60	12	13.49	9.19
2	2	26	1.05	60	24	52.42	60.40
2	2	27	1.06	36	32	51.93	59.15
2	2	28	0.88	41	32	62.55	95.99
2	2	29	0.98	46	32	56.17	71.02
2	2	30	2.04	36	39	26.98	20.73
1	3	31	2.87	36	46	19.18	13.67
2	2	32	1.42	41	39	38.76	34.60
2	2	33	1.52	46	39	36.21	31.16
1	3	34	3.53	41	46	15.59	10.79
1	3	35	3.59	46	46	15.33	10.59
1	3	36	2.51	33	55	21.93	16.02
1	3	37	4.16	35.5	55	13.23	9.00
1	3	38	4.45	38	55	12.37	8.36
1	3	39	2.41	33	68	22.84	16.83
3	4	40	nm	33	81	loose gravel	
1	3	41	4.16	35.5	68	13.23	9.00
1	3	42	3.78	38	68	14.56	10.00
3	4	43	nm	35.5	81	loose gravel	
3	4	44	nm	38	81	loose gravel	
1	1	45	2.25	70	1	24.46	18.31
1	1	46	2.38	86	1	23.13	17.09
1	1	47	1.73	70	14	31.82	25.84
1	1	48	1.57	86	14	35.06	29.69
2	2	49	1.06	72	28	51.93	59.15
2	2	50	1.51	88	28	36.45	31.47
1	3	51	2.53	72	41	21.76	15.87
1	3	52	2.51	88	41	21.93	16.02
1	3	53	3.51	71	54	15.68	10.86

1	3	54	3.41	88	54	16.14	11.22
1	3	55	2.7	105	54	20.39	14.69
1	3	56	3.44	71	56	16.00	11.11
1	3	57	3.24	71	58	16.99	11.89
1	3	58	3.38	88	56	16.29	11.33
1	3	59	4.18	88	58	13.17	8.95
1	3	60	2.52	105	56	21.84	15.94
1	3	61	3.38	105	58	16.29	11.33
1	1	62	3.16	107	3	17.42	12.23
1	1	63	3.25	115	3	16.94	11.85
1	1	64	1.6	107	12	34.40	28.88
1	1	65	1.95	115	12	28.23	21.99
2	2	66	1.2	106	28	45.87	46.12
2	2	67	0.82	137	28	67.13	123.00
2	2	68	1.3	106	35	42.34	40.00
2	2	69	1.45	137	35	37.96	33.49
1	3	70	3.43	107	55	16.05	11.15
1	3	71	2.74	109	55	20.09	14.43
1	3	72	3.39	107	58	16.24	11.30
1	3	73	2.46	109	58	22.38	16.41
1	1	74	3.35	143	1	16.43	11.45
1	1	75	2.99	149	1	18.41	13.04
1	1	76	3.26	143	12	16.88	11.81
1	1	77	4.22	149	12	13.04	8.86
2	2	78	1.88	150	41	29.28	23.08
2	2	79	1.38	154	41	39.89	36.22
2	2	80	2.33	150	50	23.62	17.54
2	2	81	2.26	154	50	24.36	18.21
1	3	82	3.07	148	67	17.93	12.65
1	3	83	2.18	164	67	25.25	19.05
1	3	84	1.93	180	67	28.52	22.29
1	3	85	3.01	148	79	18.29	12.94
1	3	86	2.66	148	91	20.69	14.95
1	3	87	3.21	164	79	17.15	12.02
1	3	88	2.58	180	79	21.34	15.50
1	3	89	2.81	164	91	19.59	14.01
1	3	90	2.61	180	91	21.09	15.29
1	1	91	3.2	182	1	17.20	12.06
1	1	92	2.78	188	1	19.80	14.19
1	1	93	3.45	194	1	15.96	11.08
1	1	94	2.64	182	10	20.85	15.08
2	2	95	0.89	182	19	61.85	92.66
1	1	96	3.04	188	10	18.11	12.79
1	1	97	1.88	194	10	29.28	23.08
2	2	98	1.33	188	19	41.39	38.49
2	2	99	1.12	194	19	49.15	52.70
2	2	100	1.41	184	29	39.04	34.99
2	2	101	1.15	201	29	47.87	50.01
2	2	102	1.25	218	29	44.04	42.83
1	3	103	4.01	184	40	13.73	9.37
1	3	104	3.64	201	40	15.12	10.43
1	3	105	2.37	218	40	23.23	17.18
1	3	106	3.97	184	51	13.87	9.47
1	3	107	3.88	201	51	14.19	9.72
1	3	108	3.97	218	51	13.87	9.47
1	3	109	2.62	202	59	21.01	15.22
1	3	110	3.22	205	59	17.09	11.97
1	3	111	2.71	208	59	20.31	14.62
1	3	112	2.66	202	63	20.69	14.95
1	3	113	2.65	205	63	20.77	15.01

1	3	114	3.2	208	63	17.20	12.06
1	3	115	2.5	202	67	22.02	16.10
1	3	116	3.44	205	67	16.00	11.11
1	3	117	3.49	208	67	15.77	10.93

SS3 additional sampling
August 4, 1993

	k [darcy]	t[seconds]	q[cc/s]		
R1	5.13	7.37	7.54		
	6.22	6.14	9.05		
	6.60	5.81	9.56		
	5.97	6.38	8.71		
	5.12	7.39	7.52		
	6.01	6.34	8.76		
	5.54	6.85	8.11		
	6.13	6.23	8.92		
	8.79	4.45	12.48		
	5.93	6.42	8.65		
	5.24	7.22	7.69		
	6.71	5.72	9.71		
	6.60	5.81	9.56		
	6.20	6.16	9.02		
	7.29	5.29	10.50		
R2	20.11	2.19	25.37		
	19.54	2.24	24.80		
	15.12	2.76	20.13		
	24.08	1.91	29.08		
	22.34	2.02	27.50		
	19.76	2.22	25.02		
	16.17	2.61	21.28		
	18.10	2.38	23.34		
	20.47	2.16	25.72		
	18.79	2.31	24.05		
	17.04	2.5	22.22		
	18.49	2.34	23.74		
	16.40	2.58	21.53		
	8.21	4.74	11.72		
	31.93	1.57	35.38		
R3	6.31	6.06	9.17		
	6.91	5.56	9.99		
	6.13	6.23	8.92		
	6.94	5.54	10.03		
	6.65	5.77	9.63		
	6.73	5.7	9.75		
	5.51	6.89	8.06		
	7.15	5.39	10.31		
	7.35	5.25	10.58		
	6.94	5.54	10.03		
	7.05	5.46	10.17		
	6.51	5.88	9.45		
	6.39	5.99	9.27		
	6.78	5.66	9.81		
	6.39	5.99	9.27		
				x	y
S1	7.67	5.05	11.00	0	0
	6.95	5.53	10.05	2	0
	8.08	4.81	11.55	4	0
	7.25	5.32	10.44	0	2
	7.18	5.37	10.34	2	2
	7.10	5.42	10.25	4	2
	5.46	6.95	7.99	0	4
	8.90	4.4	12.63	2	4

	7.52	5.14	10.81	4	4
S2	9.32	4.22	13.16	0	0
	11.33	3.54	15.69	2	0
	9.91	3.99	13.92	4	0
	6.30	6.07	9.15	0	2
	6.26	6.1	9.11	2	2
	7.23	5.33	10.42	4	2
	5.55	6.84	8.12	0	4
	5.27	7.18	7.74	2	4
	5.47	6.93	8.02	4	4
S3	12.49	3.25	17.09	0	0
	13.55	3.03	18.33	2	0
	16.32	2.59	21.45	4	0
	32.25	1.56	35.61	0	2
	24.08	1.91	29.08	2	2
	29.37	1.66	33.46	4	2
	14.20	2.91	19.09	0	4
	23.74	1.93	28.78	2	4
	12.58	3.23	17.20	4	4
S4	30.17	1.63	34.08	0	0
	55.51	1.15	48.30	2	0
	10.72	3.72	14.93	4	0
	14.44	2.87	19.36	0	2
	7.51	5.15	10.79	2	2
	5.67	6.7	8.29	4	2
	6.93	5.55	10.01	0	4
	5.33	7.11	7.81	2	4
	6.66	5.76	9.64	4	4
S5	8.13	4.78	11.62	0	0
	7.60	5.09	10.91	2	0
	6.57	5.83	9.53	4	0
	7.32	5.27	10.54	0	2
	9.52	4.14	13.42	2	2
	7.37	5.24	10.60	4	2
	27.20	1.75	31.74	0	4
	27.65	1.73	32.11	2	4
	56.56	1.14	48.73	4	4
S6	41.93	1.33	41.77	0	0
	19.10	2.28	24.36	2	0
	33.58	1.52	36.55	4	0
	43.08	1.31	42.40	0	2
	25.16	1.85	30.03	2	2
	24.08	1.91	29.08	4	2
	20.47	2.16	25.72	0	4
	22.94	1.98	28.06	2	4
	19.21	2.27	24.47	4	4
S7	10.44	3.81	14.58	0	0
	7.67	5.05	11.00	2	0
	8.08	4.81	11.55	4	0
	9.86	4.01	13.85	0	2
	6.97	5.52	10.06	2	2
	8.99	4.36	12.74	4	2
	9.04	4.34	12.80	0	4
	9.37	4.2	13.23	2	4
	10.62	3.75	14.81	4	4
S8	28.36	1.7	32.68	0	0
	22.49	2.01	27.64	2	0
	27.43	1.74	31.93	4	0
	40.84	1.35	41.15	0	2
	40.84	1.35	41.15	2	2

	45.59	1.27	43.74	4	2
	24.08	1.91	29.08	0	4
	21.36	2.09	26.58	2	4
	18.69	2.32	23.94	4	4
S9	8.46	4.61	12.05	0	0
	10.11	3.92	14.17	2	0
	7.25	5.32	10.44	4	0
	7.94	4.89	11.36	0	2
	7.78	4.98	11.15	2	2
	6.91	5.56	9.99	4	2
	4.06	9.24	6.01	0	4
	6.56	5.84	9.51	2	4
	5.00	7.56	7.35	4	4

SS4 data
October 2, 1992

region	n	time(s)	x(cm)	y(cm)	q(cc/s)	k(darcy)
1	1	5.57	0	0	9.88	6.57
1	2	6.37	47	0	8.64	5.70
1	3	4.39	94	0	12.54	8.49
1	4	5.57	0	5.5	9.88	6.57
1	5	4.42	47	5.5	12.45	8.42
1	6	5.16	94	5.5	10.67	7.13
1	7	3.42	0	11	16.10	11.19
1	8	5.41	47	11	10.17	6.78
1	9	3.91	94	11	14.08	9.63
1	10	3.43	0	35	16.05	11.15
1	11	4.3	19.5	35	12.80	8.68
1	12	3.35	39	35	16.43	11.45
1	13	2.55	0	45	21.59	15.72
1	14	4.1	19.5	45	13.43	9.14
1	15	3.4	39	45	16.19	11.26
1	16	3.98	0	55	13.83	9.45
1	17	4.45	19.5	55	12.37	8.36
1	18	4.09	39	55	13.46	9.17
1	19	6.7	0	70	8.22	5.40
1	20	5.63	16.5	70	9.78	6.49
1	21	4.89	33	70	11.26	7.55
1	22	6.05	0	82.5	9.10	6.02
1	23	4.16	16.5	82.5	13.23	9.00
1	24	4.13	33	82.5	13.33	9.07
1	25	3.23	0	95	17.04	11.93
1	26	4.37	16.5	95	12.60	8.53
1	27	2.3	33	95	23.93	17.82
1	28	5.5	0	105	10.01	6.66
1	29	4.07	15	105	13.52	9.22
1	30	4.79	30	105	11.49	7.72
1	31	4.59	0	107	11.99	8.08
1	32	4.52	15	107	12.18	8.22
1	33	5.95	30	107	9.25	6.12
1	34	4.57	0	109	12.04	8.12
1	35	4.13	15	109	13.33	9.07
1	36	3.53	30	109	15.59	10.79
1	37	3.42	40	0	16.10	11.19
1	38	4.27	55	0	12.89	8.75
1	39	3.44	70	0	16.00	11.11
1	40	3.38	40	15.5	16.29	11.33
1	41	4.71	55	15.5	11.69	7.86
1	42	4.72	70	15.5	11.66	7.84
1	43	4.06	40	31	13.56	9.24
1	44	3.77	55	31	14.60	10.03
1	45	4.74	70	31	11.61	7.81
1	46	4.61	40	35	11.94	8.05
1	47	4.2	49.5	35	13.11	8.91
1	48	3.71	59	35	14.84	10.21
1	49	2.91	40	37	18.92	13.45
1	50	4.49	49.5	37	12.26	8.28
1	51	3.73	59	37	14.76	10.15
1	52	3.34	40	39	16.48	11.49
1	53	4.5	49.5	39	12.23	8.26

1	54	3.66	59	39	15.04	10.37
1	55	3.66	40	70	15.04	10.37
1	56	4.07	44.5	70	13.52	9.22
1	57	5.29	49	70	10.41	6.94
1	58	3.41	40	82	16.14	11.22
1	59	4.34	44.5	82	12.68	8.59
1	60	2.05	49	82	26.85	20.60
1	61	3.05	40	94	18.05	12.74
1	62	3.66	44.5	94	15.04	10.37
1	63	4.66	49	94	11.81	7.95
1	64	1.76	40	105	31.28	25.24
1	65	5	42	105	11.01	7.37
1	66	2.69	44	105	20.46	14.75
1	67	2.17	40	113.5	25.37	19.16
1	68	3.72	42	113.5	14.80	10.18
1	69	2.27	44	113.5	24.25	18.11
1	70	3.45	40	122	15.96	11.08
1	71	5.12	42	122	10.75	7.19
1	72	5.53	44	122	9.95	6.62
1	73	6.47	80	0	8.51	5.61
1	74	6.59	83	0	8.35	5.50
1	75	5.59	86	0	9.85	6.54
1	76	5.66	80	9	9.73	6.46
1	77	4.99	83	9	11.03	7.39
1	78	5.66	86	9	9.73	6.46
1	79	4.42	80	18	12.45	8.42
1	80	4.74	83	18	11.61	7.81
1	81	5.2	86	18	10.59	7.07
1	82	3.22	80	35	17.09	11.97
1	83	4.42	100	35	12.45	8.42
1	84	3.91	120	35	14.08	9.63
1	85	3.31	80	37	16.63	11.61
1	86	5.74	100	37	9.59	6.36
1	87	4.55	120	37	12.10	8.16
1	88	4.47	80	39	12.31	8.32
1	89	5.39	100	39	10.21	6.80
1	90	3.94	120	39	13.97	9.55
1	91	4.3	80	70	12.80	8.68
1	92	4.47	90	70	12.31	8.32
1	93	5.4	100	70	10.19	6.79
1	94	4.56	80	78.5	12.07	8.14
1	95	6.08	90	78.5	9.05	5.99
1	96	7.02	100	78.5	7.84	5.15
1	97	3.31	80	87	16.63	11.61
1	98	3.52	90	87	15.64	10.83
1	99	4.51	100	87	12.21	8.24
1	100	4.91	80	105	11.21	7.52
1	101	3.2	92.5	105	17.20	12.06
1	102	3.49	105	105	15.77	10.93
1	103	1.81	80	118	30.41	24.29
1	104	2.42	92.5	118	22.75	16.74
1	105	5.36	105	118	10.27	6.84
1	106	5.95	80	131	9.25	6.12
1	107	3.34	92.5	131	16.48	11.49
1	108	4.31	105	131	12.77	8.66
1	109	5.96	120	0	9.24	6.11
1	110	8.95	137	0	6.15	4.00
1	111	9.24	154	0	5.96	3.87
1	112	6.36	120	8.5	8.65	5.71
1	113	6.44	137	8.5	8.55	5.63

1	114	5.07	154	8.5	10.86	7.26
1	115	4.68	120	17	11.76	7.92
1	116	3.99	137	17	13.80	9.42
1	117	4.48	154	17	12.29	8.30
1	118	5.08	120	35	10.84	7.25
1	119	4.81	124	35	11.44	7.69
1	120	4.41	128	35	12.48	8.44
1	121	5.02	120	50	10.97	7.34
1	122	5.57	124	50	9.88	6.57
1	123	3.35	128	50	16.43	11.45
1	124	4.74	120	65	11.61	7.81
1	125	3.02	124	65	18.23	12.89
1	126	5.66	128	65	9.73	6.46
1	127	3.35	120	70	16.43	11.45
1	128	6.31	128.5	70	8.72	5.76
1	129	6.09	137	70	9.04	5.98
1	130	3.71	120	85	14.84	10.21
1	131	6.58	128.5	85	8.37	5.51
1	132	5.1	137	85	10.79	7.22
1	133	6.13	120	100	8.98	5.93
1	134	3.94	128.5	100	13.97	9.55
1	135	4.53	137	100	12.15	8.20
1	136	7.94	120	105	6.93	4.52
1	137	4.41	131.5	105	12.48	8.44
1	138	4.11	143	105	13.39	9.12
1	139	3.74	120	111	14.72	10.12
1	140	4.09	131.5	111	13.46	9.17
1	141	1.67	143	111	32.96	27.16
1	142	4.72	120	117	11.66	7.84
1	143	nm	131.5	117	fracture	
1	144	3.93	143	117	14.01	9.58
1	145	10.11	160	0	5.44	3.52
1	146	10.36	168.5	0	5.31	3.44
1	147	7.23	177	0	7.61	4.99
1	148	6.21	160	17	8.86	5.85
1	149	7.88	168.5	17	6.99	4.56
1	150	8.12	177	17	6.78	4.42
1	151	5.09	160	34	10.81	7.23
1	152	5.64	168.5	34	9.76	6.48
1	153	5.56	177	34	9.90	6.58
1	154	4.75	160	35	11.59	7.79
1	155	3.02	174	35	18.23	12.89
1	156	3.44	188	35	16.00	11.11
1	157	5.09	160	38	10.81	7.23
1	158	4.34	174	38	12.68	8.59
1	159	4.67	188	38	11.79	7.94
1	160	5.85	160	41	9.41	6.23
1	161	2.06	174	41	26.72	20.47
1	162	4.52	188	41	12.18	8.22
1	163	5.18	160	70	10.63	7.10
1	164	4.72	164.5	70	11.66	7.84
1	165	4.79	169	70	11.49	7.72
1	166	nm	160	76	calcite nodule	
1	168	5.31	169	76	10.37	6.91
1	169	6.46	160	82	8.52	5.61
1	170	6.12	164.5	82	8.99	5.94
1	171	5.66	169	82	9.73	6.46
1	172	7.57	160	105	7.27	4.75
1	173	4.99	180	105	11.03	7.39
1	174	4.34	200	105	12.68	8.59

1	175	4.1	160	113	13.43	9.14
1	176	2.95	180	113	18.66	13.24
1	177	4.33	200	113	12.71	8.61
1	178	3.13	160	121	17.59	12.37
1	179	2.66	180	121	20.69	14.95
1	180	3.84	200	121	14.33	9.83
1	181	9.06	205	0	6.08	3.94
1	182	8.3	208	0	6.63	4.32
1	183	9.45	211	0	5.82	3.78
1	184	6.85	205	15.5	8.04	5.28
1	185	5.74	208	15.5	9.59	6.36
1	186	6.15	211	15.5	8.95	5.91
1	187	3.96	205	31	13.90	9.50
1	188	5.34	208	31	10.31	6.87
1	189	5.31	211	31	10.37	6.91
1	190	3.02	205	35	18.23	12.89
1	191	5.9	215	35	9.33	6.18
1	192	5.36	225	35	10.27	6.84
1	193	4.77	205	49.5	11.54	7.76
1	194	7.17	215	49.5	7.68	5.03
1	195	6.52	225	49.5	8.44	5.56
1	196	5.97	205	64	9.22	6.10
1	197	6.98	215	64	7.89	5.18
1	198	6.02	225	64	9.14	6.05
1	199	4.45	205	70	12.37	8.36
1	200	4.37	217	70	12.60	8.53
1	201	2.88	229	70	19.11	13.62
1	202	3.64	205	86.5	15.12	10.43
1	203	4.77	217	86.5	11.54	7.76
1	204	6.17	229	86.5	8.92	5.89
1	205	5.1	205	103	10.79	7.22
1	206	nm	217	103	calcite	nodule
1	207	4.6	229	103	11.97	8.07
1	208	4.4	205	105	12.51	8.46
1	209	5.23	208	105	10.52	7.03
1	210	5.55	211	105	9.92	6.59
1	211	5.13	205	108	10.73	7.17
1	212	5.23	208	108	10.52	7.03
1	213	5.85	211	108	9.41	6.23
1	214	4.7	205	111	11.71	7.88
1	215	4.05	208	111	13.59	9.27
1	216	3.9	211	111	14.11	9.66

SS4 additional sampling
August 3, 1993

	k [darcy]	t[seconds]	q[cc/s]		
1	10.38	3.83	14.50		
	12.54	3.24	17.15		
	18.20	2.37	23.44		
	10.14	3.91	14.21		
	10.20	3.89	14.28		
	7.35	5.25	10.58		
	9.89	4.00	13.89		
	9.42	4.18	13.29		
	9.47	4.16	13.35		
	11.59	3.47	16.01		
	9.60	4.11	13.52		
	9.37	4.20	13.23		
	12.07	3.35	16.58		
	8.86	4.42	12.57		
	8.44	4.62	12.02		
2	6.86	5.60	9.92		
	6.95	5.53	10.05		
	8.28	4.70	11.82		
	7.32	5.27	10.54		
	8.42	4.63	12.00		
	9.49	4.15	13.39		
	8.81	4.44	12.51		
	10.11	3.92	14.17		
	9.25	4.25	13.07		
	8.52	4.58	12.13		
	9.75	4.05	13.72		
	10.50	3.79	14.66		
	10.03	3.95	14.06		
	9.54	4.13	13.45		
	10.05	3.94	14.10		
R3	11.09	3.61	15.39		
	11.19	3.58	15.52		
	11.12	3.60	15.43		
	10.50	3.79	14.66		
	11.23	3.57	15.56		
	9.94	3.98	13.96		
	10.23	3.88	14.32		
	10.38	3.83	14.50		
	13.09	3.12	17.80		
	9.83	4.02	13.82		
	8.36	4.66	11.92		
	8.62	4.53	12.26		
	10.05	3.94	14.10		
	8.42	4.63	12.00		
	8.42	4.63	12.00		
				x[cm]	y[cm]
1	9.81	4.03	13.78	0	0
	18.49	2.34	23.74	2	0
	8.90	4.40	12.63	4	0
	12.07	3.35	16.58	0	2
	12.90	3.16	17.58	2	2
	11.63	3.46	16.05	4	2
	11.05	3.62	15.35	0	4

	14.62	2.84	19.56	2	4
	11.23	3.57	15.56	4	4
S2	10.78	3.70	15.01	0	0
	7.05	5.46	10.17	2	0
	6.82	5.63	9.87	4	0
	8.67	4.51	12.32	0	2
	7.54	5.13	10.83	2	2
	7.99	4.86	11.43	4	2
	8.21	4.74	11.72	0	4
	8.64	4.52	12.29	2	4
	7.43	5.20	10.68	4	4
S3	11.05	3.62	15.35	0	0
	7.49	5.16	10.77	2	0
	11.83	3.41	16.29	4	0
	10.75	3.71	14.97	0	2
	12.95	3.15	17.63	2	2
	11.48	3.50	15.87	4	2
	10.26	3.87	14.35	0	4
	11.95	3.38	16.43	2	4
	11.26	3.56	15.60	4	4
S4	11.67	3.45	16.10	0	0
	9.97	3.97	13.99	2	0
	10.26	3.87	14.35	4	0
	9.34	4.21	13.19	0	2
	7.97	4.87	11.41	2	2
	9.57	4.12	13.48	4	2
	9.18	4.28	12.98	0	4
	9.47	4.16	13.35	2	4
	6.02	6.33	8.78	4	4
S5	9.94	3.98	13.96	0	0
	10.47	3.80	14.62	2	0
	10.85	3.68	15.10	4	0
	10.95	3.65	15.22	0	2
	11.02	3.63	15.30	2	2
	9.97	3.97	13.99	4	2
	8.84	4.43	12.54	0	4
	9.22	4.26	13.04	2	4
	12.36	3.28	16.94	4	4
S6	8.58	4.55	12.21	0	0
	8.90	4.40	12.63	2	0
	9.81	4.03	13.78	4	0
	9.20	4.27	13.01	0	2
	6.40	5.98	9.29	2	2
	9.27	4.24	13.10	4	2
	8.60	4.54	12.24	0	4
	7.49	5.16	10.77	2	4
	10.56	3.77	14.73	4	4
S7	9.81	4.03	13.78	0	0
	7.44	5.19	10.70	2	0
	7.95	4.88	11.38	4	0
	8.42	4.63	12.00	0	2
	7.62	5.08	10.94	2	2
	9.32	4.22	13.16	4	2
	11.91	3.39	16.39	0	4
	13.05	3.13	17.75	2	4
	11.09	3.61	15.39	4	4
S8	9.67	4.08	13.62	0	0
	8.79	4.45	12.48	2	0
	8.17	4.76	11.67	4	0
	10.00	3.96	14.03	0	2

	8.64	4.52	12.29	2	2
	6.19	6.17	9.00	4	2
	7.97	4.87	11.41	0	4
	8.92	4.39	12.65	2	4
	7.57	5.11	10.87	4	4
39	9.60	4.11	13.52	0	0
	10.05	3.94	14.10	2	0
	10.41	3.82	14.54	4	0
	11.48	3.50	15.87	0	2
	10.26	3.87	14.35	2	2
	11.30	3.55	15.65	4	2
	11.30	3.55	15.65	0	4
	11.02	3.63	15.30	2	4
	11.16	3.59	15.47	4	4

SS5 data
October 3, 1992

region	n	time	x(cm)	y(cm)	q(cc/s)	k(darcy)
1	1	1.28	0	0	43.00	43.00
1	2	1.99	20	0	27.66	21.41
1	3	1.45	40	0	37.96	33.49
1	4	1.66	0	12	33.16	27.39
1	5	3.19	20	12	17.26	12.10
1	6	3.38	40	12	16.29	11.33
2	7	1.62	0	24	33.98	28.36
2	8	1.79	20	24	30.75	24.66
2	9	1.85	40	24	29.75	23.58
2	10	1.44	0	30	38.23	33.85
2	11	1.07	11	30	51.44	57.96
2	12	2.62	22	30	21.01	15.22
2	13	1.15	0	36	47.87	50.01
2	14	2.19	11	36	25.13	18.94
2	15	2.68	22	36	20.54	14.82
2	16	2.71	0	42	20.31	14.62
2	17	1.45	11	42	37.96	33.49
2	18	1.31	22	42	42.02	39.48
2	19	2.58	0	60	21.34	15.50
2	20	2.31	2	60	23.83	17.73
2	21	3.7	4	60	14.88	10.24
2	22	0.89	0	62	61.85	92.66
2	23	2.05	2	62	26.85	20.60
2	24	2.68	4	62	20.54	14.82
2	25	0.79	0	64	69.68	143.80
2	26	3.34	2	64	16.48	11.49
2	27	2.5	4	64	22.02	16.10
1	28	1.17	50	0	47.05	48.37
1	29	1.27	57	0	43.34	41.65
1	30	0.91	64	0	60.49	86.69
1	31	0.99	50	4	55.60	69.26
1	32	1.2	57	4	45.87	46.12
1	33	1.04	64	4	52.93	61.70
1	34	1.23	50	8	44.75	44.08
1	35	2.16	57	8	25.48	19.27
1	36	nm	64	8	clay drape	
2	37	1.67	50	30	32.96	27.16
2	38	nm	56	30	clay drape	
2	39	2.52	62	30	21.84	15.94
2	40	3.14	50	38	17.53	12.32
2	41	2.45	56	38	22.47	16.50
2	42	2.55	62	38	21.59	15.72
2	43	4.59	50	46	11.99	8.08
2	44	2.34	56	46	23.52	17.45
2	45	2.99	62	46	18.41	13.04
2	46	2.91	50	60	18.92	13.45
2	47	4.66	72	60	11.81	7.95
2	48	2.97	94	60	18.53	13.14
3	49	2.77	50	73	19.87	14.25
3	50	1.95	72	73	28.23	21.99
3	51	2.49	94	73	22.11	16.18
3	52	2.49	50	86	22.11	16.18
3	53	2.84	72	86	19.38	13.84

3	54	2.12	94	86	25.96	19.74
1	55	1.46	100	0	37.70	33.13
1	56	1.52	117	0	36.21	31.16
1	57	2.22	134	0	24.80	18.62
1	58	2.02	100	10	27.25	21.00
1	59	2.11	117	10	26.09	19.86
1	60	2.27	134	10	24.25	18.11
1	61	1.74	100	20	31.64	25.64
1	62	2.43	117	20	22.65	16.66
1	63	2.6	134	20	21.17	15.36
2	64	2.35	100	34	23.42	17.36
2	65	1.73	118	34	31.82	25.84
2	66	1.39	136	34	39.60	35.80
2	67	2.87	100	45	19.18	13.67
2	68	2.88	118	45	19.11	13.62
2	69	2.77	136	45	19.87	14.25
2	70	4.34	100	56	12.68	8.59
2	71	4.09	118	56	13.46	9.17
2	72	3.94	136	56	13.97	9.55
2	73	2.59	100	60	21.25	15.43
2	74	2.5	111	60	22.02	16.10
2	75	2.4	122	60	22.94	16.91
3	76	2.68	100	67	20.54	14.82
3	77	2.19	111	67	25.13	18.94
3	78	1.99	122	67	27.66	21.41
3	79	1.48	100	74	37.19	32.44
3	80	2.1	111	74	26.21	19.98
3	81	2.24	122	74	24.57	18.42
1	82	1.9	150	0	28.97	22.75
1	83	2.06	173	0	26.72	20.47
1	84	1.39	196	0	39.60	35.80
1	85	2.59	150	14	21.25	15.43
1	86	2.38	173	14	23.13	17.09
1	87	1.02	196	14	53.97	64.50
1	88	2.16	150	28	25.48	19.27
1	89	3.6	173	28	15.29	10.56
1	90	3.54	196	28	15.55	10.76
2	91	1.23	150	38	44.75	44.08
2	92	2.74	164	38	20.09	14.43
2	93	1.88	178	38	29.28	23.08
2	94	1.09	150	46	50.50	55.72
2	95	1.9	164	46	28.97	22.75
2	96	2.28	178	46	24.14	18.02
2	97	3.14	150	54	17.53	12.32
2	98	2.94	164	54	18.72	13.29
2	99	2.03	178	54	27.12	20.86
2	100	2.84	150	60	19.38	13.84
2	101	1.52	153	60	36.21	31.16
2	102	2.79	156	60	19.73	14.13
2	103	3.64	150	62	15.12	10.43
2	104	3.99	153	62	13.80	9.42
2	105	4.14	156	62	13.30	9.05
2	106	2.28	150	64	24.14	18.02
2	107	3.49	153	64	15.77	10.93
2	108	2.34	156	64	23.52	17.45
1	109	2.88	200	0	19.11	13.62
1	110	1.83	209	0	30.08	23.93
1	111	1.66	218	0	33.16	27.39
1	112	3.24	200	6	16.99	11.89
1	113	1.39	209	6	39.60	35.80

1	114	1.94	218	6	28.37	22.14
1	115	2.17	200	12	25.37	19.16
1	116	1.81	209	12	30.41	24.29
1	117	nm	218	12	hole	
1	118	2.2	200	30	25.02	18.84
1	119	1.78	222	30	30.92	24.85
1	120	2.08	244	30	26.46	20.22
2	121	2.56	200	43	21.50	15.65
2	122	3.66	222	43	15.04	10.37
2	123	2.68	244	43	20.54	14.82
2	124	3.69	200	56	14.92	10.27
2	125	2.31	222	56	23.83	17.73
2	126	2.49	244	56	22.11	16.18
2	127	2.51	200	60	21.93	16.02
2	128	4.06	216	60	13.56	9.24
2	129	2.67	232	60	20.62	14.88
2	130	3.38	200	75	16.29	11.33
2	131	3.06	216	75	17.99	12.69
2	132	3.13	232	75	17.59	12.37
3	133	1.95	200	90	28.23	21.99
3	134	3.08	216	90	17.87	12.60
3	135	2.12	232	90	25.96	19.74
1	136	3.1	250	0	17.76	12.51
1	137	2.75	273	0	20.02	14.37
1	138	nm	296	0	fracture	
1	139	2.9	250	14	18.98	13.51
1	140	2.32	273	14	23.73	17.63
1	141	nm	296	14	fracture	
1	142	2.41	250	28	22.84	16.83
1	143	3.45	273	28	15.96	11.08
1	144	nm	296	28	fracture	
1	145	2.57	250	30	21.42	15.57
1	146	2.41	260	30	22.84	16.83
1	147	2.03	270	30	27.12	20.86
2	148	3.16	250	40	17.42	12.23
2	149	2.56	260	40	21.50	15.65
2	150	2.89	270	40	19.05	13.56
2	151	2.98	250	50	18.47	13.09
2	152	1.98	260	50	27.80	21.55
2	153	3.58	270	50	15.38	10.63
2	154	3.58	250	60	15.38	10.63
2	155	3.61	255	60	15.25	10.53
2	156	3.24	260	60	16.99	11.89
2	157	3.67	250	63	15.00	10.34
2	158	2.83	255	63	19.45	13.90
2	159	2.82	260	63	19.52	13.95
2	160	3.08	250	66	17.87	12.60
2	161	3.99	255	66	13.80	9.42
2	162	2.89	260	66	19.05	13.56
3	163	2.50	250	78	22.02	16.10
3	164	3.41	260	78	16.14	11.22
3	165	2.59	270	78	21.25	15.43
3	166	2.16	250	87	25.48	19.27
3	167	2.08	260	87	26.46	20.22
3	168	2.26	270	87	24.36	18.21
3	169	2.48	250	96	22.20	16.25
3	170	2.57	260	96	21.42	15.57
3	171	3.43	270	96	16.05	11.15
1	172	2.33	300	28	23.62	17.54
1	173	2.41	309	28	22.84	16.83

1	174	2.32	318	28	23.73	17.63
1	175	1.52	300	33	36.21	31.16
1	176	3.35	309	33	16.43	11.45
1	177	3.23	318	33	17.04	11.93
1	178	2.23	300	38	24.68	18.52
1	179	2.44	309	38	22.56	16.58
1	180	2.41	318	38	22.84	16.83
2	181	3.25	300	58	16.94	11.85
2	182	3.38	307	58	16.29	11.33
2	183	3.26	314	58	16.88	11.81
2	184	5.41	300	62	10.17	6.78
2	185	3.97	307	62	13.87	9.47
2	186	4.63	314	62	11.89	8.01
2	187	1.59	300	66	34.62	29.14
2	188	3.02	307	66	18.23	12.89
2	189	2.83	314	66	19.45	13.90
2	190	3.57	300	88	15.42	10.66
2	191	3.44	319	88	16.00	11.11
2	192	3.3	338	88	16.68	11.65
3	193	4.02	300	99	13.69	9.34
3	194	4.46	319	99	12.34	8.34
3	195	2.13	338	99	25.84	19.62
3	196	1.57	300	110	35.06	29.69
3	197	1.59	319	110	34.62	29.14
3	198	3.11	338	110	17.70	12.46

SS5 additional sampling
August 4, 1993

	k [darcy]	t[seconds]	q[cc/s]		
R1	20.97	2.12	26.20		
	22.79	1.99	27.91		
	22.63	2.00	27.78		
	23.91	1.92	28.93		
	24.08	1.91	29.08		
	20.11	2.19	25.37		
	21.77	2.06	26.97		
	20.97	2.12	26.20		
	20.59	2.15	25.84		
	16.47	2.57	21.61		
	18.49	2.34	23.74		
	19.99	2.20	25.25		
	22.34	2.02	27.50		
	18.79	2.31	24.05		
	22.34	2.02	27.50		
R2	20.84	2.13	26.08		
	26.98	1.76	31.56		
	22.34	2.02	27.50		
	19.99	2.20	25.25		
	25.54	1.83	30.36		
	23.58	1.94	28.63		
	12.86	3.17	17.52		
	15.52	2.70	20.57		
	15.66	2.68	20.73		
	12.63	3.22	17.25		
	13.87	2.97	18.70		
	11.63	3.46	16.05		
	13.29	3.08	18.04		
	15.18	2.75	20.20		
	15.80	2.66	20.88		
R3	12.67	3.21	17.31		
	11.63	3.46	16.05		
	11.48	3.50	15.87		
	10.59	3.76	14.77		
	10.56	3.77	14.73		
	10.98	3.64	15.26		
	10.85	3.68	15.10		
	11.75	3.43	16.20		
	12.32	3.29	16.88		
	11.37	3.53	15.74		
	9.30	4.23	13.13		
	10.08	3.93	14.13		
	11.52	3.49	15.92		
	10.78	3.70	15.01		
	10.62	3.75	14.81		
				x[cm]	y[cm]
S1	24.61	1.88	29.55	0	0
	29.90	1.64	33.87	2	0
	21.10	2.11	26.33	4	0
	11.41	3.52	15.78	0	2
	8.01	4.85	11.45	2	2
	12.41	3.27	16.99	4	2
	10.75	3.71	14.97	0	4
	8.99	4.36	12.74	2	4

	10.17	3.90	14.24	4	4
S2	32.57	1.55	35.84	0	0
	27.43	1.74	31.93	2	0
	29.63	1.65	33.67	4	0
	27.43	1.74	31.93	0	2
	20.84	2.13	26.08	2	2
	21.36	2.09	26.58	4	2
	26.14	1.80	30.86	0	4
	19.65	2.23	24.91	2	4
	23.10	1.97	28.20	4	4
S3	10.53	3.78	14.70	0	0
	9.94	3.98	13.96	2	0
	9.67	4.08	13.62	4	0
	10.38	3.83	14.50	0	2
	11.52	3.49	15.92	2	2
	10.32	3.85	14.43	4	2
	9.97	3.97	13.99	0	4
	13.05	3.13	17.75	2	4
	14.09	2.93	18.96	4	4
S4	16.95	2.51	22.13	0	0
	20.47	2.16	25.72	2	0
	16.02	2.63	21.12	4	0
	15.52	2.70	20.57	0	2
	14.49	2.86	19.42	2	2
	15.32	2.73	20.35	4	2
	26.77	1.77	31.38	0	4
	21.63	2.07	26.84	2	4
	32.90	1.54	36.07	4	4
S5	12.23	3.31	16.78	0	0
	10.78	3.70	15.01	2	0
	9.20	4.27	13.01	4	0
	14.32	2.89	19.22	0	2
	10.26	3.87	14.35	2	2
	10.11	3.92	14.17	4	2
	12.90	3.16	17.58	0	4
	11.16	3.59	15.47	2	4
	12.81	3.18	17.47	4	4
S6	10.98	3.64	15.26	0	0
	8.67	4.51	12.32	2	0
	11.41	3.52	15.78	4	0
	15.52	2.70	20.57	0	2
	15.66	2.68	20.73	2	2
	24.08	1.91	29.08	4	2
	10.05	3.94	14.10	0	4
	17.21	2.48	22.40	2	4
	18.49	2.34	23.74	4	4
S7	11.37	3.53	15.74	0	0
	12.41	3.27	16.99	2	0
	9.75	4.05	13.72	4	0
	10.82	3.69	15.05	0	2
	14.38	2.88	19.29	2	2
	12.23	3.31	16.78	4	2
	15.05	2.77	20.05	0	4
	20.47	2.16	25.72	2	4
	12.58	3.23	17.20	4	4
S8	14.20	2.91	19.09	0	0
	12.81	3.18	17.47	2	0
	12.49	3.25	17.09	4	0
	17.46	2.45	22.67	0	2
	14.44	2.87	19.36	2	2

	23.25	1.96	28.34	4	2
	14.62	2.84	19.56	0	4
	11.95	3.38	16.43	2	4
	13.44	3.05	18.21	4	4
S9	15.95	2.64	21.04	0	0
	13.92	2.96	18.77	2	0
	19.54	2.24	24.80	4	0
	18.79	2.31	24.05	0	2
	12.81	3.18	17.47	2	2
	17.12	2.49	22.31	4	2
	10.92	3.66	15.18	0	4
	10.88	3.67	15.14	2	4
	13.09	3.12	17.80	4	4

SS6 data
May 22, 1993

time(s)	x(cm)	y(cm)	q(cc/s)	k(darcy)
2.34	0	0	23.52	17.45
3.89	5	0	14.15	9.69
1.38	10	0	39.89	36.22
3.15	15	0	17.47	12.28
1.95	40	0	28.23	21.99
3.4	43	0	16.19	11.26
5.47	58	0	10.06	6.70
6.9	68	0	7.98	5.24
7.8	78	0	7.06	4.61
7.7	6	10	7.15	4.67
5.34	15	11	10.31	6.87
4.01	26	11	13.73	9.37
6.62	40	10	8.31	5.47
4.52	48	12	12.18	8.22
3.26	60	19	16.88	11.81
5.91	70	16	9.31	6.17
3.55	79	17	15.51	10.73
2.82	90	13	19.52	13.95
8.27	2	21	6.66	4.34
6.95	12	23	7.92	5.20
9.63	22	24	5.72	3.70
7.57	38	25	7.27	4.75
12.36	41	24	4.45	2.87
4.75	45	24	11.59	7.79
5.1	56	25	10.79	7.22
2.45	68	25	22.47	16.50
11.61	75	26	4.74	3.06
10.84	85	24	5.08	3.28
3.66	97	23	15.04	10.37
10.01	1	28	5.50	3.56
4.34	11	32	12.68	8.59
3.06	18	33	17.99	12.69
3.13	26	31	17.59	12.37
7.39	34	32	7.45	4.88
4.78	40	32	11.52	7.74
6.09	48	30	9.04	5.98
4.3	55	33	12.80	8.68
6.38	59	36	8.63	5.69
8.62	64	35	6.39	4.15
3.35	68	35	16.43	11.45
7.05	73	35	7.81	5.12
3.95	77	33	13.94	9.53
3.49	85	30	15.77	10.93
9.14	2	40	6.02	3.91
6.06	9	43	9.08	6.01
17.65	14	42	3.12	1.99
7.63	19	42	7.21	4.72
5.62	22	40	9.79	6.51
4.06	32	41	13.56	9.24
4.97	37	41	11.08	7.42
3.06	39	41	17.99	12.69
6.88	43	43	8.00	5.25
3.63	47	41	15.16	10.46
3.37	51	43	16.33	11.37

4.01	56	47	13.73	9.37
2.57	66	45	21.42	15.57
4.88	75	47	11.28	7.57
4.13	77	45	13.33	9.07
3.68	90	49	14.96	10.30
4.46	94	47	12.34	8.34
5.42	99	47	10.16	6.76
9.54	2.5	44	5.77	3.74
3.41	13.5	46.5	16.14	11.22
3.59	17	48	15.33	10.59
5.94	21	47.5	9.27	6.13
6.13	30	47	8.98	5.93
5.13	34.5	48	10.73	7.17
7.97	39	49	6.91	4.51
6.25	47.5	50.5	8.81	5.81
6.47	50.5	51.5	8.51	5.61
2.92	57	54	18.85	13.40
4.43	63	55	12.43	8.40
3.78	70	55	14.56	10.00
4.38	76.5	53.5	12.57	8.51
3.55	81	52	15.51	10.73
9	85	51	6.12	3.97
4.46	97.5	56	12.34	8.34
5.8	102	56	9.49	6.29
1.73	3	54	31.82	25.84
1.45	40	55	37.96	33.49
3.36	50	55	16.38	11.41
3.77	60	59	14.60	10.03
2.81	65.5	59	19.59	14.01
2.47	69.5	59	22.29	16.33
3.65	74.5	59	15.08	10.40
5.72	81.5	60	9.62	6.39
5.88	86	60	9.36	6.20
4.24	97	61	12.98	8.81
5.99	102.5	61	9.19	6.08
2.24	109	67	24.57	18.42
3.61	102	66	15.25	10.53
3.78	96	66	14.56	10.00
2.27	92	65	24.25	18.11
4.17	82	64	13.20	8.98
7.68	11	9.5	7.17	4.68
4.91	20.5	9.5	11.21	7.52
4.45	33	9	12.37	8.36
7.22	39.5	10	7.62	5.00
3.6	54.5	13	15.29	10.56
5.49	68	16	10.03	6.67
4.41	74	16	12.48	8.44
5.16	83	19	10.67	7.13
7.41	88	21.5	7.43	4.86

SS6 additional data
August 4, 1993

	k[darcy]	t[seconds]	q[cc/s]		
R1	7.15	5.39	10.31		
	8.42	4.63	12.00		
	6.51	5.88	9.45		
	6.72	5.71	9.73		
	7.52	5.14	10.81		
	8.88	4.41	12.60		
	6.73	5.70	9.75		
	6.82	5.63	9.87		
	6.97	5.52	10.06		
	6.73	5.70	9.75		
	5.90	6.45	8.61		
	6.65	5.77	9.63		
	6.49	5.90	9.42		
	7.37	5.24	10.60		
	6.63	5.78	9.61		
R2	11.59	3.47	16.01		
	11.41	3.52	15.78		
	9.57	4.12	13.48		
	9.44	4.17	13.32		
	11.16	3.59	15.47		
	11.05	3.62	15.35		
	9.65	4.09	13.58		
	11.41	3.52	15.78		
	22.34	2.02	27.50		
	9.70	4.07	13.65		
	9.20	4.27	13.01		
	11.91	3.39	16.39		
	7.73	5.01	11.09		
	7.75	5.00	11.11		
	7.73	5.01	11.09		
R3	8.81	4.44	12.51		
	9.47	4.16	13.35		
	8.73	4.48	12.40		
	8.95	4.38	12.68		
	12.23	3.31	16.78		
	15.66	2.68	20.73		
	10.78	3.70	15.01		
	11.37	3.53	15.74		
	9.34	4.21	13.19		
	9.11	4.31	12.89		
	8.90	4.40	12.63		
	9.78	4.04	13.75		
	7.94	4.89	11.36		
	8.25	4.72	11.77		
	7.88	4.92	11.29		
				x[cm]	y[cm]
S1	4.70	8.02	6.93	0	0
	2.55	14.49	3.83	2	0
	6.30	6.07	9.15	4	0
	7.35	5.25	10.58	0	2
	5.96	6.39	8.69	2	2
	6.15	6.21	8.95	4	2
	5.90	6.46	8.60	0	4

	5.41	7.01	7.92	2	4
	8.46	4.61	12.05	4	4
S2	1.85	19.84	2.80	0	0
	1.74	21.10	2.63	2	0
	15.73	2.67	20.81	4	0
	22.34	2.02	27.50	0	2
	9.86	4.01	13.85	2	2
	16.32	2.59	21.45	4	2
	5.23	7.24	7.67	0	4
	5.97	6.38	8.71	2	4
	7.54	5.13	10.83	4	4
S3	9.81	4.03	13.78	0	0
	7.43	5.20	10.68	2	0
	2.10	17.54	3.17	4	0
	3.31	11.26	4.93	0	2
	4.19	8.95	6.21	2	2
	11.59	3.47	16.01	4	2
	3.58	10.42	5.33	0	4
	6.52	5.87	9.46	2	4
	7.87	4.93	11.27	4	4
S4	20.11	2.19	25.37	0	0
	15.05	2.77	20.05	2	0
	17.12	2.49	22.31	4	0
	4.26	8.81	6.31	0	2
	3.57	10.46	5.31	2	2
	5.58	6.81	8.16	4	2
	5.97	6.38	8.71	0	4
	10.23	3.88	14.32	2	4
	8.64	4.52	12.29	4	4
S5	17.55	2.44	22.77	0	0
	5.15	7.35	7.56	2	0
	3.42	10.91	5.09	4	0
	5.84	6.52	8.52	0	2
	3.15	11.81	4.70	2	2
	6.47	5.92	9.38	4	2
	8.86	4.42	12.57	0	4
	6.10	6.25	8.89	2	4
	5.53	6.86	8.10	4	4
S6	2.34	15.81	3.51	0	0
	5.85	6.51	8.53	2	0
	3.90	9.59	5.79	4	0
	4.69	8.03	6.92	0	2
	4.64	8.12	6.84	2	2
	8.28	4.70	11.82	4	2
	7.29	5.29	10.50	0	4
	9.18	4.28	12.98	2	4
	10.62	3.75	14.81	4	4
S7	4.17	8.99	6.18	0	0
	8.30	4.69	11.84	2	0
	4.93	7.66	7.25	4	0
	6.05	6.30	8.82	0	2
		nm		2	2
	3.30	11.29	4.92	4	2
	6.98	5.51	10.08	0	4
	4.27	8.80	6.31	2	4
	9.27	4.24	13.10	4	4
S8	8.75	4.47	12.43	0	0
	4.12	9.09	6.11	2	0
	8.08	4.81	11.55	4	0
	2.49	14.88	3.73	0	2

	4.92	7.67	7.24	2	2
	2.79	13.29	4.18	4	2
	3.88	9.64	5.76	0	4
	4.37	8.59	6.47	2	4
	2.67	13.86	4.01	4	4
S9	10.35	3.84	14.47	0	0
	4.50	8.36	6.64	2	0
	8.56	4.56	12.18	4	0
	8.88	4.41	12.60	0	2
	6.52	5.87	9.46	2	2
	13.92	2.96	18.77	4	2
	4.56	8.25	6.73	0	4
	5.12	7.38	7.53	2	4
	3.52	10.61	5.24	4	4

ES1 data
March 26, 1993

facies	x(cm)	y(cm)	time(s)	q(cc/s)	k(darcy)
a	0	183	0.88	62.55	95.99
b	0	180	1.02	53.97	64.50
b	0	178.5	2.26	24.36	18.21
b	0	177	1.13	48.71	51.77
b/c	0	175.5	1.85	29.75	23.58
c	0	174	1.10	50.04	54.67
c	0	172.5	1.24	44.39	43.44
c	0	171	1.92	28.67	22.44
c	0	169.5	1.85	29.75	23.58
c	0	168	1.68	32.76	26.93
c	0	166.5	1.63	33.77	28.11
c	0	165	2.16	25.48	19.27
d	0	163.5	1.63	33.77	28.11
d	0	162	1.78	30.92	24.85
d	0	160	2.16	25.48	19.27
e	0	158.5	2.18	25.25	19.05
f	0	157	1.57	35.06	29.69
f	0	155.5	1.60	34.40	28.88
f	0	154	2.13	25.84	19.62
f	0	152.5	2.72	20.24	14.56
g	0	151	2.44	22.56	16.58
g	0	149.5	1.69	32.57	26.70
g	0	148	1.60	34.40	28.88
g	0	146.5	1.66	33.16	27.39
g	0	145	3.02	18.23	12.89
h	0	143.5	1.94	28.37	22.14
h	0	142	2.72	20.24	14.56
h/i	0	140.5	1.97	27.94	21.69
i	0	139	1.48	37.19	32.44
i	0	137.5	1.63	33.77	28.11
i	0	136	2.20	25.02	18.84
i	0	135	2.06	26.72	20.47
i	0	133.5	1.93	28.52	22.29
i	0	132	2.16	25.48	19.27
j	0	128	0.97	56.75	72.88
j	0	125	1.09	50.50	55.72
j	0	123	0.91	60.49	86.69
k	0	120	1.13	48.71	51.77
k	0	118	1.03	53.44	63.07
l	0	116	0.96	57.34	74.84
l	0	114	1.04	52.93	61.70
l	0	112	1.24	44.39	43.44
l	0	110	1.48	37.19	32.44
l	0	108	1.38	39.89	36.22
l	0	106	1.00	55.05	67.59
l	0	101.5	1.28	43.00	41.08
l	0	100	1.13	48.71	51.77
l	0	98.5	1.42	38.76	34.60
l	0	97	1.12	49.15	52.70
l	0	95	1.04	52.93	61.70
l	0	93	1.19	46.26	46.84
l	0	91	1.31	42.02	39.48
l	0	89	0.96	57.34	74.84
l	0	87	1.07	51.44	57.96

l	0	85	1.01	54.50	66.01
l	0	83	0.94	58.56	79.14
l	0	81	nm	coarse	material
l	0	77	1.10	50.04	54.67
l	0	73	nm	coarse	material
m	0	67	1.15	47.87	50.01
m	0	60	0.92	59.83	84.01
m	0	57	1.00	55.05	67.59
m	0	53	1.29	42.67	40.53
m	0	47	0.94	58.56	79.14
m	0	43	1.10	50.04	54.67
m	0	37	1.47	37.45	32.78
n	0	30	1.92	28.67	22.44
n	0	28	2.52	21.84	15.94
n	0	26	2.02	27.25	21.00
n	0	24	2.37	23.23	17.18
n	0	22	1.99	27.66	21.41
n	0	17	2.16	25.48	19.27
n	0	15	2.00	27.52	21.27
n	0	13	2.35	23.42	17.36
o	0	10	3.31	16.63	11.61
o	0	6	3.59	15.33	10.59
p	0	3	1.18	46.65	47.59
p	0	0	1.11	49.59	53.67

APPENDIX B: Variogram calculations

Variogram estimates from second sampling data set are indicated by "*". Direction in degrees from horizonatal, angle tolerance and maximum bandwidth used in variogram calculation are also given. The number of pairs, average distance and value of the variogram are shown.

ss1 horizontal

pairs	avg dist		value	direction	0
420	0.000	*	0.024	tol	25
48	2.000	*	0.059	max bw	25
56	4.027	*	0.081		
71	7.724		0.098		
91	14.876		0.093		
73	24.375		0.153		
130	36.072		0.147		
294	47.559		0.176		
221	62.794		0.183		
256	77.714		0.189		
265	91.642		0.177		
178	107.363		0.221		
160	122.172		0.189		

ss1 vertical

pairs	avg dist		value	direction	90
420	0	*	0.024	tol	25
48	2	*	0.095	max bw	25
56	4.27	*	0.107		
62	4.5		0.110		
55	12.521		0.155		
41	19.972		0.197		
78	28.539		0.158		
84	35.277		0.160		
108	40.894		0.158		
119	47.335		0.220		
115	52.873		0.201		
100	58.879		0.240		
66	64.619		0.251		
73	71.566		0.220		

ss2 horizontal

pairs	avg dist	value	direc	0
420	0	*0.018	tol	35
48	2	*0.043	max bw	35
56	4.27	*0.085		
91	4.798	0.055		
42	14.752	0.112		
77	23.198	0.100		
213	35.022	0.130		
353	43.938	0.109		
201	53.884	0.123		
127	62.895	0.143		
218	74.23	0.120		
347	84.12	0.162		

ss2 vertical

pairs	avg dist		value		
420	0	*	0.018	direction	90
48	2	*	0.085	tolerance	35
56	4.27	*	0.076	max bw	35
106	5.226		0.098		
93	9.876		0.111		
60	17.114		0.138		
124	24.909		0.173		
182	31.587		0.143		
161	38.465		0.135		
155	45.477		0.165		
138	52.465		0.151		
217	59.624		0.169		
226	66.437		0.168		
162	73.155		0.238		
113	80.322		0.266		

SS3 horizontal

pairs	avg dist	value	direc	0
315	0.000	*0.036	tol	20
54	2.000	*0.072	max bw	20
64	4.270	*0.150		
92	10.023	0.076		
106	24.980	0.164		
160	37.064	0.202		
218	49.049	0.299		
175	62.188	0.282		
244	75.408	0.267		
154	93.280	0.266		
150	104.855	0.276		
170	116.903	0.248		
133	133.433	0.316		

SS3 vertical

pairs	avg dist	value	direc	90
315	0.000	*0.036	tol	30
54	2.000	*0.189	max bw	30
63	4.270	*0.363		
63	6.303	0.204		
94	14.601	0.456		
130	25.214	0.653		
121	34.326	0.752		
140	44.659	0.379		
134	54.935	0.210		

SS4 horizontal

pairs	avg dist	value	direc	0
315	0.000	*0.027	tol	20
54	2.000	*0.027	max bw	20
63	4.270	*0.017		
91	6.241	0.065		
132	15.982	0.094		
127	25.356	0.085		
183	35.694	0.072		
290	44.397	0.096		
234	54.323	0.106		
240	64.615	0.118		
229	75.502	0.083		
334	84.540	0.098		
193	94.141	0.101		
214	104.316	0.093		
183	115.336	0.129		
257	124.388	0.130		
148	135.179	0.131		

SS4 vertical

pairs	avg dist	value	direc	90
315	0.000	*0.027	tol	25
54	2.000	*0.019	max bw	25
63	4.270	*0.032		
87	6.252	0.077		
78	13.727	0.089		
113	19.726	0.100		
140	28.368	0.111		
242	36.149	0.101		
177	43.652	0.126		
199	52.149	0.065		
144	60.115	0.071		
238	68.485	0.096		
213	75.731	0.088		
151	83.984	0.109		

SS5 horizontal

pairs	avg dist	value	direc	0
315	0.000	*0.031	tol	20
54	2.000	*0.030	max bw	20
63	4.270	*0.050		
84	7.592	0.164		
149	20.211	0.131		
132	32.012	0.163		
254	42.578	0.163		
410	53.395	0.203		
289	65.302	0.162		
259	77.913	0.183		
223	90.129	0.207		
366	101.429	0.219		
253	113.971	0.211		
195	124.981	0.228		
231	137.338	0.203		
345	149.938	0.252		
230	161.150	0.224		
163	174.521	0.216		

SS5 vertical

pairs	avg dist	value	direc	90
315	0.000	*0.031	tol	20
54	2.000	*0.066	max bw	20
63	4.270	*0.104		
94	6.333	0.142		
108	15.164	0.214		
166	25.819	0.206		
198	34.964	0.233		
136	45.710	0.289		
122	54.952	0.225		
125	64.061	0.247		
66	75.029	0.248		

SS6 horizontal

pairs	avg dist	value	direc	0
315	0.000	*0.037	tol	30
52	2.000	*0.200	max bw	30
63	4.270	*0.301		
69	5.319	0.161		
146	12.081	0.161		
227	19.913	0.203		
262	28.129	0.227		
298	35.963	0.229		
279	44.006	0.222		
274	51.926	0.239		
263	59.975	0.286		
187	67.785	0.275		

SS6 vertical

pairs	avg dist	value	direc	90
315	0.000	*0.031	tol	25
52	2.000	*0.066	max bw	25
63	4.270	*0.104		
56	7.739	0.142		
151	15.315	0.214		
164	24.664	0.206		
231	34.680	0.233		
188	44.507	0.289		
77	54.348	0.225		

ES1 variogram

pairs	avg dist	value	direc	0
299	5.080	0.100	tol	5
284	13.694	0.155	max bw	5
279	22.650	0.222		
229	31.646	0.279		
209	40.751	0.314		
201	49.904	0.344		
170	67.771	0.338		
150	76.704	0.372		
134	85.630	0.406		
116	94.685	0.447		
95	104.089	0.444		
98	113.069	0.299		
93	122.059	0.170		
88	131.192	0.133		

APPENDIX C: Calcite nodule data

4 calcite nodule count

pprox. diameter (cm)	count	total: 31
1.0	3	avg (cm): 4.4
1.9	7	std. dev.: 3.25
2.9	1	
3.8	9	
5.7	7	
7.6	2	
11.4	1	
17.1	1	

calcite nodule count

pprox. diameter (cm)	count	total: 127
0.05	69	avg (cm): 0.7
0.8	26	std. dev.:0.87
1.3	4	
1.7	18	
2.5	9	
5.0	1	

istance is in centimeters away from center of nodule.
here no distance is indicated, measurements were taken
t points judged to be as far away as possible from calite.

S6 calcite nodule data

.(cm)	time(s)	k(darcy)	q(cc/s)
2	14.34	2.58	3.87
2	5.5	6.99	10.1
2	4.28	9.18	12.98
2	10.02	3.73	5.54
2	5.71	6.72	9.73
2	11.13	3.35	4.99
2	6.42	5.93	8.65
2	3.02	13.6	18.39
2	14.17	2.61	3.92
2	7.3	5.18	7.61
2	9.38	3.99	5.92
2	12.2	3.05	4.55
2	5.61	6.85	9.9
2	10.65	3.5	5.22
2	4.46	8.77	12.46
2	3.28	12.36	16.94
2	16.33	2.26	3.4
1	5.32	7.25	10.44
1	7.39	5.12	7.52
1	5.99	6.39	9.27
1	10.36	3.6	5.36
1	4.77	8.15	11.65
1	3.27	12.41	16.99
1	6.24	6.12	8.9
1	8.78	4.28	6.33
1	9.5	3.94	5.85
1	9.9	3.78	5.61
1	5.35	7.2	10.38
1	9.27	4.04	5.99
1	3.88	10.23	14.32
1	5.02	7.71	11.07
1	3.43	11.75	16.2
1	5.86	6.54	9.48
1	7.83	4.82	7.09
1	5.04	7.68	11.02
1	9.17	4.09	6.06
1	5.73	6.69	9.69
1	10.87	3.43	5.11
1	5.46	7.05	10.17
1	9.49	3.94	5.85
1	3.5	11.48	15.87
1	8.73	4.3	6.36
1	5.26	7.34	10.56
1	8.76	4.29	6.34
1	10.09	3.7	5.51
1	11.49	3.24	4.83
1	3.28	12.36	16.94
1	7.89	4.78	7.04
1	7.04	5.38	7.89

5.55	6.93	10.01
10.13	3.69	5.48
5.8	6.61	9.58
3.05	13.44	18.21
5.45	7.06	10.19
4.8	8.1	11.57
4.16	9.47	13.35
3.43	11.75	16.2
6.58	5.78	8.44
2.39	18.01	23.24
6.55	5.81	8.48
5.37	7.18	10.34
10.21	3.66	5.44
5.16	7.49	10.77
2.45	17.46	22.67
5.48	7.02	10.14
5.2	7.43	10.68
5.25	7.35	10.58
6.93	5.47	8.02
4.38	8.95	12.68
6.16	6.2	9.02
7.38	5.12	7.53
3.81	10.44	14.58
8.63	4.35	6.44

SS4 calcite nodule data

t(cm)	t(s)	k(darcy)	q(cc/s)
2	7.81	4.83	7.11
2	7.12	5.32	7.80
2	4.73	8.23	11.74
2	4.2	9.37	13.23
2	4.74	8.21	11.72
2	5.14	7.52	10.81
2	4.84	8.03	11.48
2	5.38	7.16	10.33
2	11.69	3.18	4.75
2	9.6	3.90	5.79
2	9.84	3.80	5.65
2	16.35	2.26	3.40
2	3.87	10.26	14.35
2	4.46	8.77	12.46
2	13.46	2.75	4.13
2	4.55	8.58	12.21
2	9.81	3.81	5.66
4	5.33	7.23	10.42
4	4.75	8.19	11.69
4	4.43	8.84	12.54
4	4.95	7.83	11.22
4	5.56	6.91	9.99
4	3.6	11.12	15.43
4	4.82	8.06	11.52
4	3.74	10.66	14.85
4	6.03	6.34	9.21
4	7.99	4.72	6.95
4	7.88	4.79	7.05
4	9.24	4.06	6.01
4	5.06	7.65	10.98
4	4.96	7.82	11.20
4	3.99	9.91	13.92
6	5.47	7.04	10.16
6	4.96	7.82	11.20
6	3.41	11.83	16.29
6	5.19	7.44	10.70
6	4.74	8.21	11.72
6	4.15	9.49	13.39
6	5.2	7.43	10.68
6	4.27	9.20	13.01
6	7.18	5.27	7.74
6	5.18	7.46	10.72
6	9.02	4.16	6.16
6	9.87	3.79	5.63
6	5.94	6.44	9.35
6	5.34	7.22	10.40
	5.42	7.10	10.25
	3.8	10.47	14.62
	4.77	8.15	11.65
	8.06	4.67	6.89
	6.17	6.19	9.00
	5.8	6.61	9.58
	5.61	6.85	9.90
	4.13	9.54	13.45
	5.21	7.41	10.66

6.44	5.91	8.63
4.2	9.37	13.23
7.27	5.21	7.64
4.66	8.36	11.92
6.31	6.04	8.80
4.63	8.42	12.00
4.22	9.32	13.16
4.21	9.34	13.19
5.63	6.82	9.87
5.91	6.48	9.40
5.44	7.08	10.21
3.44	11.71	16.15
6.16	6.20	9.02
3.41	11.83	16.29
4.27	9.20	13.01
4.46	8.77	12.46

APPENDIX D: Diagrams of sampling locations

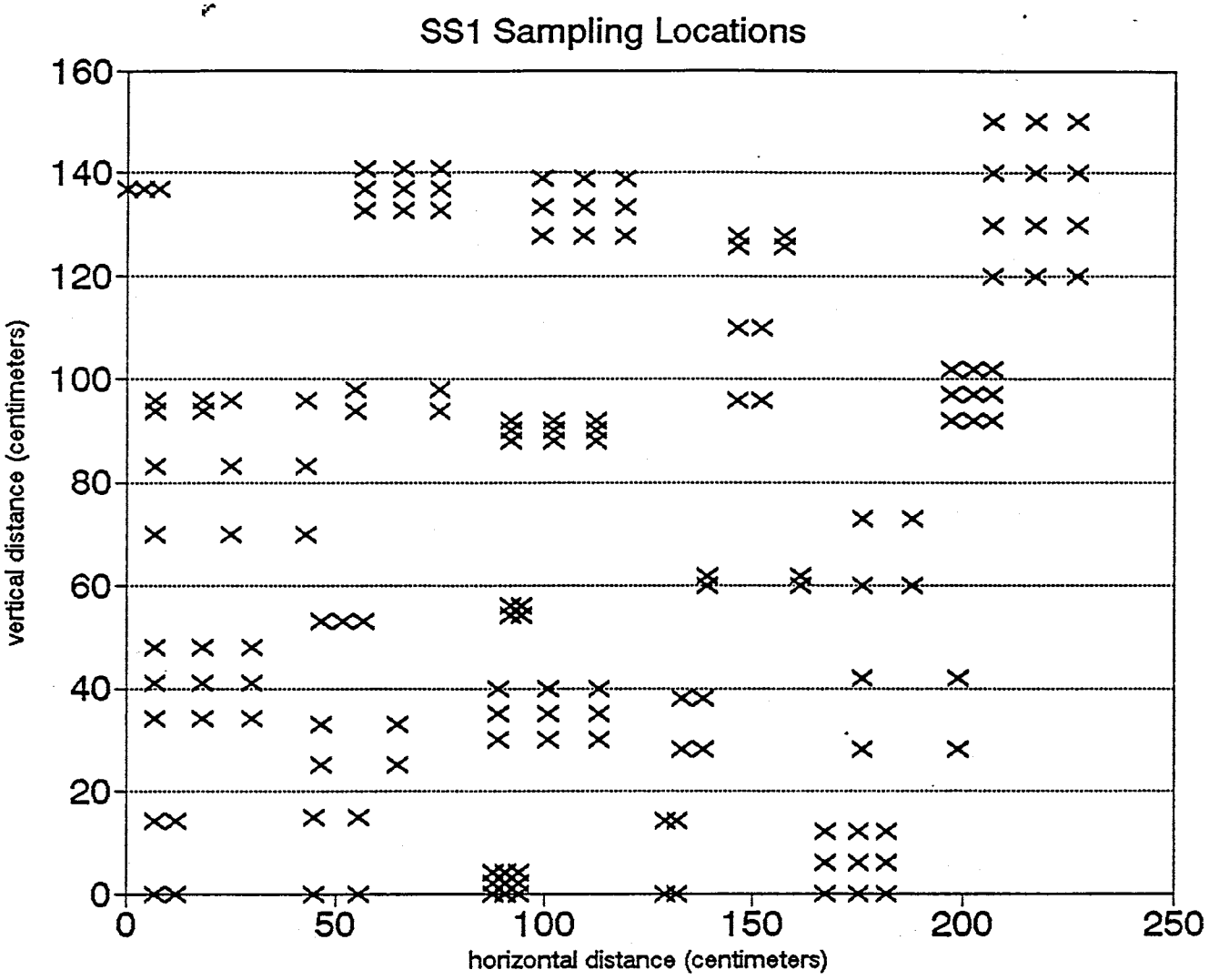
SS1 Sampling Locations
vertical distance (centimeters)
horizontal distance (centimeters)
0
20
40
60
80
100
120
140
160
0
50
100
150
200
250

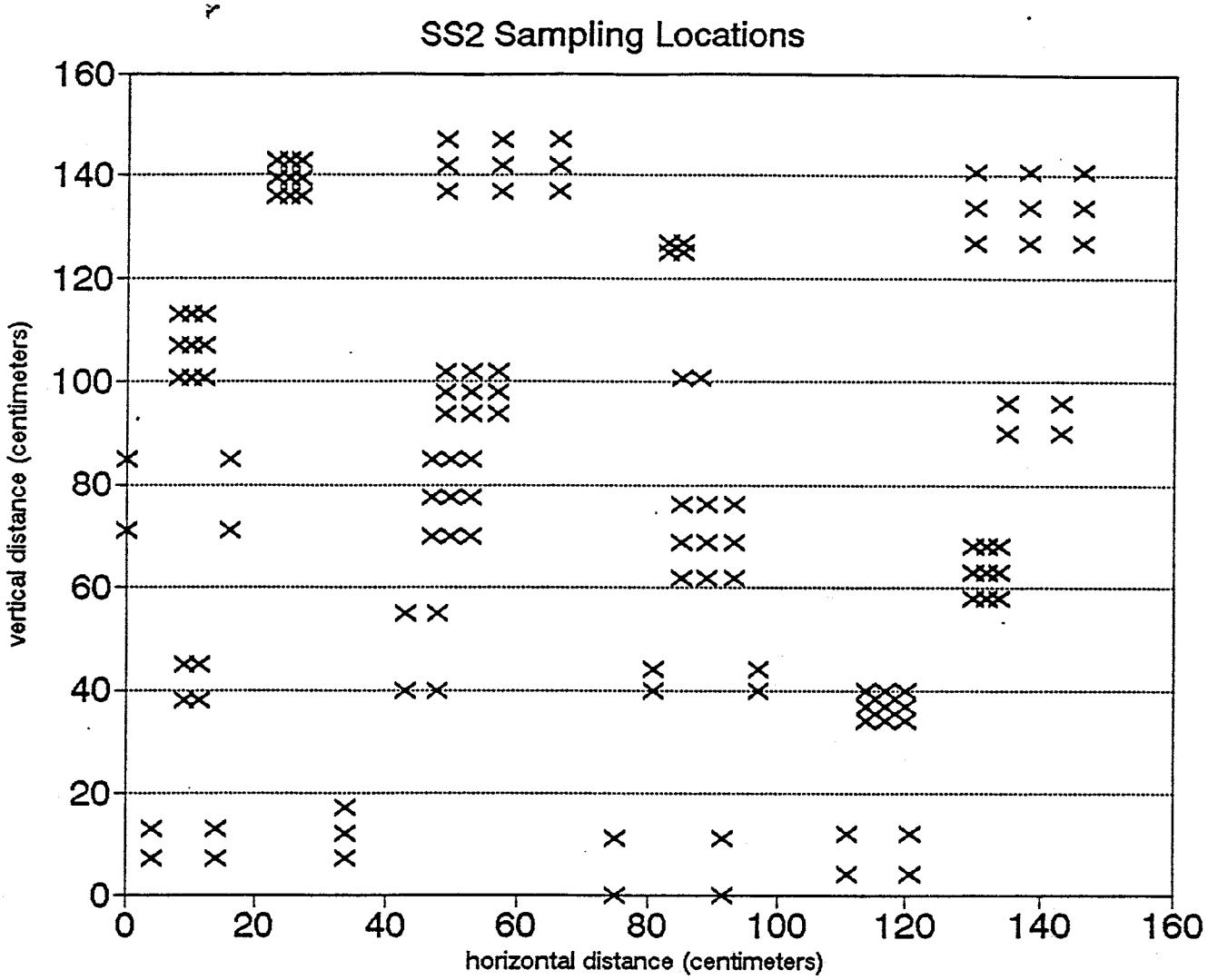
SS2 Sampling Locations
vertical distance (centimeters)
horizontal distance (centimeters)
0
20
40
60
80
100
120
140
160

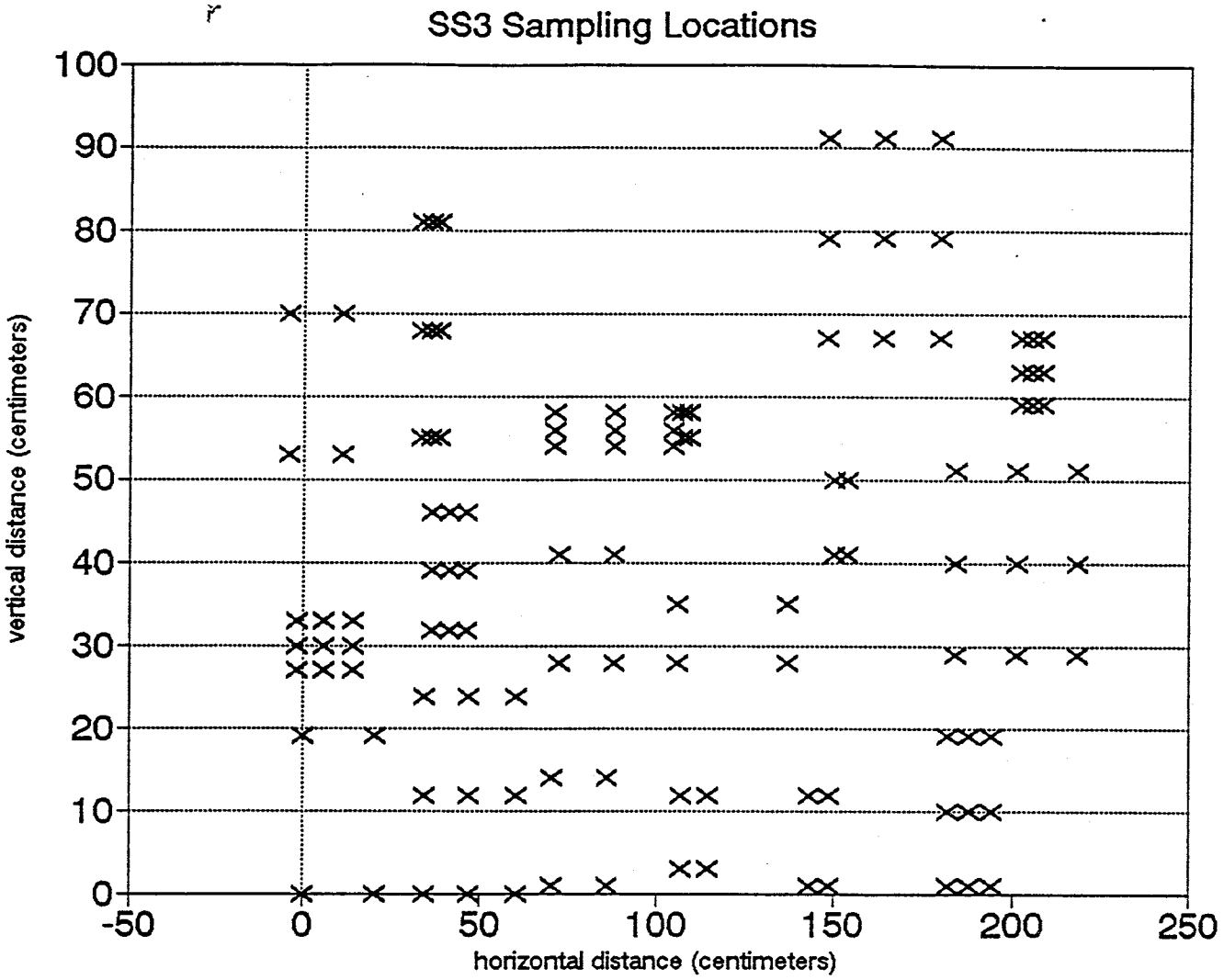
SS3 Sampling Locations
vertical distance (centimeters)
horizontal distance (centimeters)
100
90
80
70
60
50
40
30
20
10
0
-50
0
50
100
150
200
250

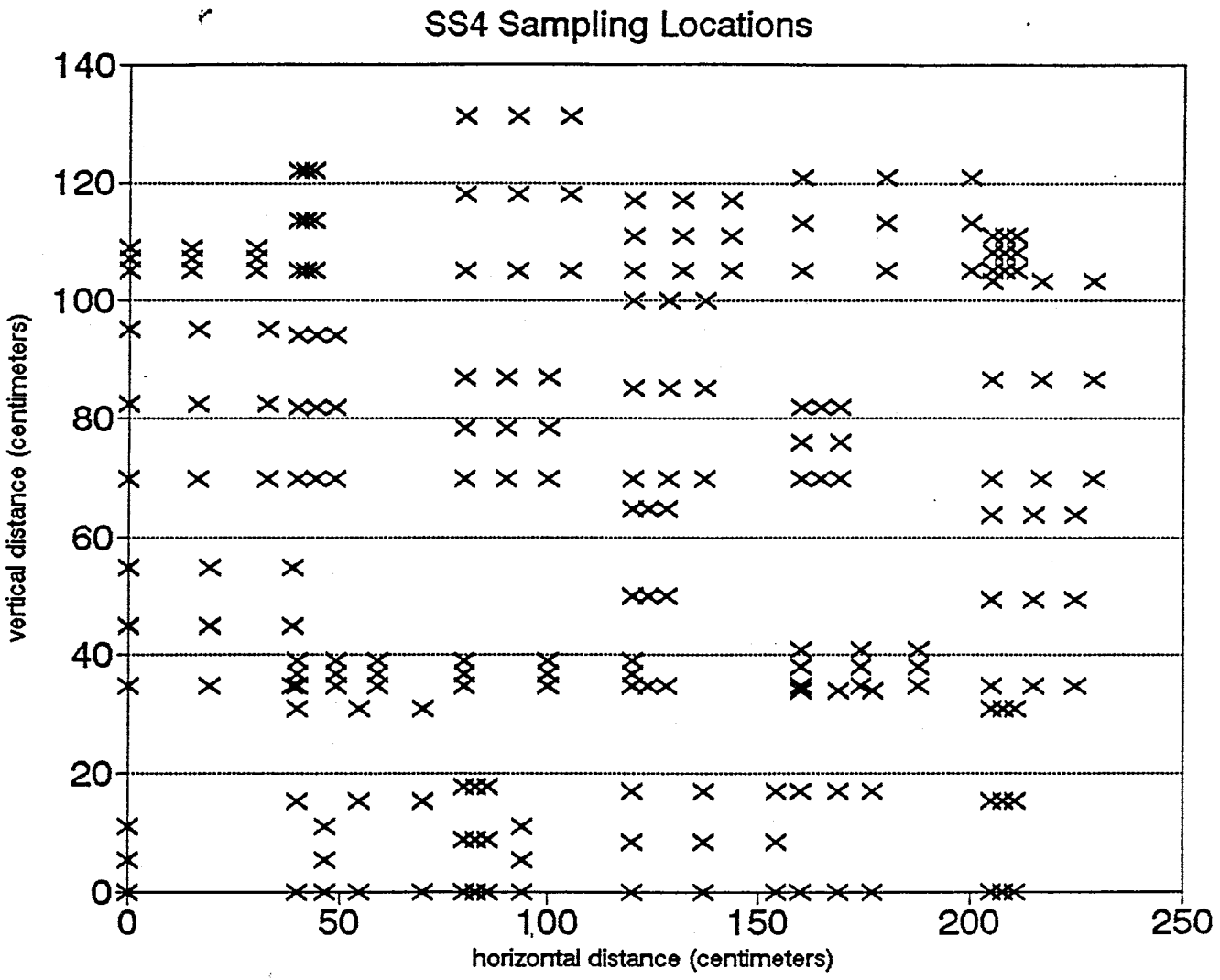
SS4 Sampling Locations
140
120
100
80
60
40
20
0
vertical distance (centimeters)
0
50
100
150
200
250
horizontal distance (centimeters)

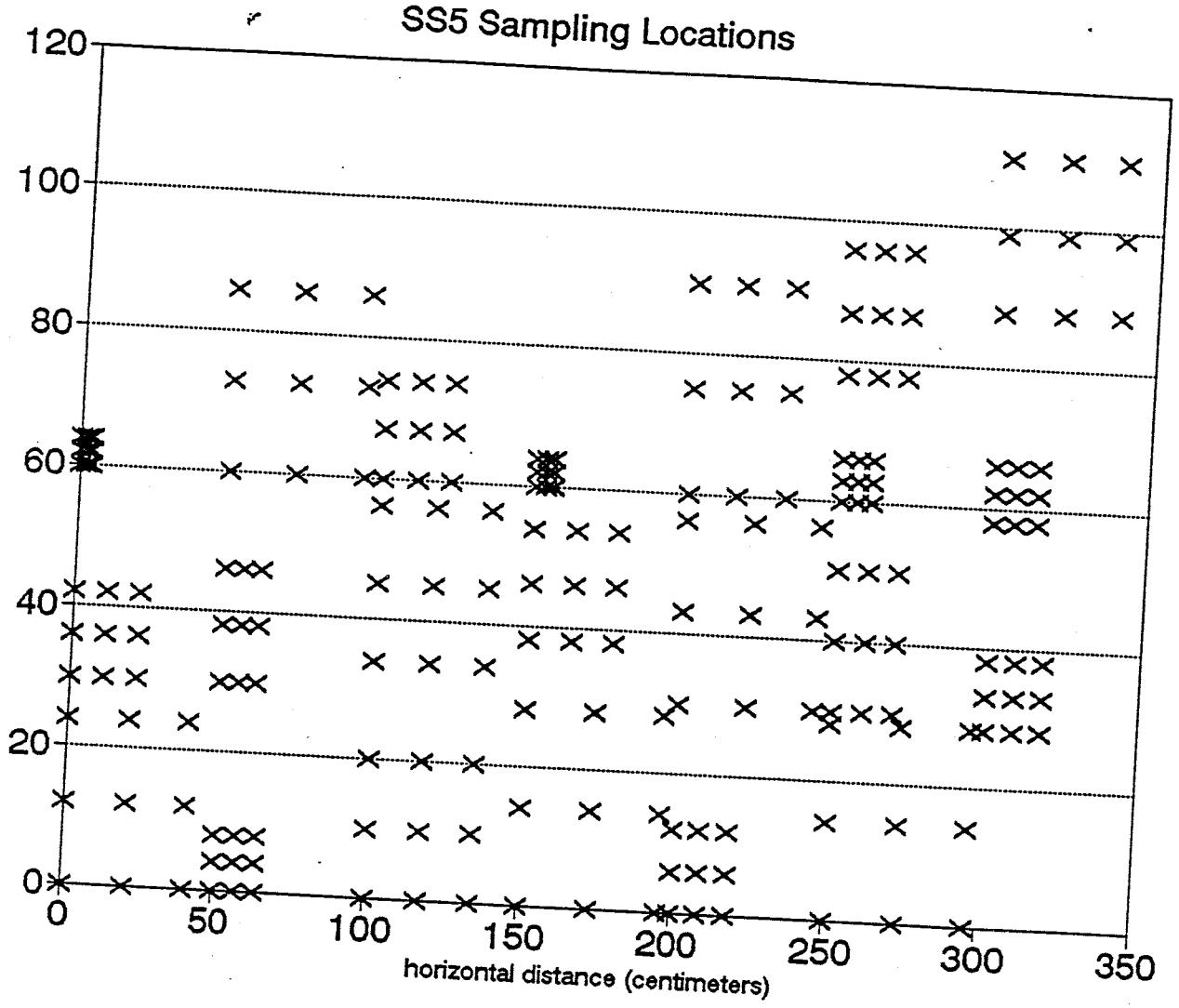
SS5 Sampling Locations
120
100
80
60
40
20
0
0
50
100
150
200
250
300
350
horizontal distance (centimeters)

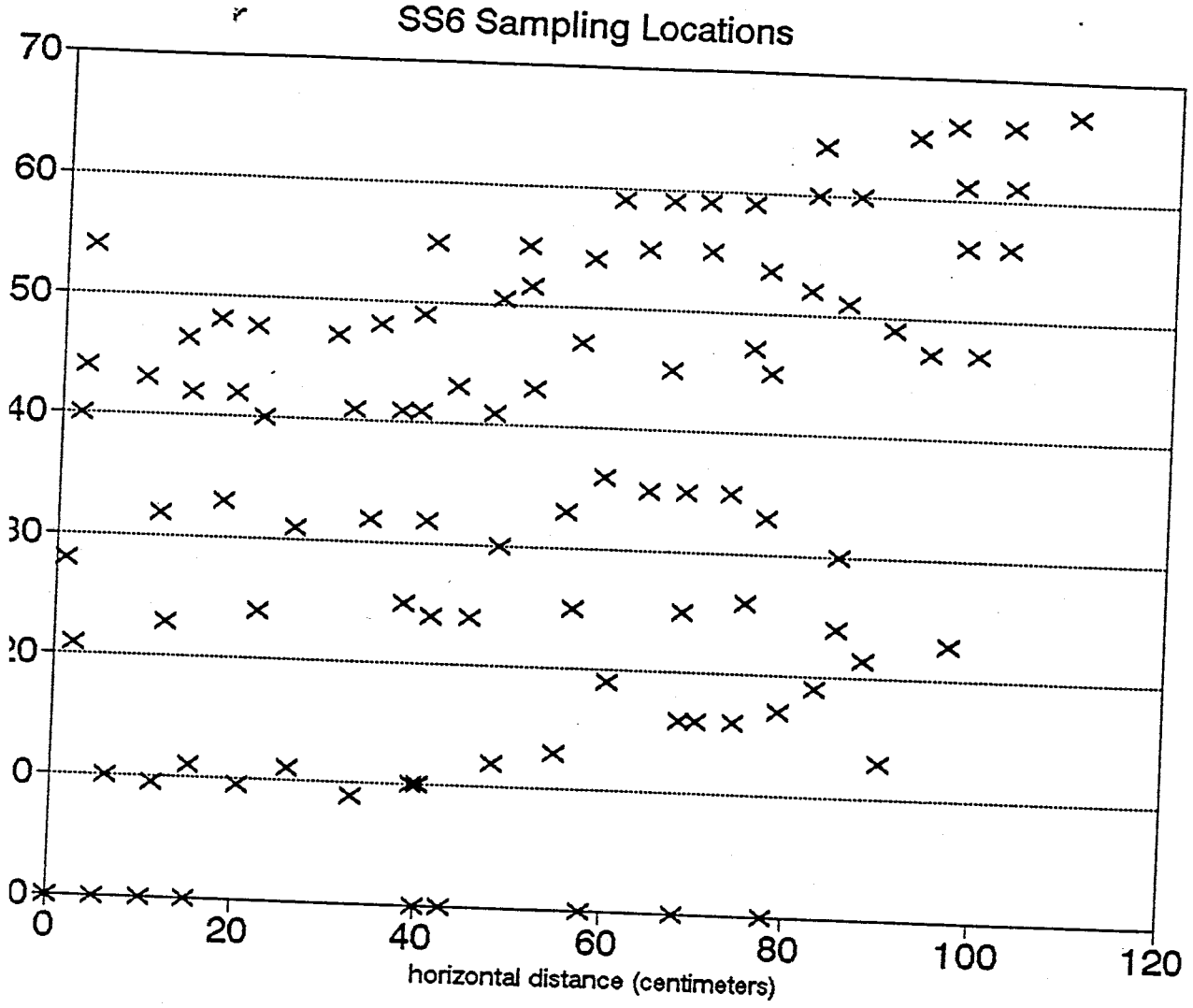
SS6 Sampling Locations
70
60
50
40
30
20
0
0
0
20
40
60
80
100
120
horizontal distance (centimeters)

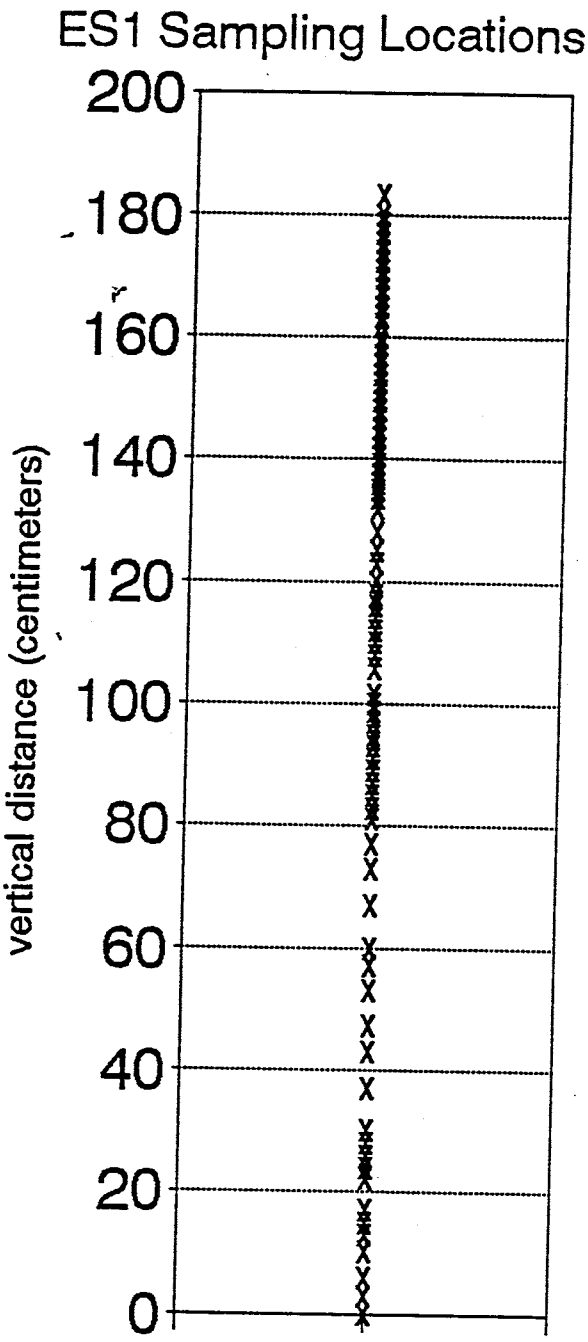
ES1 Sampling Locations
vertical distance (centimeters)
200
180
160
140
120
100
80
60
40
20
0